

**Effects of 2-methoxyestradiol, an endogenous estrogen metabolite, on SNO and
WHCO3 oesophageal cancer cell growth**

by

Veneesha Rambalee

Submitted in fulfillment of part of the requirements for the degree

Master of Science (Physiology)

in the Faculty of Health Sciences

University of Pretoria

Pretoria

May 2003

Supervisor: Dr AM Joubert

Co-supervisor: Dr M-L Lottering

Summary

Oesophageal squamous cell carcinoma ranks amongst the ten most frequently occurring cancers in the world with some of the highest incidences being reported in the Eastern Cape region of South Africa (Transkei). The etiology of this disease remains obscure.

2-Methoxyestradiol (2 ME), an endogenous estrogen metabolite, may be a defense mechanism against tumors. The aim of this study was to investigate whether 2 ME affects proliferation and/or induces apoptosis in oesophageal cancer cell lines and if so, by what mechanism.

2 ME decreased cell numbers in two oesophageal cell lines investigated. Cells treated with 2 ME showed morphological hallmarks of apoptosis, G2/M arrest and spindle disruption. Increased expression of death receptor 5 protein suggested that the extrinsic pathway was activated to induce apoptosis in oesophageal cancer cells.

2 ME has antitumor effects on oesophageal cancer cells by inducing apoptosis. It can be suggested that 2 ME can be considered to be a potential chemotherapeutic for the treatment of oesophageal cancer.

Acknowledgements

My thanks go to:

- Prof TJ Mariba, Dean of Faculty of Health Sciences for kind words of inspiration
- Prof D van Papendorp, Head of Dept of Physiology
- Drr ML Lottering and AM Joubert for expert supervision during this study
- Prof N Dippenaar for words of encouragement and little laughs that kept me going
- Mrs M Terblanche all her help and kindness
- Prof J Coetzee and Mr C van der Merwe for the help at the EM unit
- Dr K Lazenby, Miss M Williams, Miss A van Zyl and Miss S Coetzee for all the support
- Jenine, Pinks and Shoba for all your kind gestures
- Francina and Ezekiel for helping in the lab
- My Mum, Dad and brothers Treveen and Prevlen for believing in me
- Josh and Simone who aren't here yet but "heah, I'm doing this for you"
- My husband, Vernon-the best thing that could ever happen to me
- My LORD JESUS CHRIST, without whom none of this would have been possible

...

Table of Contents

Summary	i
Acknowledgements	ii
List of Figures	ix
List of Tables	xiii
List of Abbreviations	xiv

Chapter 1

Literature Review

1.1	Cancer of the oesophagus	1
1.1.1	Structure of the oesophagus	1
1.1.2	Incidence of oesophageal cancer	2
1.1.3	Etiology of oesophageal cancer	4
1.2	Estrogen and its major metabolites	7
1.2.1	Introduction.....	7
1.2.2	17 β -Estradiol metabolism.....	8
1.2.3	Hydroxylation and methylation	9
1.2.4	17 β -Estradiol and cell growth.....	10
1.2.5	2-Methoxyestradiol	11
1.3	Forms of cell death.....	13
1.3.1	Characteristics of apoptosis	14

a)	Morphological features of apoptosis.....	14
b)	Biochemical features of apoptosis.....	17
1.3.2	Mechanisms of apoptosis induction.....	18
a)	The extrinsic pathway.....	20
b)	The intrinsic pathway.....	22
1.3.3	Initiators of apoptosis.....	24
1.3.4	Apoptosis in cancer.....	25
1.3.5	Apoptosis in chemotherapeutic application.....	27
1.4	Aim of study	28
1.4.1	Specific aims of this study.....	28

Chapter 2

	General Procedures.....	30
2.1	Maintenance of cell cultures	30
2.1.1	Materials	30
2.1.2	Cell cultures	30
2.1.3	Maintenance of cell cultures.....	32
2.1.4	Subculturing of a monolayer.....	32
2.1.5	Procedure for trypsinization.....	32
2.1.6	Preservation of human cells grown in a cell culture.....	33
2.1.7	Determination of number of viable cells	34
2.2	Preparation of 2 ME stock solutions.....	35

2.3	Exposure of cells to 2 ME.....	36
2.4	Statistical analysis of data.....	37

Chapter 3

Analytical Experimental Protocols

3.1	Concentration-dependent growth studies.....	38
	a) Materials	38
	b) Methods.....	39
3.2	Morphology studies	39
3.2.1	Light microscopy	39
	a) Materials	39
	b) Methods.....	39
3.2.2	Transmission electron microscopy	40
	a) Materials	40
	b) Methods.....	40
3.2.3	Scanning electron microscopy	41
	a) Materials	41
	b) Methods.....	41
3.2.4	Immunofluorescent β -tubulin detection.....	42
	a) Materials	42
	b) Methods.....	42
3.2.5	Cell death type confirmation.....	43
	a) Materials	43

b)	Methods.....	43
3.3	Cell cycle studies	44
3.3.1	Determining the length of the cell cycle.....	44
a)	Materials	44
b)	Methods.....	44
3.3.2	Flow cytometry analysis	46
a)	Materials	46
b)	Methods.....	46
3.4	Apoptotic pathway studies/identification	47
3.4.1	B-cell lymphoma 2 immunohistochemistry.....	47
a)	Materials	47
b)	Methods.....	47
3.4.2	Death Receptor 5 immunohistochemistry.....	48
a)	Materials.....	48
b)	Methods.....	48

Chapter 4

Results	49
4.1 Concentration-dependent growth studies.....	49
4.2 Morphology studies	52
4.2.1 Light microscopy	52
4.2.2 Transmission electron microscopy	57
4.2.3 Scanning electron microscopy	60
4.2.4 Immunofluorescent β -tubulin detection.....	63
4.2.5 Cell death type confirmation.....	66
4.3 Cell cycle studies	69
4.3.1 Cell cycle length	69
4.3.2 Flow cytometry analysis	72
4.4 Apoptotic pathways studies/identification.....	75
4.4.1 B-cell lymphoma 2.....	75
4.4.2 Death Receptor 5.....	78

Chapter 5

Discussion	81
-------------------------	----

Chapter 6

Conclusion	90
-------------------------	----

References.....92

List of Figures

Figure 1:	A cross-sectional diagram showing the anatomy of the oesophagus.....	1
Figure 2:	Map of South Africa showing the Eastern Cape where prevalence of oesophageal cancer is the highest in the world.....	3
Figure 3:	Enzymes involved in the regulation of E concentrations in human mammary cells.....	9
Figure 4:	A cell dying through apoptosis undergoes distinctive changes	16
Figure 5:	Intrinsic and extrinsic pathways of apoptosis in cells eventually lead to cell death.....	19
Figure 6:	Extrinsic pathway of apoptosis induction.....	21
Figure 7:	Intrinsic pathway of apoptosis induction.....	23
Figure 8:	Standard haemocytometer chamber.....	35
Figure 9a:	SNO cells treated with different concentrations of 2 ME 10^{-6} , 10^{-7} , 10^{-8} , 10^{-9} M for 72 h	50
Figure 9b:	WHCO3 cells treated with different concentrations of 2 ME 10^{-6} , 10^{-7} , 10^{-8} , 10^{-9} M for 72 h.....	51
Figure 10a:	Haematoxylin and Eosin staining of SNO control cells exposed to 0.1% DMSO (vehicle) for 24 h.....	53
Figure 10b:	Haematoxylin and Eosin staining of SNO cells exposed to 1×10^{-6} M 2 ME for 24 h.....	53
Figure 11a:	Haematoxylin and Eosin staining of WHCO3 control cells exposed to 0.1% DMSO (vehicle) for 24 h.....	54
Figure 11b:	Haematoxylin and Eosin staining of WHCO3 cells exposed to 1×10^{-6} M 2 ME for 24 h.....	54

Figure 12a: Haematoxylin and Eosin staining of SNO control cells exposed to 0.1% DMSO (vehicle) for 24 h	55
Figure 12b: Haematoxylin and Eosin staining of SNO cells exposed to 1×10^{-6} M 2 ME for 24 h.....	55
Figure 13a: Haematoxylin and Eosin staining of WHCO3 control cells exposed to 0.1% DMSO (vehicle) for 24 h.....	56
Figure 13b: Haematoxylin and Eosin staining of WHCO3 cells exposed to 1×10^{-6} M 2 ME for 24 h.....	56
Figure 14a: Transmission electron microscopy of SNO control cells exposed to 0.1% DMSO (vehicle) for 24 h	58
Figure 14b: Transmission electron microscopy of SNO cells exposed to 1×10^{-6} M 2 ME for 24 h.....	58
Figure 15a: Transmission electron microscopy of WHCO3 control cells exposed to 0.1% DMSO (vehicle) for 24 h.....	59
Figure 15b: Transmission electron microscopy of SNO cells exposed to 1×10^{-6} M 2 ME for 24 h.....	59
Figure 16a: Scanning electron microscopy of SNO control cells exposed to 0.1% DMSO (vehicle) for 24 h	61
Figure 16b: Scanning electron microscopy of SNO cells exposed to 1×10^{-6} M 2 ME for 24 h.....	61
Figure 17a: Scanning electron microscopy of WHCO3 control cells exposed to 0.1% DMSO (vehicle) for 24 h.....	62
Figure 17b: Scanning electron microscopy of WHCO3 cells exposed to 1×10^{-6} M 2 ME for 24 h.....	62

Figure 18a: β -Tubulin detection of SNO control cells exposed to 0.1% DMSO (vehicle) for 24 h.....	64
Figure 18b: β -Tubulin detection of SNO cells exposed to 1×10^{-6} M 2 ME for 24 h	64
Figure 19a: β -Tubulin detection of WHCO3 control cells exposed to 0.1% DMSO (vehicle) for 24 h.....	65
Figure 19b: β -Tubulin detection of WHCO3 cells exposed to 1×10^{-6} M 2 ME for 24 h.....	65
Figure 20a: Propidium iodide and Hoechst 33342 staining of SNO control cells exposed to 0.1% DMSO (vehicle) for 24 h.....	67
Figure 20b: Propidium iodide and Hoechst 33342 staining of SNO cells exposed to 1×10^{-6} M 2 ME for 24 h.....	67
Figure 21a: Propidium iodide and Hoechst 33342 staining of WHCO3 control cells exposed to 0.1% DMSO (vehicle) for 24 h.....	68
Figure 21b: Propidium iodide and Hoechst 33342 staining of WHCO3 cells exposed to 1×10^{-6} M 2 ME for 24 h.....	68
Figure 22a: Percentage of synchronized SNO cells in mitosis at 2-h intervals	70
Figure 22b: Percentage of synchronized WHCO3 cells in mitosis at 2-h intervals	71
Figure 23a: Flow cytometric analysis of the effects of 24 h exposure to 10^{-6} M 2 ME on the cell cycle and apoptosis induction in SNO cells.....	73
Figure 23b: Flow cytometric analysis of the effects of 24 h exposure to 10^{-6} M 2 ME on the cell cycle and apoptosis induction in the WHCO3 cells	74
Figure 24a: Bcl2 immunocytochemistry of SNO control cells exposed to 0.1% DMSO (vehicle) for 24 h.....	76

Figure 24b: Bcl2 immunocytochemistry of SNO cells exposed to 1×10^{-6} M 2 ME for 24 h.....	76
Figure 25a: Bcl2 immunocytochemistry of WHCO3 control cells exposed to 0.1% DMSO (vehicle) for 24 h.....	77
Figure 25b: Bcl2 immunocytochemistry of WHCO3 cells exposed to 1×10^{-6} M 2 ME for 24 h.....	77
Figure 26a: Death receptor 5 immunocytochemistry of SNO control cells exposed to 0.1% DMSO (vehicle) for 24 h.....	79
Figure 26b: Death receptor 5 immunocytochemistry of SNO cells exposed to 1×10^{-6} M 2 ME for 24 h.....	79
Figure 27a: Death receptor 5 immunocytochemistry of WHCO3 control cells exposed to 0.1% DMSO (vehicle) for 24 h.....	80
Figure 27b: Death receptor 5 immunocytochemistry of WHCO3 cells exposed to 1×10^{-6} M 2 ME for 24 h.....	80
Figure 28: Increased Bax/Bcl2 ratio inhibits the anti-apoptotic function of Bcl2	84
Figure 29: 2 ME may induce apoptosis via the extrinsic pathway and cross-talk between pathways can occur at caspase 8 and 10 cleavage.....	87

List of Tables

Table 1:	Factors contributing to oesophageal cancer	3
Table 2:	Anti-proliferative, anti-angiogenic and apoptosis-inducing properties of 2-Methoxyestradiol	12
Table 3:	Inhibitors and inducers of apoptosis	25
Table 4:	Summary of structural proteins processed by caspases associated with apoptotic morphology	89

List of Abbreviations

AIDS	Acquired Immune Deficiency Syndrome
ANT	Adenine-Nucleotide Translocator
Apaf-1	Apoptosis protease activating factor-1
Bcl2	B-cell lymphoma 2
CAD	Caspase-activated DNase
COMT	Catechol- <i>O</i> -methyl transferase
CE	Catechol estrogen
Cyt c	Cytochrome c
DNA	Deoxyribonucleic acid
DMSO	Dimethyl sulphoxide
DAB	Diaminobenzidine
DEDS	Death effector domains
DFF 40	DNA fragmentation factor
DR5	Death Receptor 5
E	17 β -Estradiol
EDTA	Ethylene diamine tetra acetic acid
EGF	Epidermal growth factor
ER	Estrogen receptor
FAD	Fas-associated protein domain
FADD	Fas-associated death domain
FAK	Focal adhesion kinase
FasL	Fas ligand
FLICE	Fas-related ICE protease

FCS	Heat-inactivated fetal calf serum
FITC	Fluoroisothiocyanate
h	hour
H ₂ O ₂	Hydrogen peroxide
HO	Hoechst
2 HE	2-hydroxy-estradiol
HU	Hydroxyurea
IgG	Immunoglobulin G
I	Interphase
ICAD	Inhibitor of Caspase-Activated Deoxyribonuclease
ICE	Interleukin-1 beta-converting enzyme
MAPK	Mitogen Activated Protein Kinase
MEKK1	Map/Erk Kinase Kinase 1
MEM	Minimum Essential Medium
2 ME	2-Methoxyestradiol
M	Molar
NuMa	Nuclear Matrix Associated protein
OC	Oesophageal cancer
PAK2	p21 activated kinase
PBS	Phosphate buffered saline
PTP	Permeability-Transition Pore
PI	Propidium iodide
SEM	Scanning electron microscopy
SAANDs	Selective Apoptotic Antineoplastic Drugs
T	Telophase

TEM	Transmission electron microscopy
TGF α	Transforming growth factor α
TNF	Tumor necrosis factor
TRAIL	TNF-related apoptosis-inducing ligand
UV	Ultraviolet
VDAC	Voltage-Dependent Anion Channel

Chapter 1

Literature Review

Oesophageal cancer is the third most common cancer amongst males and the most common among black African males in South Africa (1). This devastating cancer affects 1 in 32 black male South Africans. The disease has been poorly understood and the cause is unknown.

1.1 Cancer of the oesophagus

1.1.1 Structure of the oesophagus

The normal oesophagus is a hollow, highly distensible muscular tube that extends from the pharynx to the gastro-oesophageal junction. In the human newborn the oesophagus (figure 1) measures 10 to 11 cm in length and 23 to 25 cm in the adult.

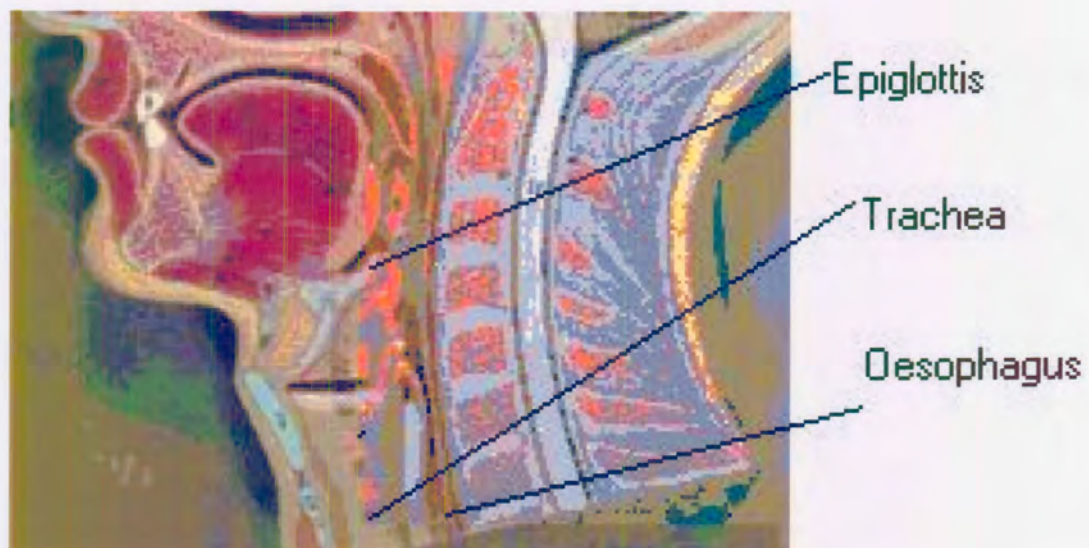


Figure 1: A cross-sectional diagram showing the anatomy of the oesophagus (2).

a disease occurring in men. In a pilot study done at the King Edward VIII hospital, Durban, it was shown that the male: female ratio was as high as 20:1 (5).



Figure 2: Map of South Africa showing the Eastern Cape where prevalence of oesophageal cancer is the highest in the world (6).

Patients remain asymptomatic and present to hospital when the disease has reached its malignant stages. Since the majority of patients are from the Transkei region they first consult traditional healers. At Tygerberg Hospital (Cape Town, South Africa) it is not unusual to see 3 or 4 new cases (7) of advanced OC per week. OC is a disease that is rarely curable. Curative surgery is only an option in small tumors without distant

The wall of the oesophagus consists of 4 layers, from the inside outwards: the mucosa, submucosa, muscularis propria and adventitia, reflecting the general structural organization of the gastrointestinal tract. The mucosa is composed of a non-keratinizing stratified squamous epithelial layer that overlies the lamina propria. A number of specialized cell types, such as melanocytes, endocrine cells, and Langerhans cells are found in the deepest portion of the epithelial layer.

The lamina propria is the non-epithelial portion of the mucosa. It consists of areolar connective tissue and contains vascular structures and scattered leukocytes. The submucosa consists of loose connective tissue containing blood vessels. The muscularis propria contains striated muscle fibers.

The function of the oesophagus is to conduct food and fluids from the pharynx to the stomach.

1.1.2 Incidence of oesophageal cancer

While squamous cell carcinoma of the oesophagus occurs throughout the world, its incidence varies widely among countries and within the regions of the same country. There is large geographical variation in the incidence of oesophageal cancer (OC), with some well defined areas of high incidence near the Caspian Sea in Kazakhstan and Iran, in Brittany (France) and especially in China (3). However, the area with the highest prevalence of OC in the world is the Eastern Cape region, Transkei, of South Africa (4) as shown in figure 2. It has also been found that blacks in South Africa are at a higher risk to develop oesophageal cancer than whites and that it is predominantly

metastases (7). However, current research has shown that the overall five-year survival in OC is less than 10% (8). Five-year survival of patients with tumors confined to the mucosa and without lymph node metastasis is estimated at 60%, but less than 10% of stomach carcinomas are diagnosed when they have reached the malignant stage (9). OC is relatively resistant to radiotherapy, but chemotherapy may be associated with improved response rates (9).

1.1.3 Etiology of oesophageal cancer

The marked differences in epidemiology strongly implicate dietary and environmental factors, with an ill-defined contribution from genetic predisposition. The majority of oesophageal cancers are attributable to excessive alcohol and tobacco usage (3). Some alcoholic drinks contain significant amounts of carcinogens as polycyclic hydrocarbons and nitrosamines along with other mutagenic compounds (Table 1). Dietary deficiencies in vitamins and essential amino acids have also been documented to cause OC (10). Dietary factors such as salt and high carbohydrate intake probably increase the risk, while intake of vegetables, fruit, beta-carotene and vitamin C seems to reduce the risk of OC by neutralizing free radicals produced in the body (11). Nutritional deficiencies associated with alcoholism may contribute to the process of carcinogenesis. In general though, dietary deficiencies have not been shown to initiate events. Epidemiological and experimental studies provide strong evidence for dietary substances in promotion, progression and inhibition of cancer (12). It has also been found that zinc and selenium deficiencies may contribute to the etiology of OC (13). All the factors thought to contribute to OC are summarized in Table 1 below.

Table 1: Factors contributing to oesophageal cancer (11).

Factors associated with development of squamous cell carcinoma of the oesophagus

Dietary

Deficiency of vitamins (A, C, riboflavin, thymine and pyridoxine)

Deficiency of trace metals (zinc, molybdenum)

High content of nitrites and nitrosamines

Fungal contamination of food

Lifestyle

Alcohol consumption, tobacco use, urban environment

Oesophageal disorders

Acute oesophagitis, Achalasia

Genetic predisposition

Acute celiac disease, Endodermal dysplasia

Other carcinogens, such as fungus-contaminated food, may play a role in oesophageal cancer. *Fusarium verticilloides* (*F.moniliforme*) and *F.subglutinans* produce metabolites called mycotoxins that are toxic to humans and animals. A majority of the incidents of oesophageal cancer in the Transkei region is associated with contaminated foodstuffs that contain mycotoxins produced by the fungus *F.moniliforme* that have been implicated in the etiology of oesophageal cancer. It is believed that these mycotoxins interfere with sphingolipid metabolism (14). Their worldwide appearance in food is well documented, particularly in under-developed and developing countries such as South Africa (14). Most rural black South Africans eat mycotoxin-contaminated maize several times a day with meat and imfino (a herb-like tea, brewed from roots) supplements, increasing the risk of oesophageal carcinomas.

1.2 Estrogen and its major metabolites

1.2.1 Introduction

Estrogen and progesterone are the two most important steroid hormones in the adult female. Estrogens are formed from androgenic precursors through aromatization. 17β -Estradiol (E) is the most potent estrogen in premenopausal, non-pregnant women and is mainly synthesized by the granulosa cells of the ovarian follicles. E is secreted into the bloodstream, binds partially to a circulating sex hormone-binding globulin and is then transported to cells in the body (15).

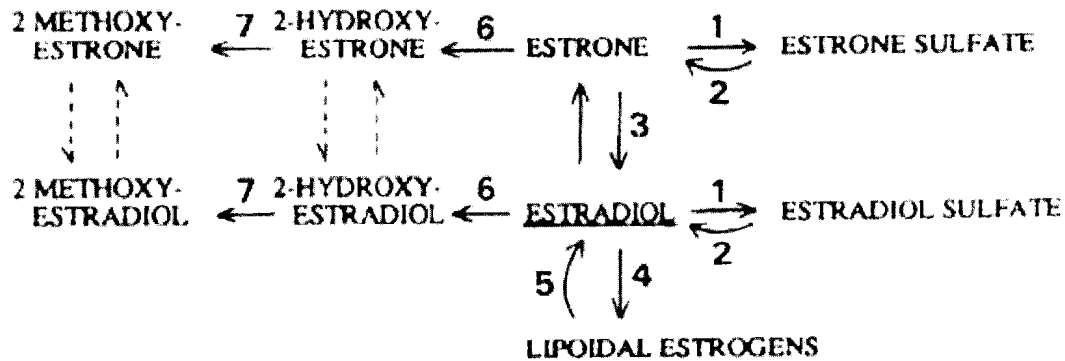
Many functions of E are mitogenic of nature. E is therefore generally regarded as a proliferating agent. However, examples of anti-mitogenic E effects have been reported (16). E is mainly responsible for normal development, growth and maintenance of the female reproductive system and the development of the secondary sexual characteristics. E is also known to be involved in both the etiology and maintenance of growth of cancers in reproductive tissues (17).

In 1980, it was suggested that the metabolism of various gonadal hormones by their target tissues is critical for the expression of the physiological actions of these hormones (18). Diverse functions have been attributed to E. In an effort to explain the variety of these effects, possible metabolic pathways whereby E is converted to other physiologically active metabolites were investigated to ascertain whether certain classical E functions may be ascribed to some of its metabolites. One such pathway that has attracted much attention is the 2-carbon metabolic pathway, with its major

metabolites, 2-hydroxy-E (2 HE) and 2-Methoxyestradiol (2 ME), being quantitatively the most important estrogen derivatives in humans (19).

1.2.2 17 β -Estradiol metabolism

The levels of E found in the blood do not accurately reflect the concentrations found within the cells of target tissues (20). The hormone microenvironment within the cell is regulated by a number of steroid hormone-metabolizing enzymes, which may be under metabolite and/or hormonal (estrogen, progesterone) control (21). Some enzymes catalyze the production of biologically inactive derivatives, which are rapidly eliminated from the cell, while others catalyze the production of exclusively intracellular derivatives, which act as reserve forms of E. Still, others catalyze the formation of cytotoxic E metabolites (21). Enzymes involved in the regulation of E concentration via the 2-carbon pathway in human mammary cells are depicted in figure 3.



1. Estrogen sulfotransferase
2. Estrogen sulfatase
3. Estradiol-17 β hydroxydehydrogenase
4. Fatty acyl Coenzyme A: estradiol-17 β acyltransferase
5. Lipoidal estrogen esterase
6. Estradiol 2-hydroxylase
7. Catechol estrogen *o*-methyl transferase

Figure 3: Enzymes involved in the regulation of E concentrations in human mammary cells (21).

1.2.3 Hydroxylation and methylation

E is metabolized to hydroxylated products, such as 2-, 4-, 6-, 7-, 15- and 16-substituted estradiols (22). Generally, metabolism via 2-hydroxylation is predominant (22) though in certain target tissues, *e.g.* brain, 4-hydroxylation may be also prominent (23). The enzyme that catalyzes the synthesis of 2 HE (a catechol estrogen-CE) is a microsomal cytochrome P450-dependent monooxygenase, known as 2-hydroxylase (24) and is located in the liver, brain and estrogen-responsive tissues (25).

CEs are extremely labile compounds. Chemically, 2 HE is readily oxidized to a quinone, which leads to cleavage of the aromatic ring (26), and biologically, it is

rapidly metabolized to the monomethyl ether, 2 ME, by the enzyme catechol-*O*-methyl transferase (COMT) (27). COMT is a ubiquitous cytosolic and microsomal enzyme. COMT levels are increased in most malignant mammary tumors. 2 ME can be demethylated by a specific, cytochrome P450-dependent demethylase, which is distinct from the 2 Methoxyestrone-demethylase (27).

1.2.4 17 β -Estradiol and cell growth

As a mitogen, E stimulates DNA synthesis and subsequent proliferation of estrogen receptor (ER) positive (28,29) and sometimes ER negative cells (30,31). Stimulation by E is biphasic, with significant stimulation occurring at 10^{-11} M, optimal stimulation occurring at *ca* 10^{-8} M and inhibition of growth and/or cell death occurring at concentrations equal to, or exceeding 10^{-6} M (32). However, involvement of E in the control of cell proliferation and/or cell death has not been clarified.

Breast epithelium undergoes cyclic apoptotic programmed cell death with fluctuation in B-cell lymphoma 2 (Bcl2) levels during the menstrual cycle (33). E was found to increase Bcl2 production without affecting Bax (34), thus protecting cells from apoptosis. This effect is ER mediated (33,34). With E ablation, however, regression of E-sensitive tissues occurs through the process of apoptosis *e.g.* vaginal and cervical epithelia after menopause (35).

1.2.5 2-Methoxyestradiol

This study focuses on 2 ME, an endogenous estrogen metabolite (synthesis discussed in section 1.2.3). It is accepted that 2 ME does not bind to ER (36) though there has been reports of weak 2 ME-ER binding (37). Partly because of this, 2 ME was initially regarded as being biologically inactive. Only in the past decade, evidence for its biological activity has started to accumulate. In recent years several researchers have shown that 2 ME displays definite anti-proliferative, anti-angiogenic and pro-apoptotic activity (30,38,39,40) as summarized in Table 2.

2 ME is a potent inhibitor of arterial smooth muscle, fibroblast, epithelial and endothelial cell proliferation, as well as angiogenesis *in vitro*. 2 ME targets actively cycling cells, showing no effect on quiescent cells.

The first mechanism of action identified for 2 ME, is its interaction with the colchicine binding (39) and it inhibits tubulin polymerization, thereby causing abnormal microtubule assembly (39). This disruption of microtubules leads to abnormal spindle formation and uneven chromosome distribution (30) with a resultant block of mitotic cells in metaphase (30). Of 30 naturally occurring estrogens and their derivatives tested, 2 ME showed the strongest microtubule-disrupting activity (30). Moreover, it has been shown that 2 ME is toxic to 55 different tumor cell lines, some of which are ER positive and ER negative (40,41). These actions are independent from ER activity (41,42). In addition to this mechanism, recent studies have proposed that 2 ME also targets apoptosis-inducing signaling pathways (41,42).

Table 2:

ANTI-PROLIFERATIVE, ANTI-ANGIOGENIC AND APOPTOSIS-INDUCING ACTIONS OF 2 ME

1. Anti-proliferative action of 2 ME

- *Lottering et al. (20), 1991-cell growth on MCF7 and HeLa cells*
- *Fotsis et al. (38), 1994-tumor cell growth in fibroblasts and epithelial cells*
- *Nishigaki et al. (43), 1995-smooth muscle cell growth*
- *Wassberg et al. (44), 1999, Lin 2000, Shumacher 1999-anti-proliferative activity on various cell lines*

2. Anti-angiogenic action of 2 ME

- *Fotsis et al. (38), 1994- angiogenesis in metastatic diseased models in mice.*
- *Katotaka et al. (45), 1998- controls metastatic invasion of cancer.*
- *Pribluda et al. (46), 2000-regulates various steps in the angiogenesis cascade such as migration, invasion, collagen, collagen matrix and tubule formation.*
- *Chauhan et al. (47), 2002-2 ME has anti-angiogenic activity in multiple myeloma cells.*

3. Apoptosis-inducing action of 2 ME

- *Quaningo et al. (42), 2002-2 ME-induced apoptosis in pancreatic cancer cell lines via the mitochondria-dependent pathway.*
 - *Chauhan et al. (47), 2002- 2 ME induces apoptosis in leukemic cells.*
 - *LaVallee et al. (41), 2002-2 ME induces apoptosis in breast cancer cell lines independently of estrogen receptors.*
-

1.3 Forms of cell death

Several forms of cell death exist. Studies of dying cells have demonstrated the need for precise definitions of various forms of cell death that include apoptosis, oncosis, necrosis and programmed cell death.

Apoptosis occurs as a result of a preprogrammed process contained within the cell and can be either activated by the cell itself or external stimuli (48). Apoptosis is a physiological energy-dependent cell death marked by cell shrinkage, intact cell membrane, chromatin condensation, margination of chromatin and eventually the formation of apoptotic bodies. This form of cell death causes destruction of individual cells that represent a threat to the integrity of an organism (49).

Apoptosis is involved in morphogenesis of embryonic tissue as well as homeostasis of adult organs and tissues (50). The formation of proper connection synapses between neurons in the brain requires the elimination of surplus cells via apoptosis (50). Removal of tissue in the embryo for proper formation of fingers and toes occurs via apoptosis. In the female body, apoptosis is responsible for the sloughing off of the inner lining of the uterus (the endometrium) at the start of menstruation (50).

Apoptosis is therefore a vital biological process, a mechanism by which an organism maintains health and homeostasis through ridding itself of aging, excess, infected, or mutated cells.

The term oncosis has been coined for cell death caused specifically by ischemia (51). Oncosis is a form of cell death characterized by cell swelling due to accumulation of water and electrolytes, early plasma membrane rupture, and disruption of cellular organelles (52).

Necrosis is defined as a pathologic form of cell death resulting from acute cellular injury which is typified by rapid cell swelling and lysis (53). Metabolic collapse, cell and mitochondrial swelling, flocculation of nuclear chromatin, rupture of the cytoplasmic and nuclear membranes and shedding of cellular contents into the extracellular space are associated with necrosis.

According to Van Cruchten and Van Den Broeck (54), the term programmed cell death refers to a fixed pathway followed by dying cells, whether or not with the characteristics of apoptosis.

1.3.1 Characteristics of Apoptosis

a) Morphological features of apoptosis

The definition of apoptosis was first based on a distinct sequence of morphological features observed by electron microscopy described by Kerr *et al.* (55). As briefly mentioned in section 1.3 apoptosis is characterized by a series of typical morphological features such as shrinkage of the cell, blebbing of the cell's surface (52), fragmentation into membrane-bound apoptotic bodies and rapid phagocytosis by neighboring cells (52).

The cell's nucleus shrinks, followed by condensation of nuclear chromatin into sharply delineated masses that become marginated against the nuclear membrane. Following this, the nuclear membrane breaks up (karyorrhexis) (52). The cells detach from the surrounding tissue and become convoluted to form extensions. The cell extensions separate and the plasma membrane seals to form a separate membrane around the detached solid material. The latter process is termed budding and is responsible for the formation of apoptotic bodies as shown in figure 4. Apoptotic bodies are packed with cellular organelles, like mitochondria and fragments of the nucleus. These apoptotic bodies are then rapidly phagocytosed by neighboring cells including macrophages and parenchyma cells (52). Another morphological characteristics of apoptosis include the fusion of the outer cisternae of the endoplasmic reticulum with the cell membrane.

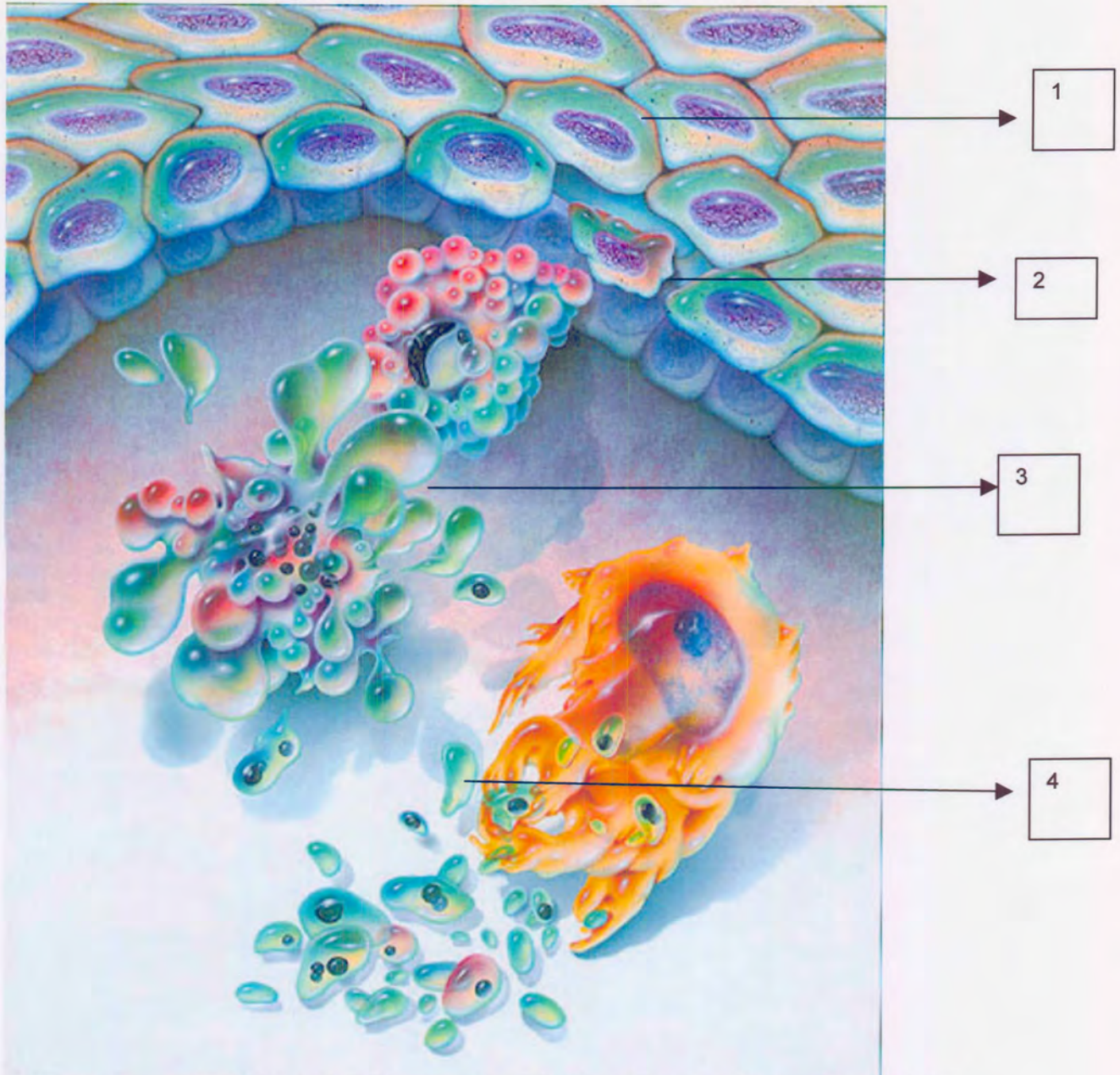


Figure 4: A cell dying through apoptosis, undergoes distinctive changes. First it shrinks and pulls away from its neighbors. Then blebs appear on the surface, and the chromatin condenses at the edge of the nucleus. Soon fragments break off and apoptotic bodies are formed (56).

1. Normal cell
2. Cell beginning apoptosis
3. Blebbing of cell
4. Formation of apoptotic bodies

b) Biochemical features of apoptosis

The biochemical hallmark of apoptosis is degradation of DNA by endogenous DNases (52). The DNases initially cut the internucleosomal regions of DNA into large fragments of 50-300 kilobases and subsequently into smaller fragments of 180-200 bases (57). The two main enzymes responsible for fragmentation during apoptosis include:

- DNA fragmentation factor (DFF 40) (58)
- Caspase activated DNase (CAD) (59)

These enzymes are selectively activated upon cleavage by caspase 3 (49). Caspases are a family of cysteine proteases. These intracellular proteases cleave their targets at aspartic acid residues (cysteine aspartases). At least 14 of such proteases have been reported thus far (49).

Initiator caspases are responsible for cleavage of cytoskeletal proteins such as vimentin, actin and fodrin (a membrane associated cytoskeletal protein) (49). These early apoptotic events are thought to be responsible for characteristic blebbing of the cell surface (60).

Cleavage of translocase (flippase) and /or activation of scramblase (floppase) leads to a subsequent flip of phosphatidyl serine from the inner to the outer leaflet of the plasma membrane. This is a very early event during the initiation stages of apoptosis (52).

Activation of the enzyme type II transglutaminase, leads to cross-linking of proteins to the envelope of apoptotic bodies (61). Transglutaminase II therefore protects the endangered plasmalemma by cross-linking proteins and by the formation of sub-plasmalemma protein scaffolds that are shifted to directly underneath the plasma membrane (49).

An increase in intracellular Ca^{2+} levels, loss of mitochondrial transmembrane potential leading to the release of cytochrome c (47) and proteolytic degradation are also biochemical characteristics of apoptosis.

1.3.2 Mechanisms of apoptosis induction

Multiple signaling pathways lead from death-triggering extracellular or intracellular agents to a central control and execution stage (62). Two major pathways for induction of apoptosis have been identified namely the extrinsic (ligand-receptor interaction) (49) and the intrinsic pathway (mitochondria-dependent) as shown in figure 5. The extrinsic pathway, triggered by death activators binding to receptors at the cell surface, is represented by the tumor necrosis factor (TNF) family of receptors. The TNF family of receptors utilize protein interaction modules known as death domains and death effector domains (DEDS) to assemble receptor-signaling complexes. Receptor-signaling complexes recruit and activate cell death proteases (called caspases), namely pro-caspase 8 and 10 (63).

The intrinsic pathway, generated by signals within the cell, involves the participation of mitochondria that release caspase-activating proteins. Proteins of the Bcl2 family govern this mitochondria-dependent apoptosis (64).

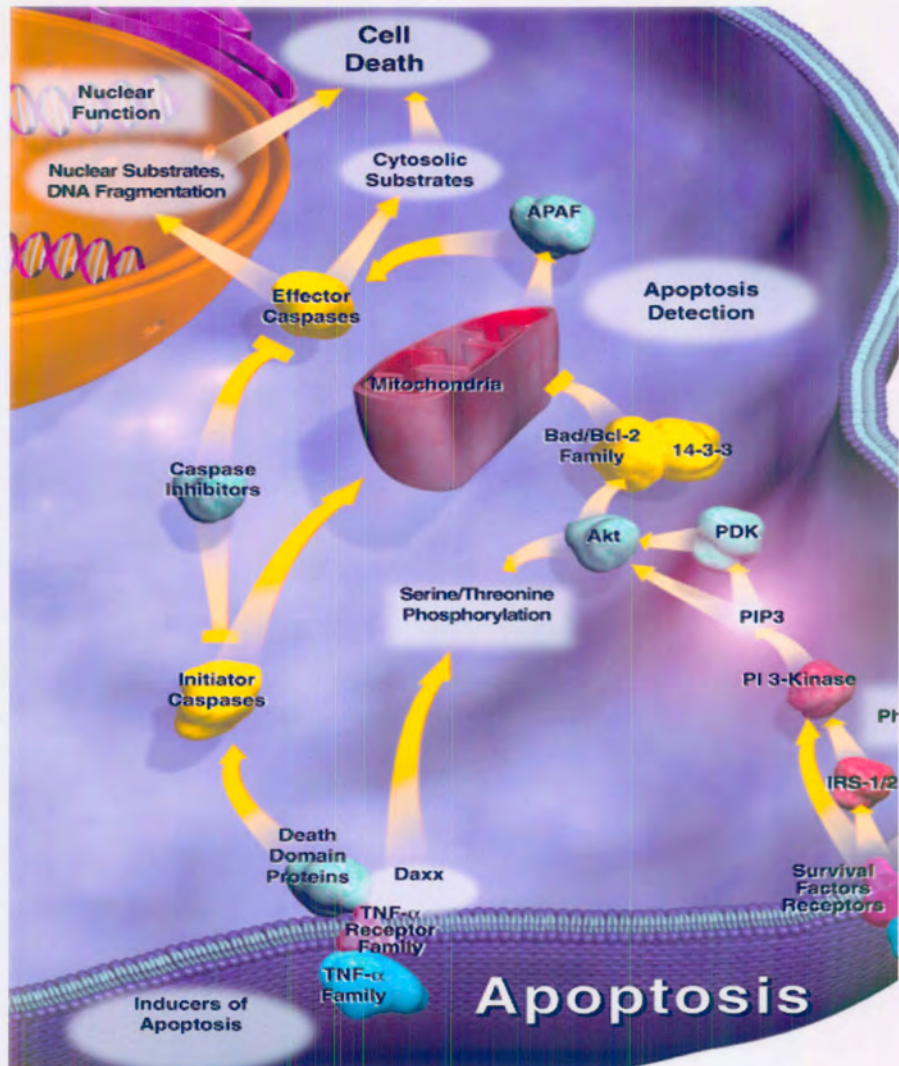


Figure 5: Intrinsic and extrinsic pathways of apoptosis in cells eventually lead to cell death (65).

a) The extrinsic pathway

Cell surface proteins, belonging to the TNF receptor (Fas Death Receptor 5, TNF-related apoptosis-inducing ligand (TRAIL) receptor 2, Apo2, Killer), superfamily (66) are characterized by conserved cysteine-rich extracellular domains and the presence of an intracellular “death domain” in a subset of its members (63). These receptors share a specific intracellular domain, termed the death domain, activation of which triggers the apoptosis cascade (67). Subsequent mutational analysis of Fas and TNF indicated that the cytoplasmic domain (about 70 amino acids) is necessary and sufficient to transmit a signal to the cytoplasm that leads to apoptotic cell death, as shown in figure 6 (68).

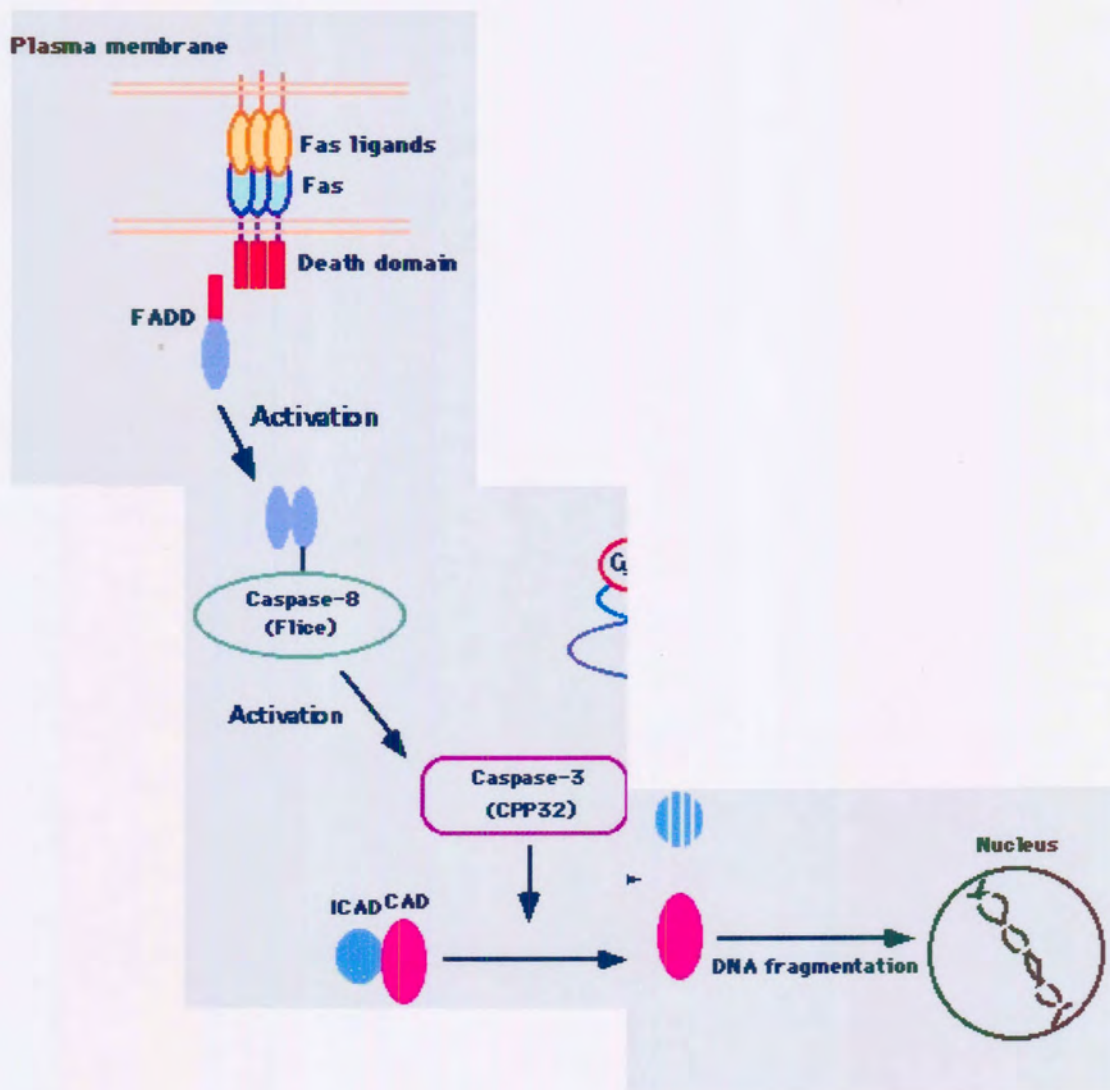


Figure 6: Extrinsic pathway of apoptosis induction (68).

b) The intrinsic pathway

The intrinsic pathway is also known as the mitochondria-dependent pathway. Mitochondria appear to be core components of the cell death machinery (69). Several death signals have been reported to release cytochrome c (Cyt c) from the mitochondria into the cytosol (70). Released Cyt c (also known as apoptosis protease activating factor-2) then binds to apoptosis protease activating factor-1 (Apaf-1) to form an apoptosome complex with procaspase 9 in an energy-dependent manner (59). Subsequently, activated caspase 9 cleaves downstream caspases such as caspase 3 and 7 (71). These downstream caspases, through the cleavage of several death substrates, are believed to cause execution of cell death (42) that leads to DNA fragmentation as shown in figure 7.

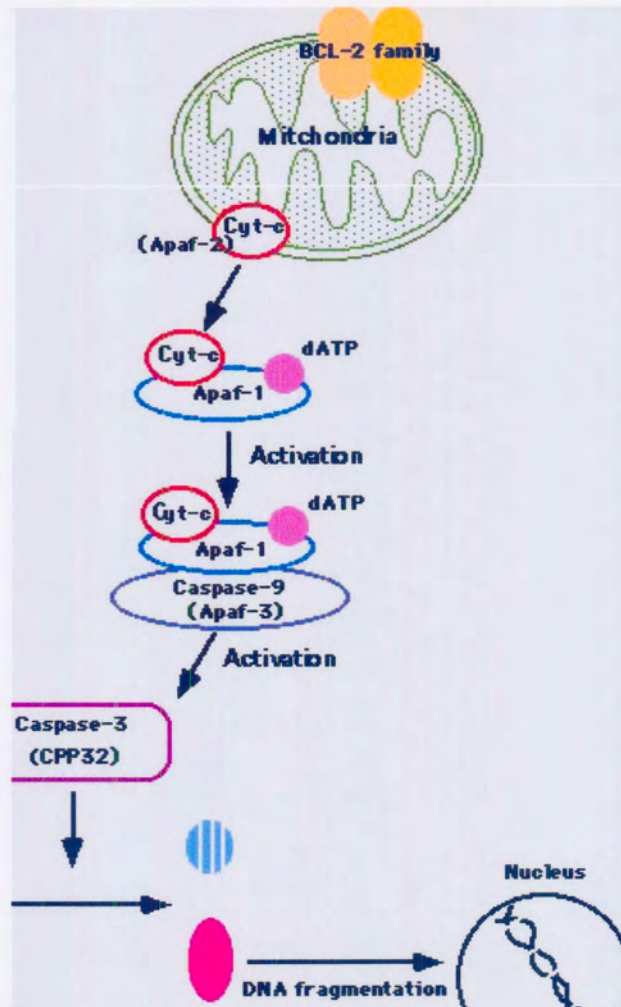


Figure 7: Intrinsic pathway of apoptosis induction (68).

1.3.3 Initiators of Apoptosis

Recently, considerable research has focussed on identifying the molecular sensors or triggers of apoptosis. Apoptosis can be initiated by a variety of extrinsic and intrinsic signals (72). This type of regulation allows for elimination of cells that have been produced in excess, that have developed improperly, or that have sustained genetic damage. Physiological inhibitors/activators, viral genes, pharmacological agents, toxins and therapy-associated agents (refer to p25) can either induce or inhibit apoptosis and are summarized in Table 3.

Table 3: Inhibitors and inducers of apoptosis (53).

<i>Inhibitors of Apoptosis</i>	<i>Inducers of apoptosis</i>
<i>Physiological inhibitors</i>	<i>Physiological activators</i>
1. Growth factors	1. TNF family (TNF, Fas ligand)
2. Extracellular matrix	2. Neurotransmitters
3. Neutral amino acids	3. Glucocorticoids
4. Zinc	4. Loss of matrix attachment
5. Androgens	<i>Damage-related inducers</i>
6. Estrogens	1. Viral infection
<i>Viral genes</i>	2. Bacterial toxins
1. Adenovirus	3. Oncogenes
2. Baculovirus	4. Tumor suppressors
3. Cowpox virus	5. Cytotoxic T cells
4. Epstein Barr virus	6. Oxidants
<i>Pharmacological agents</i>	7. Free radicals
1. Calpain inhibitors	<i>Theraphy-associated agents</i>
2. Cysteine protease inhibitors	1. Chemotherapeutic drugs
3. Phenobarbital	2. Gamma radiation
	3. UV radiation

1.3.4 Apoptosis in cancer

Although apoptosis is important for the normal development and health of an animal, its aberrant activation may contribute to a number of diseases, for example, Acquired Immune Deficiency Syndrome (AIDS), neurodegenerative disorders (Parkinson's and

Alzheimer's disease), and ischemic injury (53). Impaired apoptosis may be a significant factor in the etiology of diseases such as cancer, autoimmune disorders, and viral infections (53).

The "program" for orderly cell death of the organism's survival may become corrupted by injury, such as in stroke or heart attack, or via a genetic aberration *e.g.* the inactivation of the p53 tumour suppressor gene by a virus, a chemical, or radiation (54).

Cells from a wide variety of human malignancies have a decreased ability to undergo apoptosis in response to at least some physiological stimuli (24). This is most apparent in metastatic tumors. Most normal cells depend on environment-specific factors to maintain their viability (53). Metastatic tumor cells have circumvented this homeostatic mechanism and can survive at sites distinct from the tissue where they arose. To do this, tumor cells have developed some degree of independence from the survival factors that restrict the distribution of their nontransformed counterparts. Advances are beginning to shed some light on the molecular basis for increased resistance of tumor cells to undergo apoptosis, however the mechanism still remains unclear (53).

1.3.5 Apoptosis in chemotherapeutic application

Cancer therapies are currently designed to arrest and kill rapidly dividing cancer cells. However they are non-selective. Traditional chemotherapy and radiation therapy kill both normal and tumor cells. A wide variety of chemotherapeutic agents work by initiating DNA damage. Cell death in response to DNA damage has been shown to result from apoptosis (53).

Selective Apoptotic Antineoplastic Drugs (SAANDs) such as Aptosyn® (exisulind) is a first-generation compound in a new class of first-generation drugs, selectively inducing apoptosis in precancerous and cancerous cells (72). Only precancerous and cancerous tissues are directed to self-destruct, with minimal impact on healthy tissue. Another potential chemotherapeutic drug is 2 ME, the estrogen metabolite that has been shown to have antitumor activity on fifty-five cell lines (40).

1.4 Aim of study

OC is amongst the ten most frequently occurring cancers in the world. The Transkei region in the Eastern Cape, South Africa is the area with the highest prevalence of oesophageal cancer in the world (4). By comparing the risk factor patterns of two target populations (Colored and Xhosas) in the Western Cape Province, smoking and the use of alcohol have been indicated as possible common determinants (73). Differences in dietary habits associated with an increased risk for oesophageal cancer also became apparent. (74). However, in communities where all members have the same lifestyle and dietary habits, it was shown that OC is more prevalent in males than in females (5). It raises the question: What is the protective factor present in females? Could this protection be due to the protective effects of estrogen metabolites in women?

Though 2 ME showed anti-proliferative activity in 55 different tumor cell lines, its cellular actions have not been studied in OC. It has been proposed that increased formation of 2 ME, can be an endogenous defense mechanism against tumors, since 2 ME selectively inhibits the *in vitro* growth and induces apoptosis in transformed cells only (19,30). Therefore we chose to investigate whether 2 ME has any *in vitro* antitumor effects on oesophageal cancer cell lines, more specifically anti-mitogenic and pro-apoptotic actions.

1.4.1 Specific aims of this study

1. To determine the effects of 2 ME on cell growth and morphology of two oesophageal cancer cell lines of different origin.

2. To investigate whether 2 ME induces cell death via apoptosis in OC cells.

3. To identify the pathway whereby 2 ME may induce apoptotic cell death.

Chapter 2

General Procedures

2.1 Maintenance of cell cultures

2.1.1 Materials

2 ME, Eagles's Minimum Essential Medium with Earle's salts, L-glutamine and NaHCO₃ (MEM), Trypsin-EDTA, and Trypan blue were supplied by Sigma Chemical Co. (St. Louis, United States of America). Heat-inactivated fetal calf serum (FCS), sterile cell culture flasks and plates were obtained through Sterilab Services (Johannesburg, South Africa). Phosphate buffered saline (PBS), penicillin, streptomycin and fungizone were obtained from Highveld Biological (Sandringham, South Africa). All other chemicals were of analytical grade and supplied by Sigma Chemical Co. (St. Louis, United States of America).

2.1.2 Cell cultures

Highveld Biological (Sandringham, South Africa) supplied both SNO and WHCO3 oesophageal carcinoma cell lines.

SNO cells were obtained through a biopsy from a male patient from the Transkei Hospital and cultured by Dr Elke Bay at Highveld Biological. SNO cells are described as a non-keratinizing squamous epithelium cell line.

WHCO3 cells were a gift from Professors Veale and Thornley (Department of Zoology, University of Witwatersrand, Johannesburg, South Africa). WHCO3 cells were obtained through a biopsy from a patient with squamous oesophageal carcinoma and is described as a poorly differentiated, non-keratinizing cell line.

Continuous cell lines were used in this study rather than primary cultures, since they can be propagated, expanded and divided into identical replicates several times to maintain consistency during experimental procedures. Primary cultures die off after a few rounds of subculturing, after which a new primary culture has to be grown which has different properties than the first primary culture. It is therefore difficult to maintain consistency in experiments conducted. Also, biopsies are difficult to obtain and separation of different cell types from the biopsy is needed to obtain the required cell type.

Furthermore, the advantages of using continuous cell lines are: their greater growth rates to higher cell densities and resultant higher yield, their lower serum requirement and the ease of maintenance in simple media (75). However there are also disadvantages of using continuous cell lines. The disadvantages of primary cultures are the mixed nature of each preparation, limited lifespan of the culture and potential contamination problems.

2.1.3 Maintenance of cell cultures

The media used is dependent on the cell type and the company of purchase supplier's instructions. Eagle's minimum essential medium (MEM) is used for most cell types. It is a balanced salt solution containing L-glutamine and a combination of organic salts, glucose, amino acids and vitamins. A variety of cells are grown in monolayers (SNO and WHCO3 cells grow as monolayers).

Cells were grown as monolayers in minimum essential medium at 37°C in a humidified atmosphere containing 5% CO₂. Media were supplemented with 10% heat inactivated FCS, penicillin (100µg/l), streptomycin (100µg/l) and fungizone (250µg/l).

2.1.4 Subculturing of a monolayer

A primary culture is grown to near-confluency in a 25 cm² tissue culture flask containing 5 ml medium. Cells are dispersed by trypsin treatment. These cells are then seeded to produce secondary cultures. This process is called subculturing or propagating.

2.1.5 Procedure for trypsinization

All medium was removed from the primary culture by pouring off into a waste bottle. 5 ml of PBS was added to the adhering monolayer to remove dead cells and any adhering FCS. 1 ml of trypsin (0.25% in PBS) was added to the cells to allow trypsin

digestion to continue for approximately 2 min at 37 °C. The cells were observed microscopically for cell rounding but not dislodging. Trypsin was removed with a sterile pasteur pipette. 1.5 ml of complete cell culture media was added to the flasks and the cells were dispersed into suspension by tapping the flasks hard against the hand and pipetting the resultant solution with a sterile pasteur pipette. 0.5 ml of the cell suspension was transferred to a new flask containing 4 ml of fresh medium. The new flasks with cells were capped and incubated at 37 °C without further disturbance. Cells were monitored until the color of the media changed orange.

2.1.6 Preservation of human cells grown in cell culture

When freezing was necessary the SNO and WHCO3 cell suspensions were centrifuged at 200 x g for 5 minutes. The supernatant was then discarded and the pellet was suspended in 1ml freeze medium (80% medium, 15% serum and 5% glycerol). This was transferred to a cryotube, which was immediately placed in a – 70 °C deepfreeze. This procedure results in a cooling rate of approximately 1 °C/minute.

Aseptic techniques were applied throughout and all cellular experiments were carried out in a laminar flow cabinet.

2.1.7 Determination of number of viable cells

Determining the number of cells in culture is important in standardization of culture conditions and performing accurate quantitation experiments. A haemocytometer is a thick glass slide with a central area designed as a counting chamber (figure 8).

Cells were trypsinized as described above. The cell suspension was then centrifuged at 200 xg for 5 minutes. The supernatant was discarded and 1 ml of media was added to the pellet and the cells were gently resuspended in the media using a pipette. 100 μ l of this cell suspension was added to a micro tube as well as 100 μ l of Trypan blue dye (0.1%). Cells were stained with (0.1%) Trypan blue to determine cell viability. Dead cells take up the dye and are not counted. In contrast, cells that are viable do not take up Trypan blue and are counted. Cells are counted on a haemocytometer to give an approximate estimate of cells in suspension.

Cells per ml is determined by the following calculation:

Cells/ml = Average count per square x dilution factor x 10^{-4} (see figure 8)

Total cells = cells/ml x original volume of cell suspension from which the sample was taken.

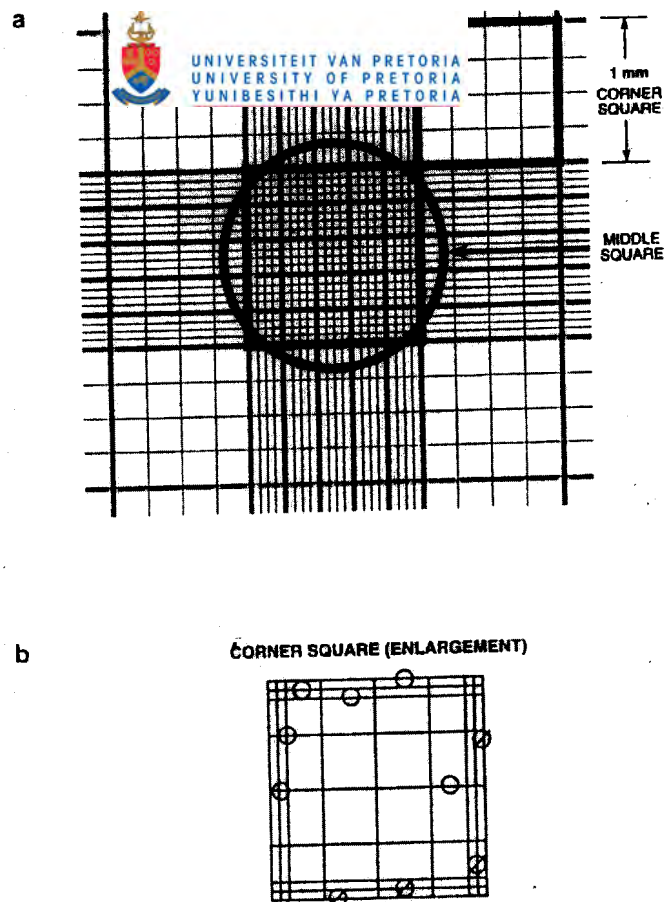


Figure 8: a) Standard haemocytometer chamber. The circle indicates the approximate area covered at 100x microscope magnification. The procedure for counting cells on the haemocytometer is as follows: a) Count 4 corner squares and middle square in both chambers. b) Count cells in the top and left touching middle line (o). Do not count cells touching middle line at bottom and right (75).

Thereafter the cell suspension was diluted with medium to give the required cell number and seeded into appropriate vessels (on heat-sterilized coverslips in 6 well culture plates or 96 well culture plates for experiments).

2.2 Preparation of 2 ME stock solutions

2 ME was dissolved in dimethyl sulphoxide (DMSO) to give a final concentration of 2×10^{-3} M. This stock solution was diluted with medium to the desired concentrations

for the experiments. The medium of all control cells was supplemented with an equal concentration of DMSO. The concentrations of the DMSO never exceeded 0.1% (v/v) in the final dilutions.

2.3 Exposure of cells to 2 ME

SNO and WHCO3 cells were seeded on heat-sterilized coverslips in the appropriate vessels and allowed to settle for 24 h. After 24 h the control cells were exposed to 0.1 % DMSO and the other cells were exposed to different concentrations of 2 ME ranging from 10^{-6} to 10^{-9} M at different time intervals.

2.4 Statistical analysis of data

Statistical analysis of the data was conducted as discussed with Dr. Becker of the unit for Biostatistics at the MRC. Variation in results could be due to A) variation between subjects in a random sample, B) variation within subjects (biological variation) or C) variation in the analytical procedure. Comparing two cell lines was similar to comparing two subjects. The sample size (n) is therefore one in each category and thus too small to compare statistically. When exposing cells to the effects of 2 ME, biological variation is introduced within each cell line. The analytical variation in the experimental procedures and biological variation within each cell line were analyzed by determining ANOVA and students' t-test for paired samples, respectively. Quantitative experiments were repeated thrice, with $n=6$ in each experiment. All experiments included a set of appropriate controls.

Chapter 3

Analytical experimental protocols

3.1 Concentration-dependent growth studies

a) Materials

Glutaraldehyde, crystal violet and Triton X-100 were purchased from Sigma Chemical Co. (Munich, Germany).

b) Methods

SNO and WHCO3 cells were seeded in 96 well culture plates at a density of 5000 viable cells per well and exposed to 4 different concentrations of 2 ME (10^{-6} , 10^{-7} , 10^{-8} , 10^{-9} M) for 72 h at 37°C, to determine which concentration of 2 ME was most effective in inhibiting cell growth. The experiment was terminated by replacing the growth medium with 300µl of 1% glutaraldehyde in PBS for 15 minutes. Crystal violet (1%, in PBS) was added for 30 minutes, hereafter the culture wells were immersed in running tap water for 15 minutes. After the plates had dried, 500µl of 0.2% Triton X-100 was added to each well. The plates were incubated for 90 minutes and 200µl of the liquid content were transferred to 96 well plates (76). The absorbance (measured at 570nm) of the samples was analyzed using an EL_X800 Universal Microplate Reader (Bio-Tek Instruments Inc., Analytical Diagnostic Products, Weltevreden SA). Results shown are representative of three independent experiments (each conducted in triplicate).

3.2 Morphology studies

3.2.1 Light microscopy

a) Materials

Bouin's fixative, Haematoxylin, eosin, ethanol, xylol and Entellan[®] fixative were purchased from Sigma Chemical Co. (Munich, Germany).

b) Methods

SNO and WHCO3 cells (250 000) were seeded onto heat-sterilized coverslips in 6 well plates. They were exposed to 1×10^{-6} M of 2 ME for a period of 24 h at 37°C. An exposure time of 24 h was chosen, to show morphological changes occurring during this period when studying the influence of 2 ME on cell numbers of SNO and WHCO3 cells. Cells were fixed in Bouin's fixative for 60 minutes and stained by standard haematoxylin and eosin staining procedure. Coverslips were removed with a tweezer and transferred to a staining dish. Bouin's fixative was added to the coverslips for 30 minutes. The fixative was discarded from the staining dish. 70% ethanol was added to the coverslips for 20 minutes. The coverslips was thereafter incubated in Mayers Hemalum for 20 minutes and rinsed in running tap water for 2 minutes. The coverslips were then subjected to 1% eosin for 2 minutes and rinsed twice with 70%, 96%, and 100% ethanol and xylol, respectively for 5 minutes (77). The coverslips were mounted on microscope slides with resin and left to dry and thereafter evaluated with a light microscope (Olympus-420).

3.2.2 Transmission electron microscopy

a) Materials

Osmium, quetol, 'Reynolds' lead citrate, aqueous uranyl acetate and toluidine blue were purchased from Merck Co. (Munich, Germany).

b) Methods

500 000 cells were seeded in 25 cm³ flasks. Cells were then exposed to 0.1% DMSO (vehicle control), and to 1 x 10⁻⁶M 2 ME for 24 h. Cells were washed in PBS three times and scraped off the bottom of the flask. Subsequently, ultrathin sections of cells were prepared to study the two-dimensional structure of cells. Cells were fixed in 2.5% glutaraldehyde in 0.075M phosphate buffer, (pH 7.4-7.6) for 1 h and rinsed 3 times for 5 min each with 0.075M phosphate buffer. Thereafter sections were fixed in 0.25% aqueous osmium tetroxide and rinsed three times in distilled water in a fume hood. Samples were dehydrated in ethanol (70%, 100%), and infiltrated with 30% quetol in acetone or ethanol for 1 h. Samples were infiltrated with 60% quetol in ethanol for 1 h and thereafter with pure quetol for 4 h or longer. Sections were polymerized at 65 °C for 24-36 h. Ultrathin sections were mounted on grids, contrasted for 10 min in 4% aqueous uranyl acetate, and rinsed in water. Enhancement of contrast was obtained by placing the samples in Reynolds' lead citrate for 2 min, and rinsing the samples in water. Thereafter cells were cut into 0.5µm monitor sections stained with toluidine blue and immersed in immersion oil for transmission electron microscopy.

3.2.3 Scanning microscopy (SEM)

a) Materials

DMSO, glutaraldehyde, phosphate buffer, aqueous osmium tetroxide and gold were purchased from Merck Co. (Munich, Germany).

b) Methods

500 000 cells were seeded in 25 cm² flasks and allowed to attach for a day. Cells were exposed to 0.1% DMSO and to 1 x 10⁻⁶ M 2 ME for 24 h. Thereafter cells were washed in PBS three times and scraped off the bottom of the flask. Cells were fixed in 2.5% glutaraldehyde in 0.075M phosphate buffer (pH 7.4-7.6) for 1 h and rinsed three times for 5 min each in 0.075M phosphate buffer. The cells were fixed in 0.25% aqueous osmium tetroxide (in a fume hood) and rinsed three times consecutively in distilled water. Cells were dehydrated in ethanol (70%, 100%) and dried at critical point (when the specific temperature and pressure of a substance is reached the interface between the liquid and the vapour disappears) (78) in liquid CO₂. The cells were then mounted on a stub and sprayed with gold.

3.2.4 Immunofluorescent β -tubulin detection

a) Materials

β -tubulin, formalin, methanol, anti-mouse IgG, Extravidin FITC conjugate were purchased from Sigma Chemical Co. (Munich, Germany).

b) Methods

To visualize the effect of 2 ME on spindle formation in SNO and WHCO3 cells, indirect immunofluorescence was employed. Cells (500 000) were seeded onto heat-sterilized glass coverslips in 6 well plates. Cells were allowed to adhere for 48 h before half-confluent layers were exposed to 2 ME or DMSO controls for a period of 24 h at 37°C. The cells were then fixed in 10% formalin and 2 mM EGTA in PBS for 10 min and permeabilized in ice cold 97% methanol containing 2mM EGTA at -20°C for 10 min. Cells were subsequently washed in PBS (3 x 5 min) before incubation for 1 h with a mouse monoclonal antibody against human β -tubulin (Clone 2-28-33; 1:1000). After washing with PBS, the cells were incubated with biotin-conjugated anti-mouse IgG (Fab-specific, developed in goat) in PBS as secondary antibody for 1 h (1:100). Following washing, cells were finally incubated with Extravidin®-FITC conjugate (1:200 in FITC-conjugate diluent) for 1 h. The coverslips were mounted with a glycerol-based mounting fluid after the final 3 x 5-minute wash step. The cells were examined with a Nikon Optiphot microscope equipped with an episcopic fluorescence attachment and an excitation-emission filter with an average wavelength of 495 nm for FITC.

3.2.5 Cell death type confirmation

a) Materials

Hoechst 33342, propidium iodide were purchased from Sigma Chemical Co. (Munich, Germany).

b) Methods

To study their viability and the presence of apoptotic cells after 2 ME treatment, SNO and WHCO3 cells were seeded onto chamber slides and 500 000 sub-confluent cells were exposed to 1×10^{-6} M of 2 ME for 24 h. The medium was removed and the cells were gently rinsed with PBS. After staining the cells with 0.5 mg/ml Hoechst 33342 (HO) in PBS, the cells were incubated for 20 min at 37 °C followed by an addition of 0.5 mg/ml propidium iodide (PI). Without delay cells were examined under a fluorescence microscope to assess whether they were viable, apoptotic or necrotic and photographs were taken. While all cells take up HO, only cells with intact cell membranes can exclude PI. Cells stained pink with PI are therefore necrotic, while apoptotic cells stain blue, indicating that these cells still have functional cell membranes capable of excluding PI, although they have an aberrant appearance.

3.3 Cell cycle studies

3.3.1 Determining the length of each cell cycle

a) Materials

Thymidine and hydroxyurea were purchased from Sigma Chemical Co. (Munich, Germany).

b) Methods

SNO cells were trypsinized and 5000 cells per well were seeded onto pre-cleaned, sterile coverslips in 6 well culture plates. Sub-confluent cell cultures were supplemented with 2mM hydroxyurea (HU) for 20 h. This procedure allows the cells to enter the S-phase at a normal rate. HU inhibits DNA synthesis by inhibiting the conversion of ribonucleotides to deoxyribonucleotides (79), and thereafter a block in the early S-phase (80).

WHCO3 cells were synchronized using the double thymidine method, as preliminary studies showed that HU is toxic to these cells. Cells were seeded as described above and were supplemented with 2mM thymidine for 18 h. After rinsing with fresh media without thymidine, cells were incubated for 10 h in medium and thereafter exposed again to thymidine for 18 h.

At this stage both cell lines were blocked in early S-phase. To allow the synchronized cell population to continue through the S-phase, medium was changed three times with fresh media (without hydroxyurea or thymidine), incubating the cells for 15

minutes at 37 °C after each change. Duplicate coverslips were fixed at 2-h intervals for up to 24 h after the HU/thymidine-containing medium was removed and at 1-h intervals around the expected mitotic peak. The fixed cells were stained with haematoxylin and eosin (H + E) and their mitotic indices were determined.

3.3.2 Flow cytometry analysis

a) Materials

Propidium iodide was purchased from DAKO Chemical Supplies (San Diego, United States of America).

b) Methods

SNO and WHCO3 cells (500 000) were seeded into 25cm² flasks. Cell cycle analysis were performed after exposure of cells to 1×10^{-6} M of 2 ME at 37°C for 24 h when optimal morphological characteristics associated with apoptosis were observed. Cells were trypsinized in equal volumes of trypsin (0.25%) and EDTA (1mM), fixed in 99.5% methanol and stored at -20°C. Methanol was removed by centrifugation at 200 x g for 10 minutes. The cells were resuspended in 1ml 1% CaCl₂ and 50µg/ml propidium iodide and incubated for 20 minutes while shaking gently. The amount of cells in apoptosis was measured. Each analysis was based on at least 10 000 events employing a Coulter Epic-XS flow cytometer. The data were analyzed using a multicycle analysis program (MulticycleAV software).

3.4 Apoptotic pathway studies/identification

3.4.1 Bcl2 immunohistochemistry

a) Materials

Anti-human Bcl2 antibody was purchased from Sigma Co. (Munich, Germany). DAKO LSAB Kit was purchased from DAKO Corp. (San Diego, United States of America).

b) Methods

Cells (500 000) were seeded onto heat-sterilized glass coverslips in 6 well plates. Cells were allowed to adhere for 48 h before half-confluent layers were exposed to 2 DMSO controls or ME for a period of 24 h at 37°C. The cells were then fixed in 10% formalin (2 mM EGTA in PBS) for 10 min and permeabilized in ice cold 97 % methanol containing 2 mM EGTA at -20°C for 10 min. Cells were subsequently washed in PBS (3 x 5 min) before incubation for 1 h with a mouse monoclonal antibody against human Bcl2. Cells were incubated with prediluted biotinylated antibody for 30 min followed by streptavidin-horseradish peroxidase conjugate for 30 minutes. After washing, peroxidase activity was detected using 3,3'-diaminobenzidine (DAB) as chromagen with H₂O₂ as a substrate. Cells were counterstained with haematoxylin and were mounted with a glycerol-based mounting fluid after the final 3 x 5-minute wash step. The cells were examined with a Nikon Optiphot microscope.

3.4 Death Receptor 5 (DR5) immunocytochemistry

a) Materials

Death Receptor 5 antibody, human anti-goat IgG were purchased from Calbiochem (Oslo, Norway).

b) Methods

Cells (500 000) were seeded onto heat-sterilized glass coverslips in 6 well plates. Cells were allowed to adhere for 48 h before half-confluent layers were exposed to 2 ME or DMSO controls for a period of 16 h at 37°C. The cells were then fixed in 10% formalin and 2 mM EGTA in PBS for 10 min and permeabilized in ice cold 97 % methanol containing 2 mM EGTA at -20°C for 10 min. Cells were subsequently washed in PBS (3 x 5 min) before incubation for 1 h with a mouse monoclonal antibody against human Death Receptor 5 (Clone 2-28-33; 1:1000). After washing with PBS, the cells were incubated with biotin-conjugated anti-mouse IgG (Fab-specific, developed in goat) in PBS as secondary antibody for 1 h (1:100). Following washing, cells were finally incubated with ExtrAvidin®-FITC conjugate (1:200 in Extravidin-FITC conjugate diluent) for 1 h. The coverslips were mounted with a glycerol-based mounting fluid after the final 3 x 5-minute wash step. The cells were examined with a Nikon Optiphot microscope equipped with an episcopic-fluorescence attachment and an excitation-emission filter with an average wavelength of 495 nm for FITC.

Chapter 4

Results

4.1 Concentration-dependent growth studies

Growth studies were conducted to determine whether 2 ME has an antitumor effect on the growth of the SNO and WHCO3 cell lines. 4 different concentrations of 2 ME were used ranging from 1×10^{-6} to 1×10^{-9} M. 5000 cells were seeded per well in 96 well plates and exposed for a period of 72 h. Crystal violet staining was used to determine cell viability.

Figure 9a and figure 9b presented below show that 2 ME reduced cell numbers with **40%** and **60%** in SNO and WHCO3 cells respectively, after exposure to 10^{-6} M 2 ME for 72 h, in both cell lines with a significant *p*-value of < 0.05 . This revealed that 2 ME does reduce cell numbers in the SNO and WHCO3 cell lines. This is consistent with studies in the past decade that have revealed 2 ME as a promising anti-angiogenic and anti-cancer agent (46).

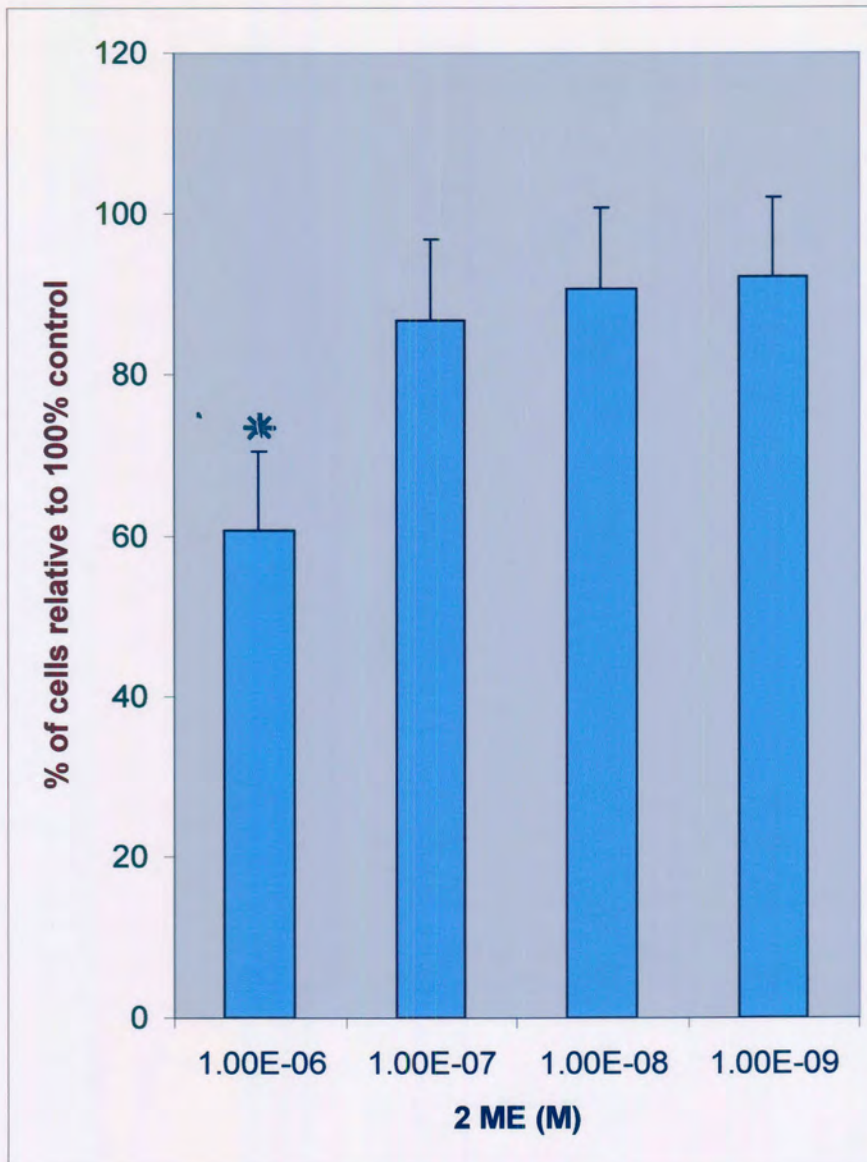


Figure 9a: Graph of SNO cells treated with different concentrations of 2 ME (10^{-6} , 10^{-7} , 10^{-8} , 10^{-9} M) for 72 h. A 40% decrease in cell number was noted at concentration 10^{-6} M of 2 ME. * indicates a p -value < 0.05 .

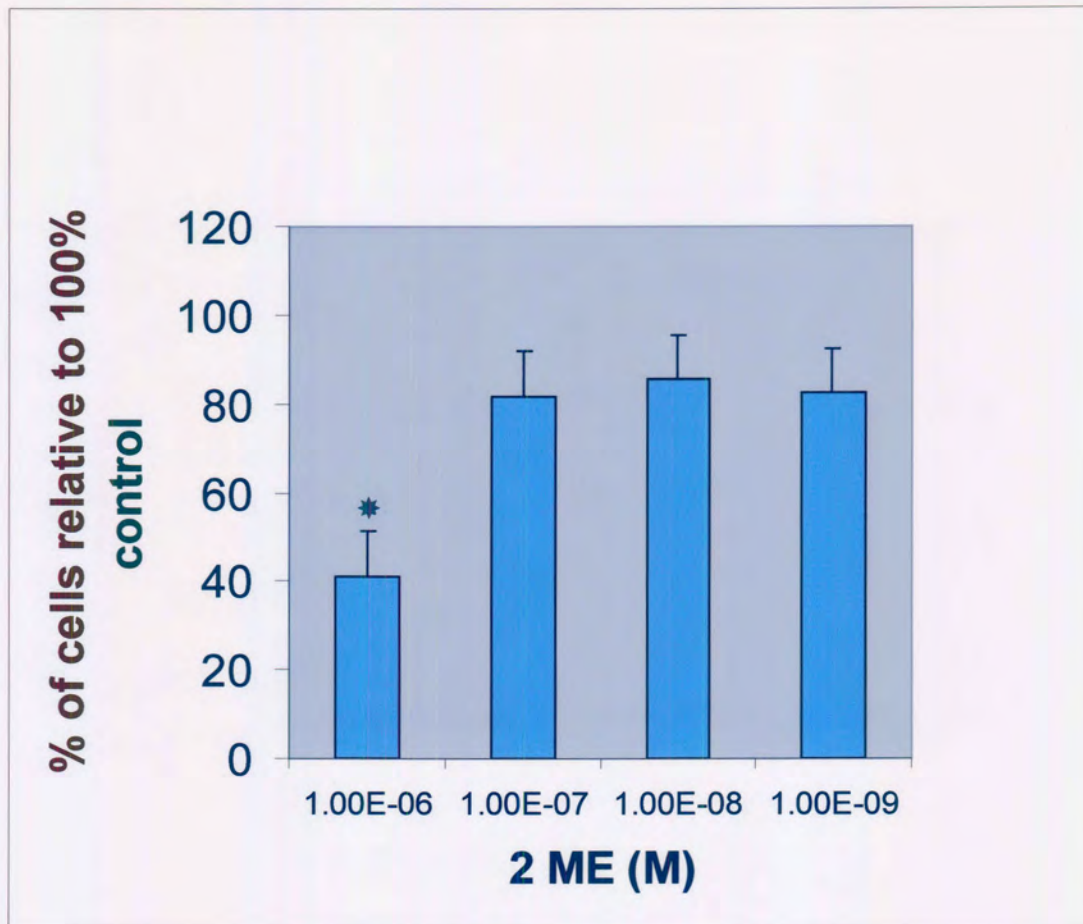


Figure 9b: Graph of WHCO3 cells treated with different concentrations of 2 ME 10^{-6} , 10^{-7} , 10^{-8} , 10^{-9} M for 72 h. A 60% decrease in cell number was noted at concentration 10^{-6} M of 2 ME. * indicates a p -value < 0.05 .

4.2 Morphology Studies

4.2.1 Light microscopy

The anti-proliferative effect of 2 ME observed in the growth studies could be due to either growth inhibition (cytostatic effect) or induction of cell death. Morphological characteristics of cytoplasm and nuclear components of the cells treated with 2 ME were studied in haematoxylin and eosin stained cells, to find an indication of the cause of 2 ME's anti-mitogenic effect.

Our observations revealed that cells were rounded and shrunken in appearance after treatment with 2 ME for 24 h. Morphological characteristics of apoptosis, including nuclear membrane blebbing, condensed chromatin and cell membrane budding with intact cell membranes were observed in 2 ME exposed cells and are shown in the figure 10b and figure 11b. These results indicated apoptosis as the form of cell death induced by 2 ME in OC cells. In various other tumor cell lines studied, the anti-proliferative activity of 2 ME was also found to arise mainly from triggering of apoptosis (44,81,82).

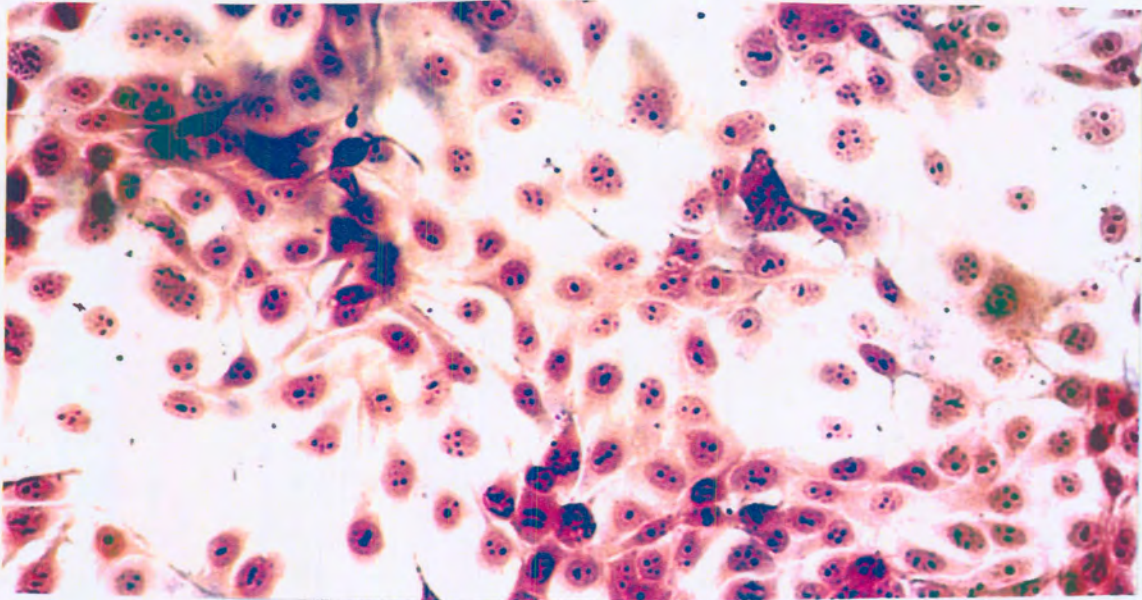


Figure 10a: Haematoxylin and Eosin staining of SNO control cells exposed to 0.1% DMSO (vehicle) for 24 h. A dense population of spindle-shaped cells is observed (X 10 magnification).

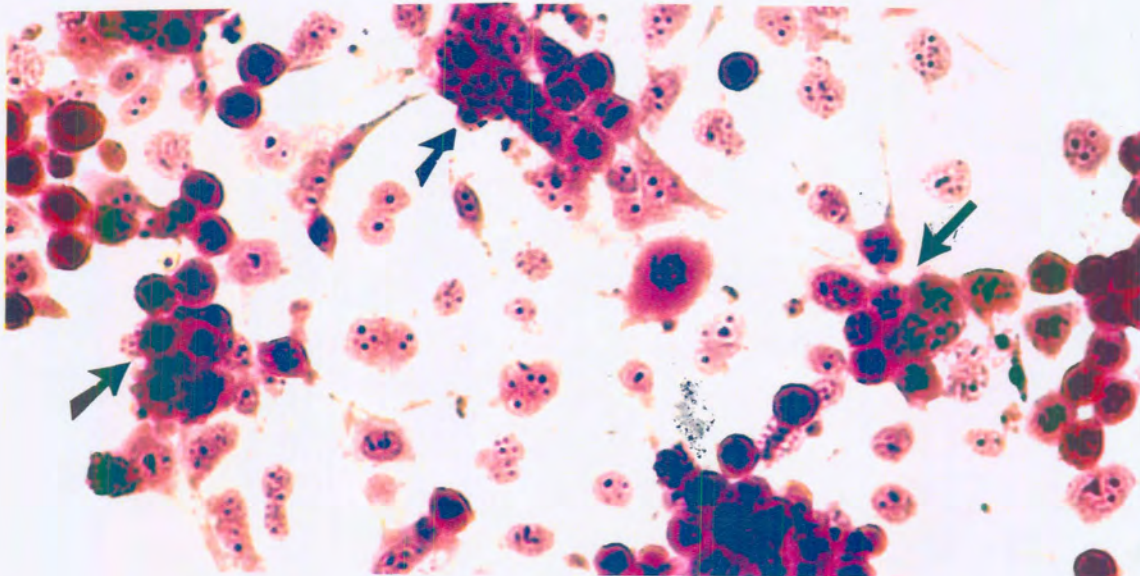


Figure 10b: Haematoxylin and Eosin staining of SNO cells exposed to 1×10^{-6} M 2 ME for 24 h. Arrows indicate clusters of rounded cells and clumping of cells. The field is also less densely populated (X 10 magnification).



Figure 11a: Haematoxylin and Eosin staining of WHCO3 control cells exposed to 0.1% DMSO (vehicle) for 24 h. Cell membranes are intact. Cells are spindle-shaped. No membrane blebbing is visible.

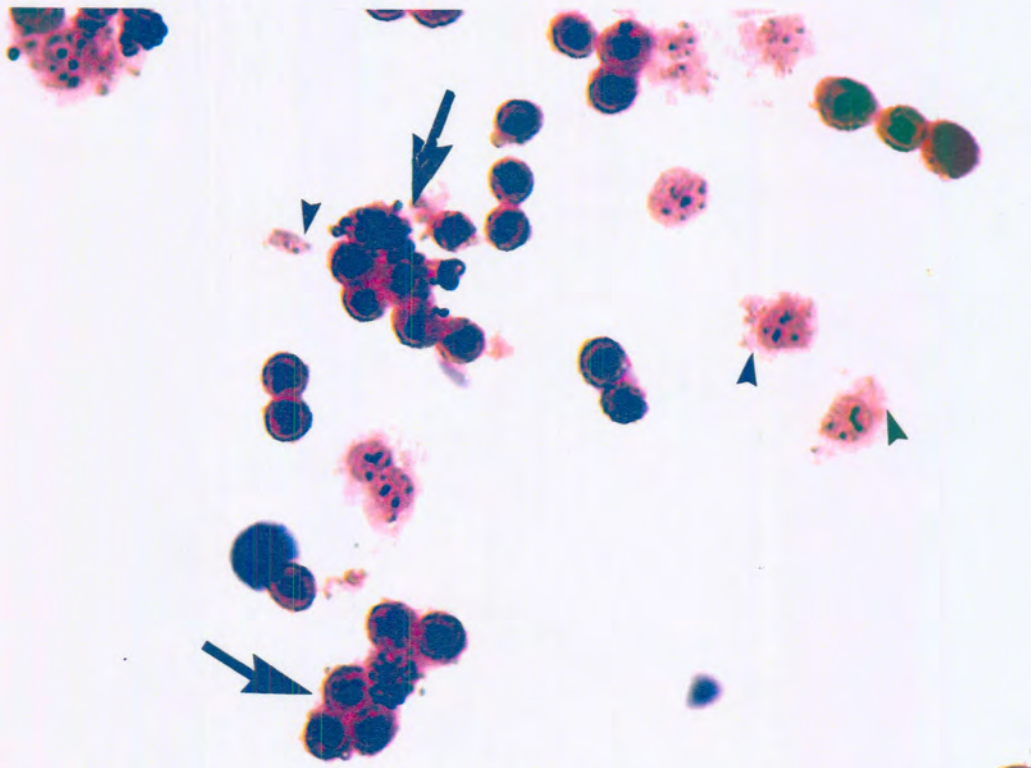


Figure 11b: Haematoxylin and Eosin staining of WHCO3 cells exposed to 1×10^{-6} M 2 ME for 24 h. Arrows indicate clumps of rounded cells with condensed content. Arrowheads indicate degraded cytoplasm. Cells visibly shrink (this is an early apoptotic feature) (X 10 magnification).

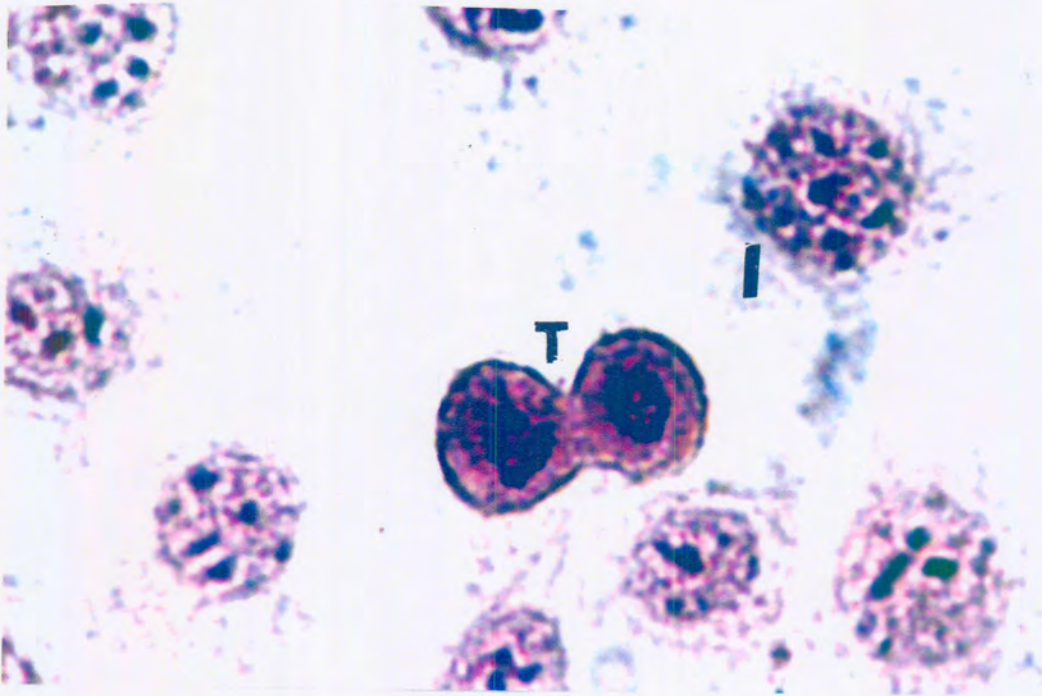


Figure 12a: Haematoxylin and Eosin staining of SNO control cells exposed to 0.1% DMSO (vehicle) for 24 h. Cells in interphase (I) and telophase (T) with intact cell and nuclear membranes are observed (X 40 magnification).

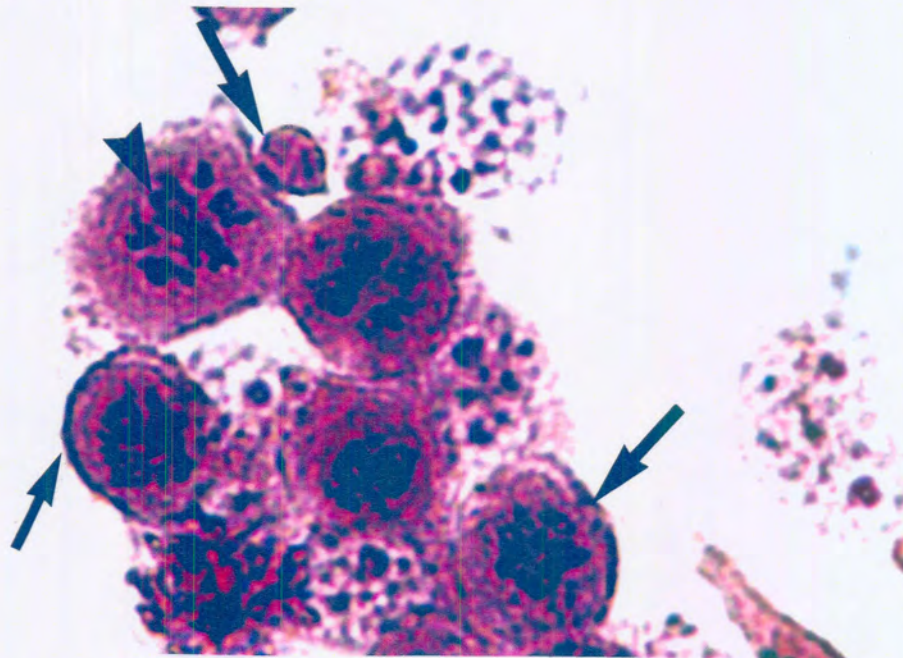


Figure 12b: Haematoxylin and Eosin staining of SNO cells exposed to 1×10^{-6} M 2 ME for 24 h. Clusters of rounded cells show condensed chromatin (arrows) and nuclear and cell membrane blebbing. Abnormal chromosome distribution (arrowhead) is noted as well as budding off of apoptotic bodies (X 40 magnification).

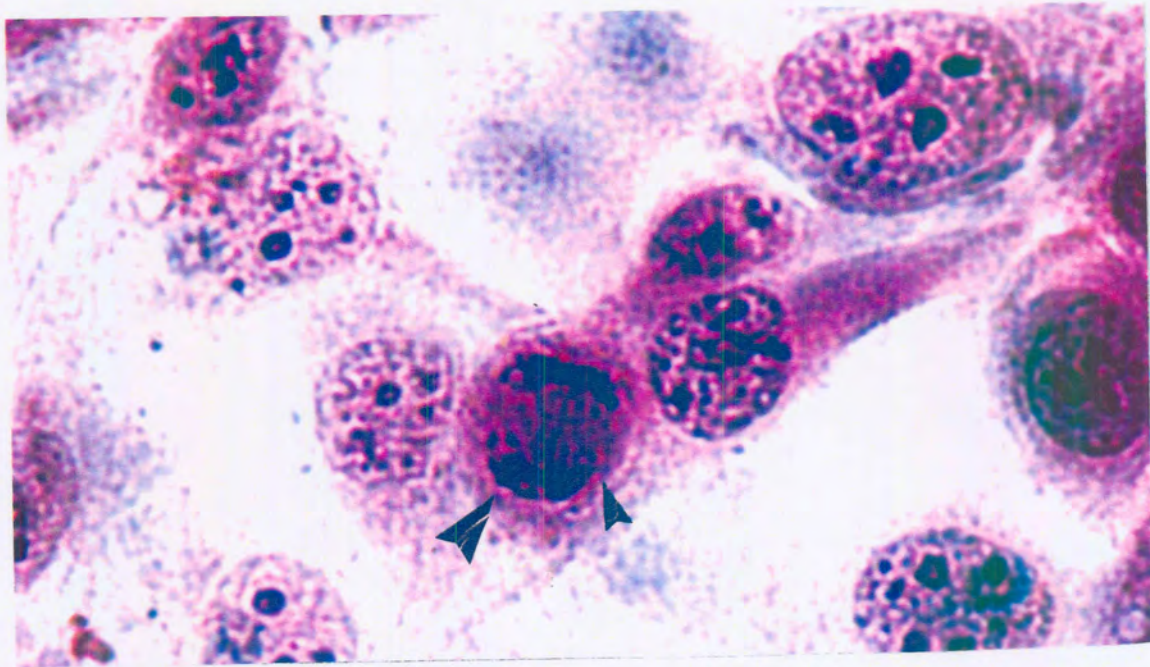


Figure 13a: Haematoxylin and Eosin staining of WHCO3 control cells exposed to 0.1% DMSO (vehicle) for 24 h. Arrowheads indicate a normal anaphase cell. Cells are adherent to each other (X 40 magnification).

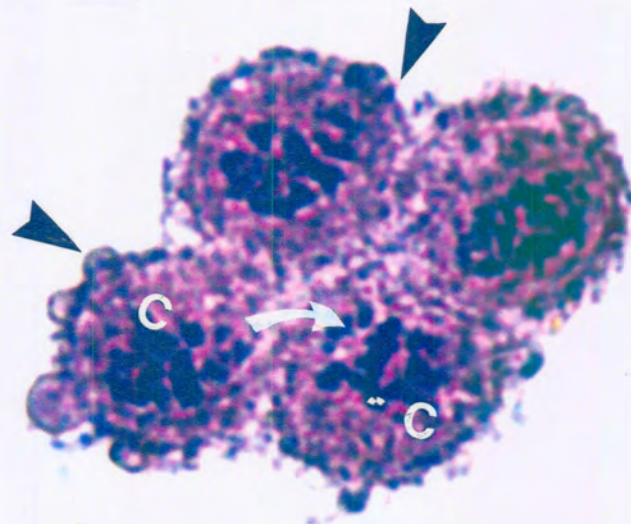


Figure 13b: Haematoxylin and Eosin staining of WHCO3 cells exposed to 1×10^{-6} M 2 ME for 24 h. Arrowheads indicate a sparse population of rounded cells blocked in metaphase, showing nuclear membrane blebbing (arrow) and chromatin condenses and becomes granular and convoluted (C), not present in the controls (X 40 magnification).

4.2.2 Transmission electron microscopy (TEM)

TEM was employed to view sub-cellular structures in two dimensions. Figure 14a showed that SNO control cells had an intact nucleolus in contrast to SNO and WHCO3 cells treated with 2 ME that showed homogenous condensed chromatin, irregular nuclear membrane and increased mitochondrial aggregation toward the nucleus. Chromatin condensation is a feature of cells undergoing apoptosis. However, treated cells showed irregular nuclear membranes (figure 14b and figure 15b). Control cells had evident smooth nuclear membranes.

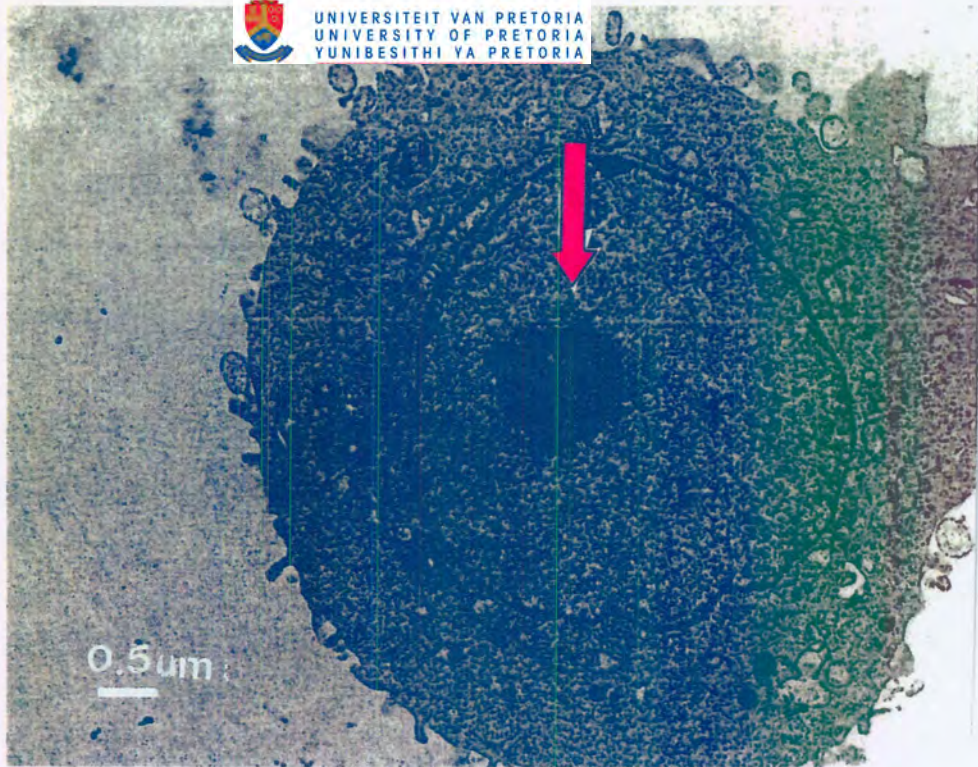


Figure 14a: Transmission electron microscopy of SNO control cells exposed to 0.1% DMSO (vehicle) for 24 h. Arrow indicates the nucleolus.

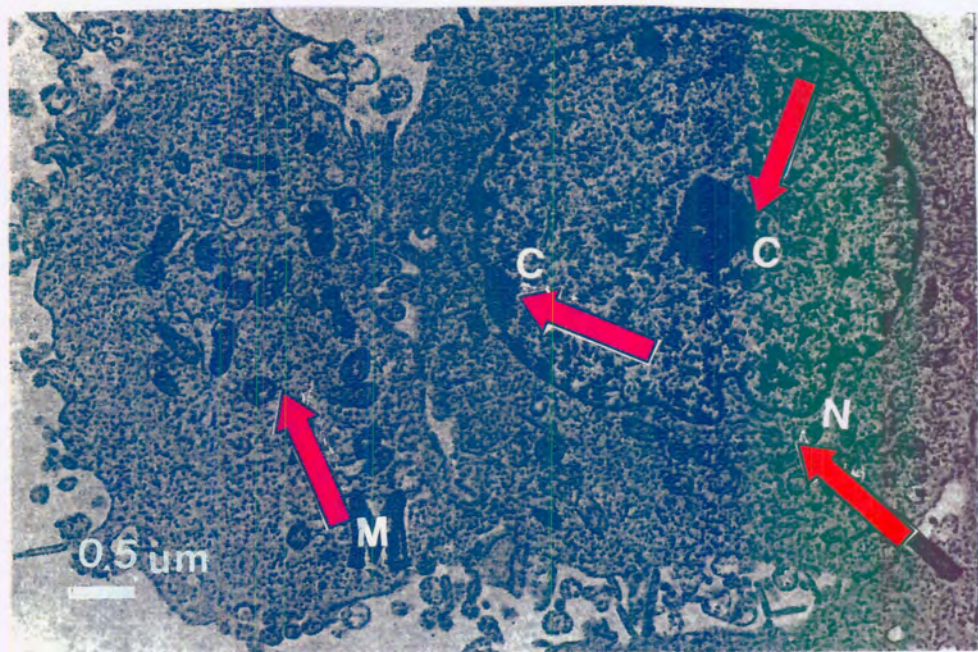


Figure 14b: Transmission electron microscopy of SNO cells exposed to 1×10^{-6} M 2 ME for 24 h. Arrows indicate darker areas of condensed chromatin (pyknotic) (C), chromatin forms aggregates near the nuclear membrane, irregular nuclear membrane (N) and increased mitochondrial aggregation (M). Internal organelles such as mitochondria still remain intact.

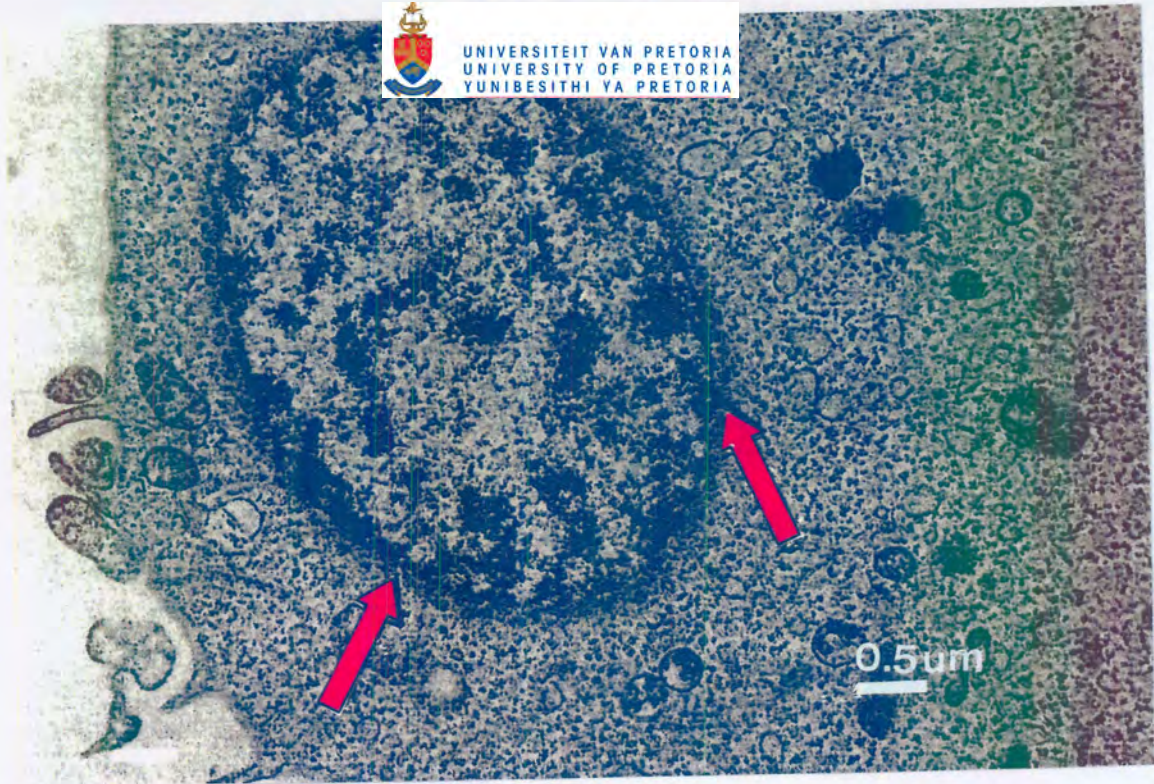


Figure 15a: Transmission electron microscopy of WHCO3 control cells exposed to 0.1% DMSO (vehicle) for 24 h. Arrows indicate a rounded intact nuclear membrane.

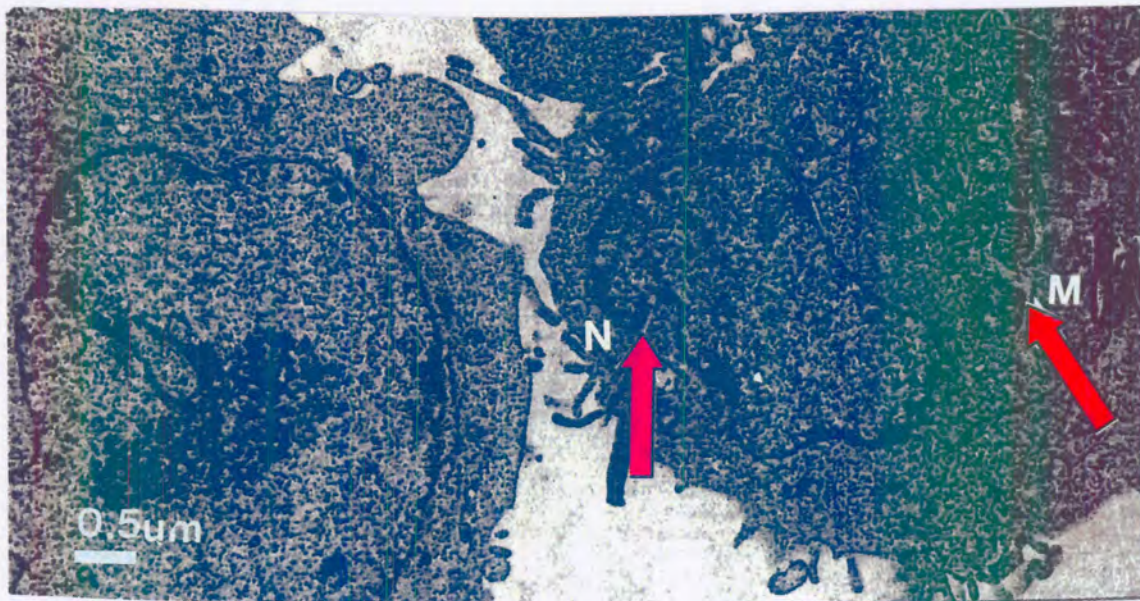


Figure 15b: Transmission electron microscopy of WHCO3 cells exposed to 1×10^{-6} M 2 ME for 24h. Arrows indicate an irregular nuclear membrane (N) and increased mitochondrial aggregation (M). Organelles within the shrunken apoptotic cytoplasm retain a largely normal appearance.

4.2.3 Scanning electron microscopy (SEM)

SEM was used to view the surface of the SNO and WHCO₃ cells in a three dimensional view. SEM revealed increased membrane blebbing as compared to control cells. This could possibly be early morphological features of apoptosis, after treatment with 2 ME. It could also be due to phosphatidyl serine that relocates from the inner to the outer membrane of the cell to enhance cell death (the flip of phosphatidyl serine from the inner membrane of the cell to the outer membrane of the cell is used as a marker for apoptosis). The surface of the treated cells also appeared rough and stringy in the WHCO₃ cell line as shown in figure 17b.

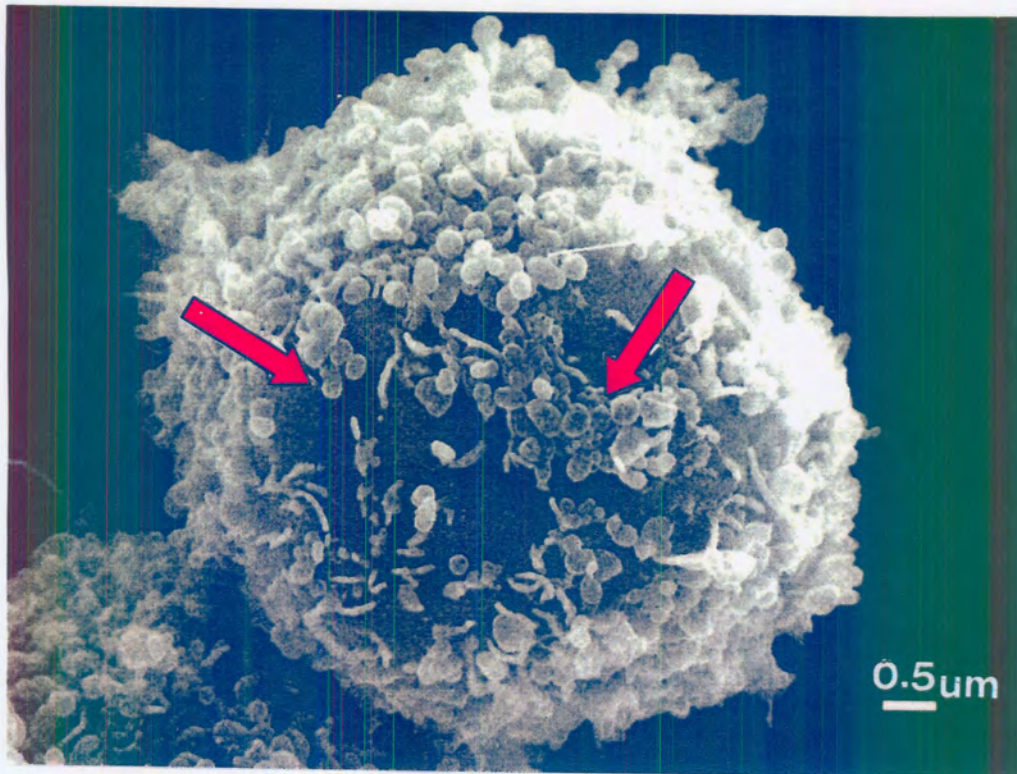


Figure 16a: Scanning electron microscopy of SNO control cells exposed to 0.1% DMSO (vehicle) for 24 h. Arrows indicate smooth cell surface.

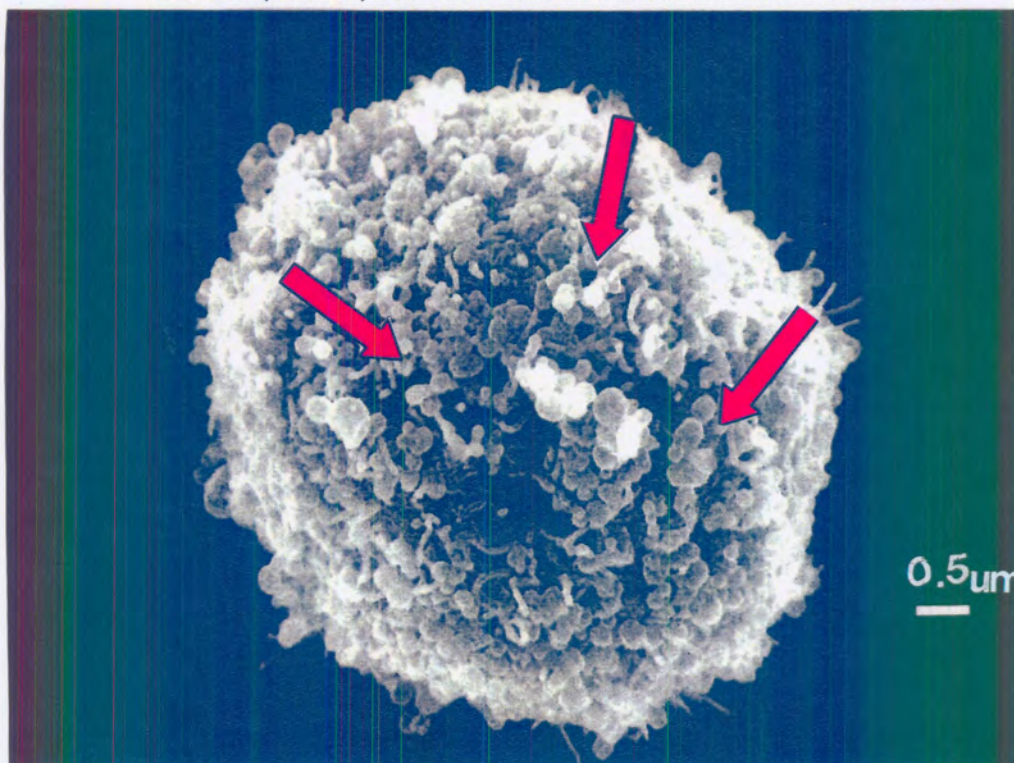


Figure 16b: Scanning electron microscopy of SNO cells exposed to 1×10^{-6} M ME for 24 h. Distinct protuberances or membrane blebs become discernable (arrows).

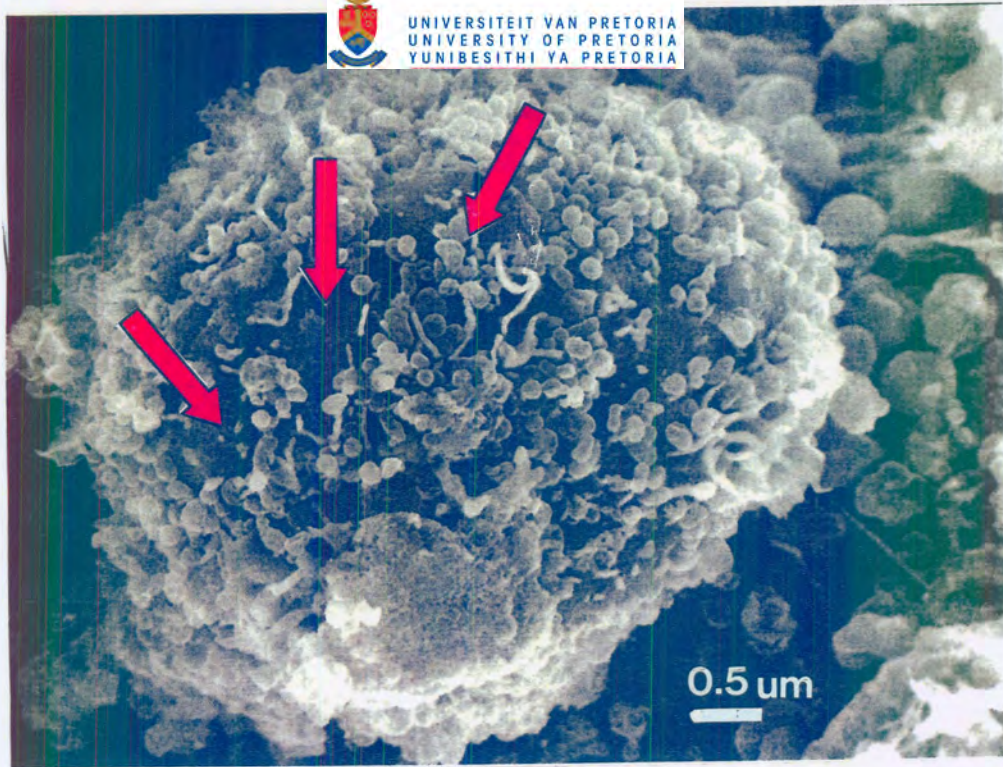


Figure 17a: Scanning electron microscopy of WHCO3 control cells exposed to 0.1% DMSO (vehicle) for 24 h. Arrows indicate the rounded surface of the cell.

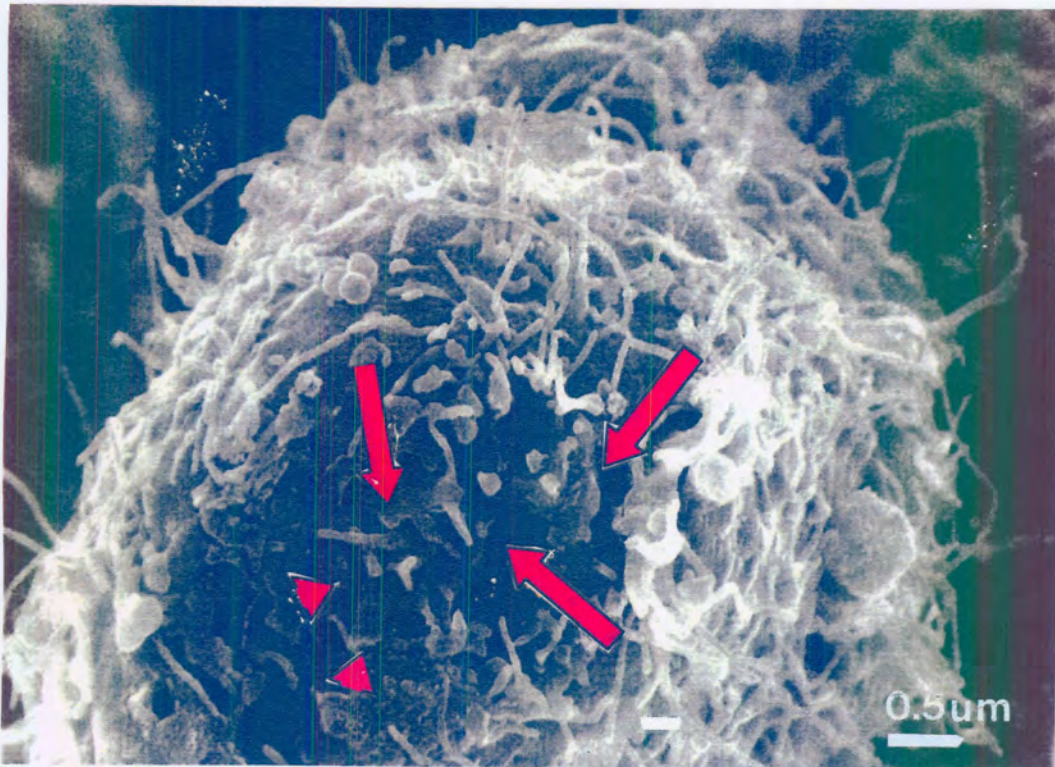


Figure 17b: Scanning electron microscopy of WHCO3 cells exposed to 1×10^{-6} M 2 ME for 24 h reveal a cell surface with a very different appearance as that of the control. Arrows shows the irregular surface of the cell. Note the increased blebbing of the cell membrane and cell shrinkage (arrowheads).

4.2.4 Immunofluorescent β -tubulin detection

Before investigating new action mechanisms for 2 ME's induction of apoptosis, the well-established mechanism of tubulin disruption had to be confirmed in the OC cells. Tubulin has been identified as a molecular target in the pursuit to unravel the mechanism of action of 2 ME (39,83). Previous research has shown that 2 ME induces cell death by causing microtubule disruption and blocking cells in metaphase. These cells cannot proceed through the cell cycle, thereby resulting in cell death via apoptosis. Therefore immunofluorescent staining of β -tubulin was included in this study.

Figure 18b and figure 19b showed that the cells treated with 2 ME were rounded, accumulated in the metaphase and thus could not progress through the cell cycle. Cells also showed spindle disruption with fragmented polar formations. This confirmed that 2 ME does act by causing microtubule disruption in both cells lines as indicated by the photographs below.

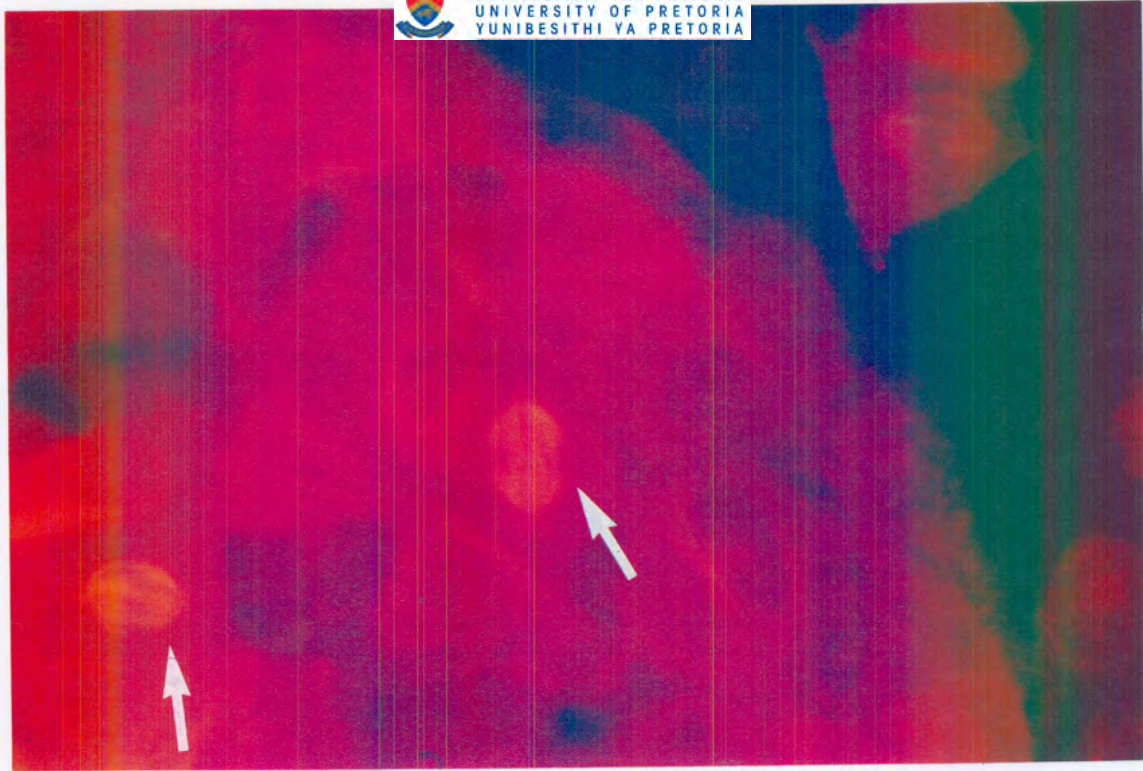


Figure 18a: β -Tubulin detection of SNO control cells exposed to 0.1% DMSO (vehicle) for 24 h. Arrows indicate normal spindle formation as cells proceed through the cell cycle.

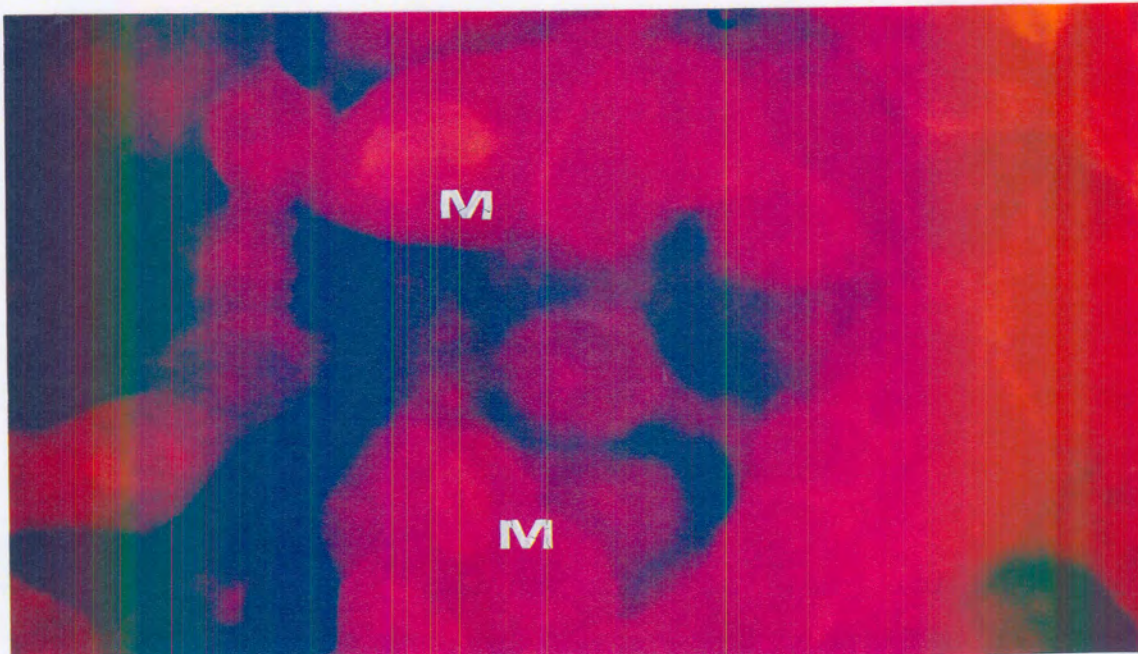


Figure 18b: β -Tubulin detection of SNO cells exposed to 1×10^{-6} M 2 ME for 24 h. (M) indicates cells in metaphase.

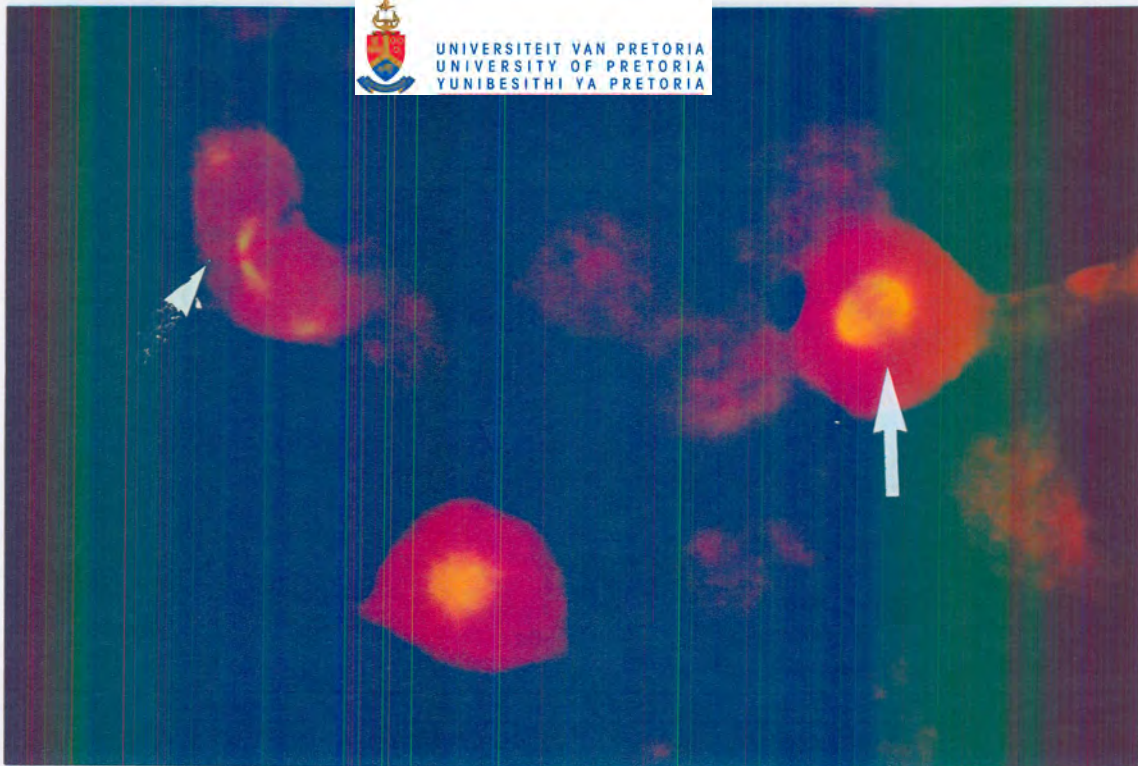


Figure 19a: β -Tubulin detection of WHCO3 control cells exposed to 0.1% DMSO (vehicle) for 24 h. Normal spindle formation during metaphase (arrow) as well as during telophase (arrowhead) can be seen as cells proceeded through the cell cycle.

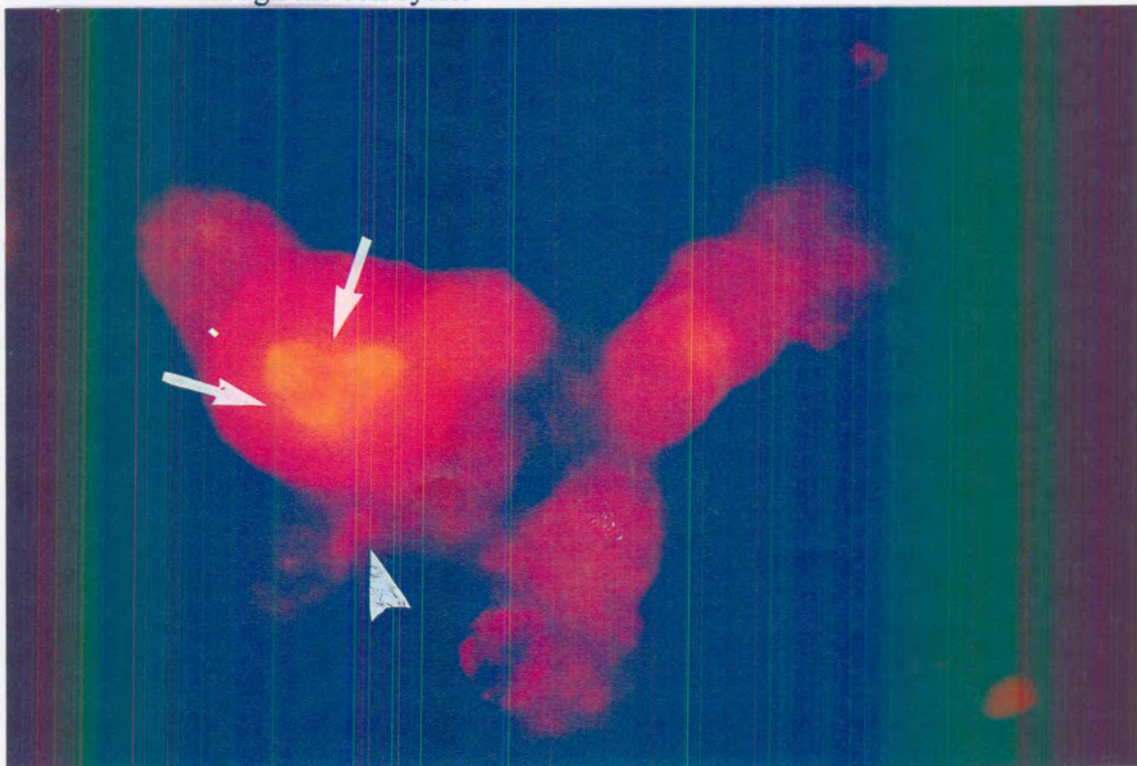


Figure 19b: β -Tubulin detection of WHCO3 cells exposed to 1×10^{-6} M 2 ME for 24 h. Arrows show spindle disruption with fragmented tripolar formations. Membrane blebs become visible (arrowhead).

4.2.5 Cell death type confirmation

To differentiate between apoptosis and necrosis, and to further confirm that the morphological characteristics observed in 2 ME-treated cells were indeed those of apoptosis, PI and HO staining were conducted to confirm the presence of apoptotic cells after treatment with 2 ME. Viable cells and cells that are undergoing apoptosis have intact cell membranes and can only take up the blue Hoechst stain (Hoechst 33342 can penetrate the intact plasma membrane without permeabilization), while cells that are necrotic have lost their membrane integrity and can take up the propidium iodide stain. Co-staining of cells with PI and HO allows discrimination of “necrotic” from apoptotic cells. After 2 ME treatment most nuclear membranes of the cells were rounded in appearance due to a metaphase block and showed apoptotic features like nuclear membrane blebbing (figure 20b and figure 21b). They stained blue, indicating an intact nuclear membrane, which is a feature of apoptosis.

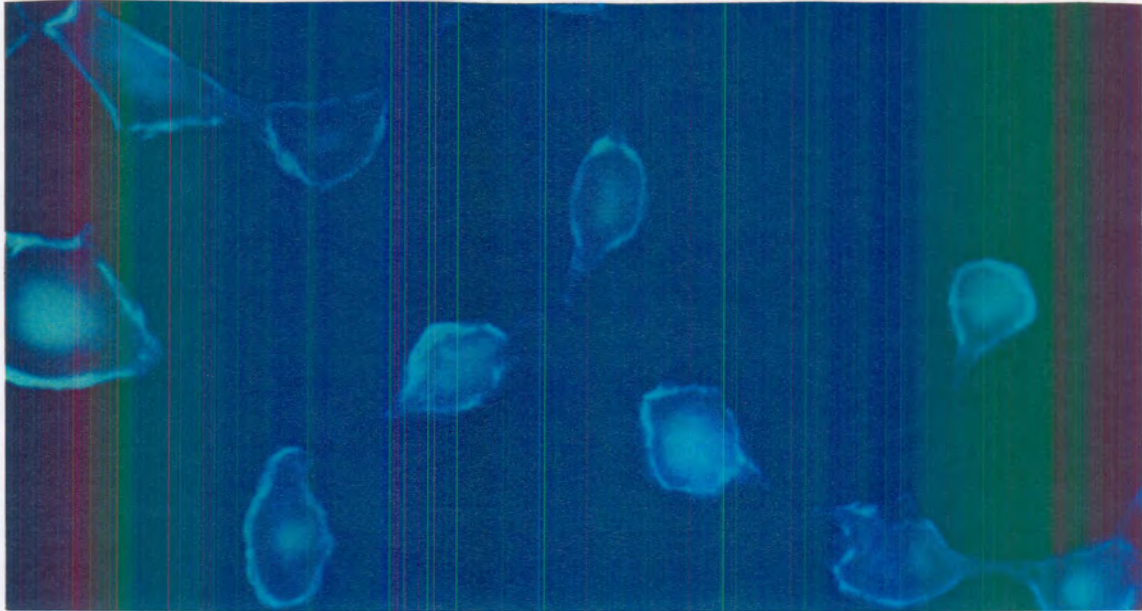


Figure 20a: Propidium iodide and Hoechst staining of SNO control cells exposed to 0.1% DMSO (vehicle) for 24 h. Nuclear membranes are intact. No nuclear membrane blebbing is visible.

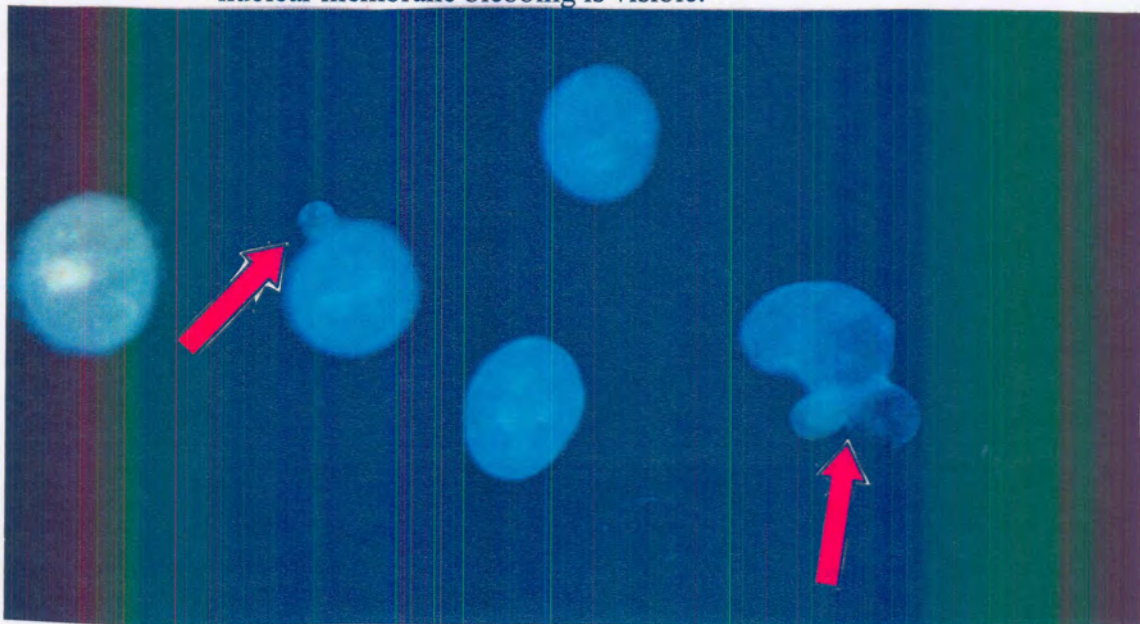


Figure 20b: Propidium iodide and Hoechst staining of SNO cells exposed to 1×10^{-6} M 2 ME for 24 h. Nuclear membrane integrity is compromised. Arrows show nuclear membrane blebbing in cells undergoing apoptosis.

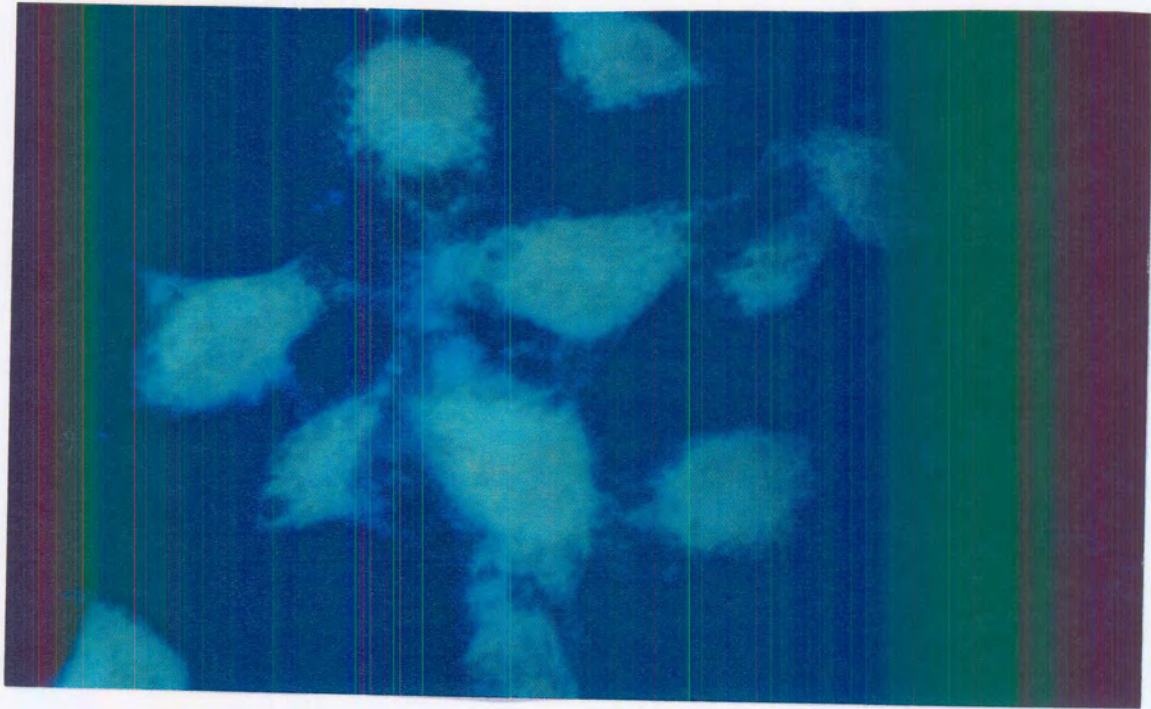


Figure 21a: Propidium iodide and Hoechst staining of WHCO3 control cells exposed to 0.1% DMSO (vehicle) for 24 h.

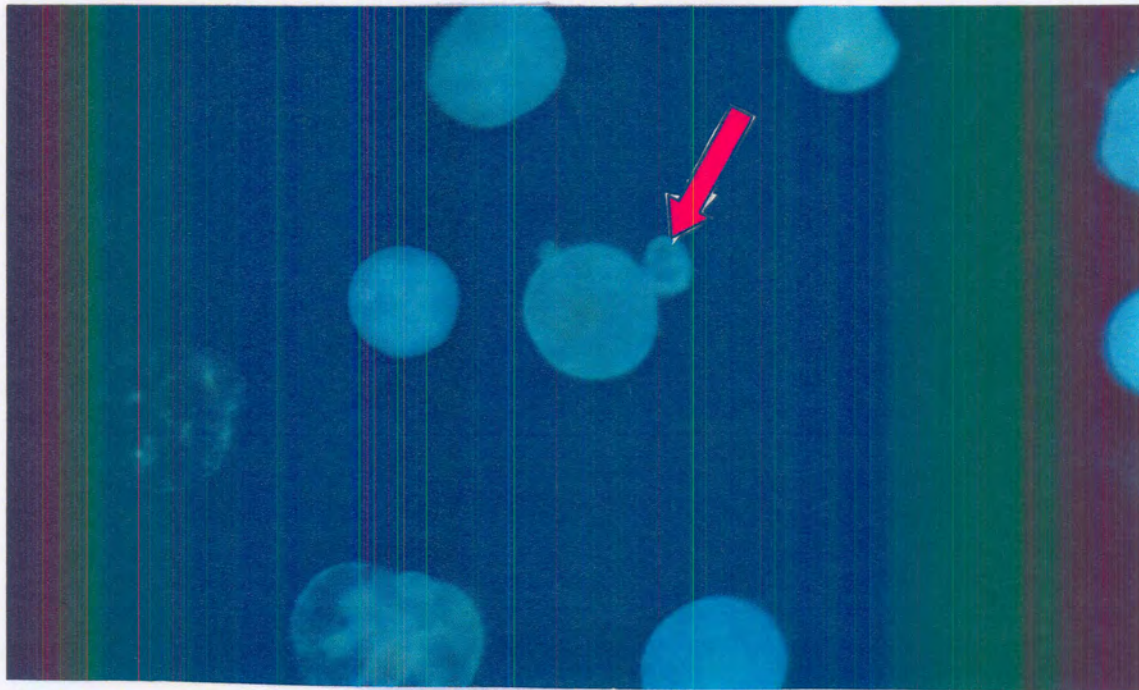


Figure 21b: Propidium iodide and Hoechst staining of WHCO3 cells exposed to 1×10^{-6} M 2 ME for 24 h. Arrow shows nuclear membrane blebbing in cells undergoing apoptosis.

4.3 Cell cycle studies

4.3.1 Cell cycle length

Synchronized cell lines were monitored at 2-h intervals over a period of 24 h, to determine the cell cycle length and thereby determining the hour at which peak mitosis occurred. Cells were stained at 2-h intervals. Mitotic indices were determined using a light microscope to determine the hour at which peak mitosis occurs. Peak mitosis occurred at 12 h in both cell lines (figure 22a and figure 22b).

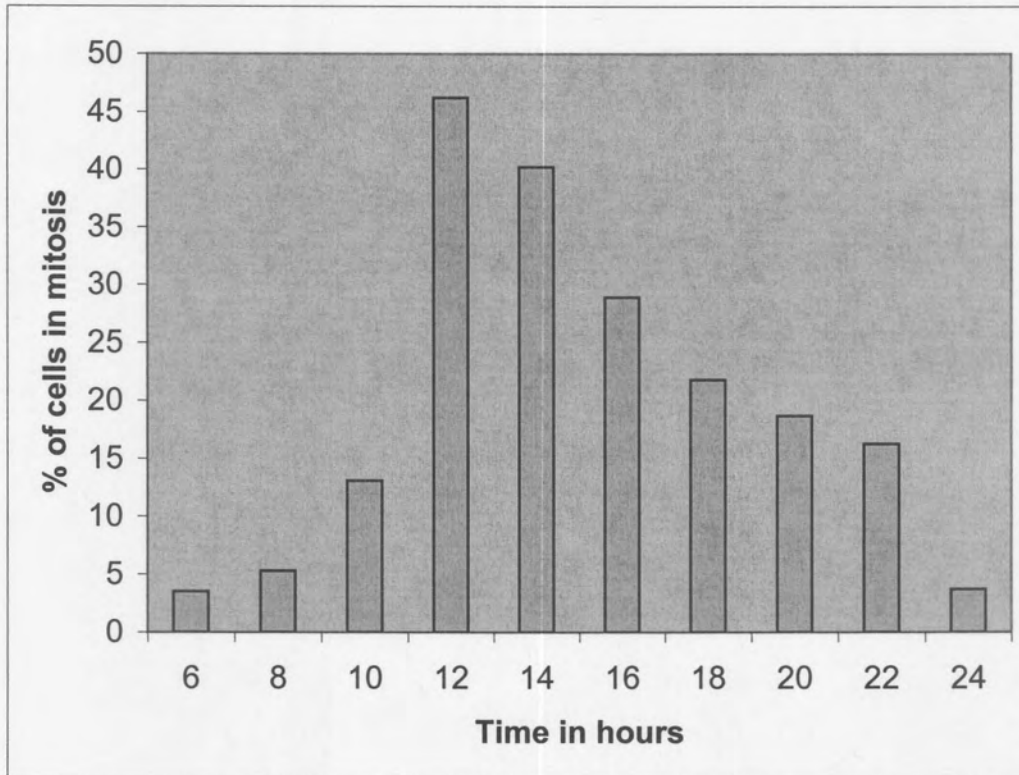


Figure 22a: Percentage of synchronized SNO cells in mitosis at 2-h intervals. Peak amount of cells in mitosis occurred at 12 h.

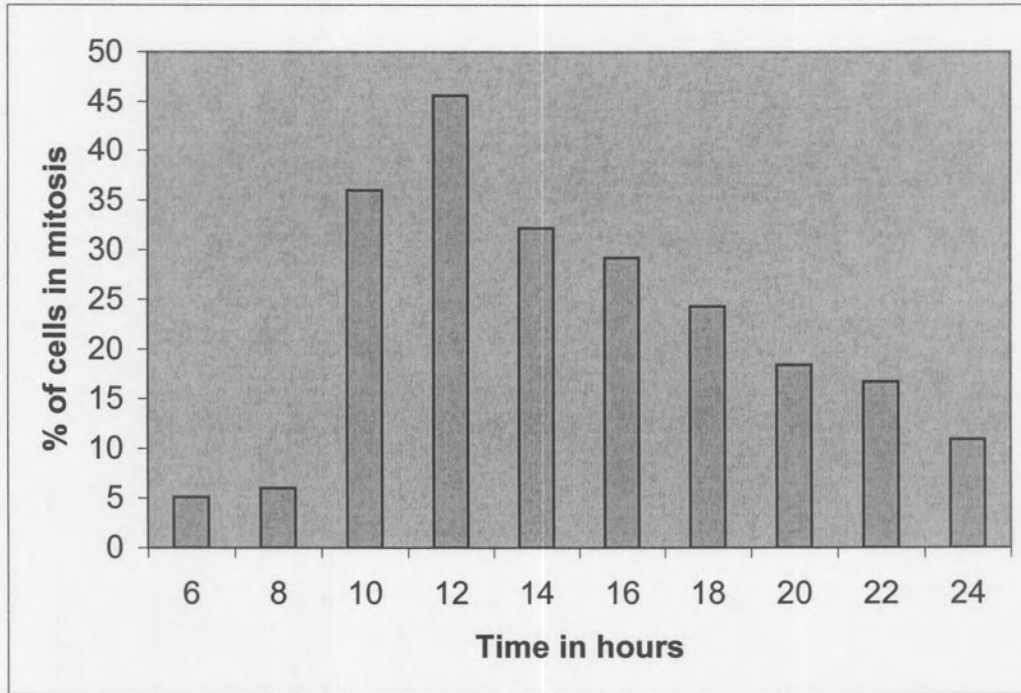


Figure 22b: Percentage of synchronized WHCO3 cells in mitosis at 2-h intervals.

Peak amount of cells in mitosis occurred at 12 h.

4.3.2 Flow cytometry analysis

The distribution of cells proceeding through the cell cycle phases after exposure to 10^{-6} M 2 ME was investigated by means of flow cytometry. Cells treated with 2 ME showed a higher sub G1/G0 peak that is indicative of apoptosis. Flow cytometry revealed that peak apoptosis occurred after 24 h of exposure to 2 ME in SNO cells and WHCO3 cells as shown in figure 23a and figure 23b. Subsequently, we attempted to investigate whether 2 ME-induced apoptosis via the intrinsic or extrinsic pathway.

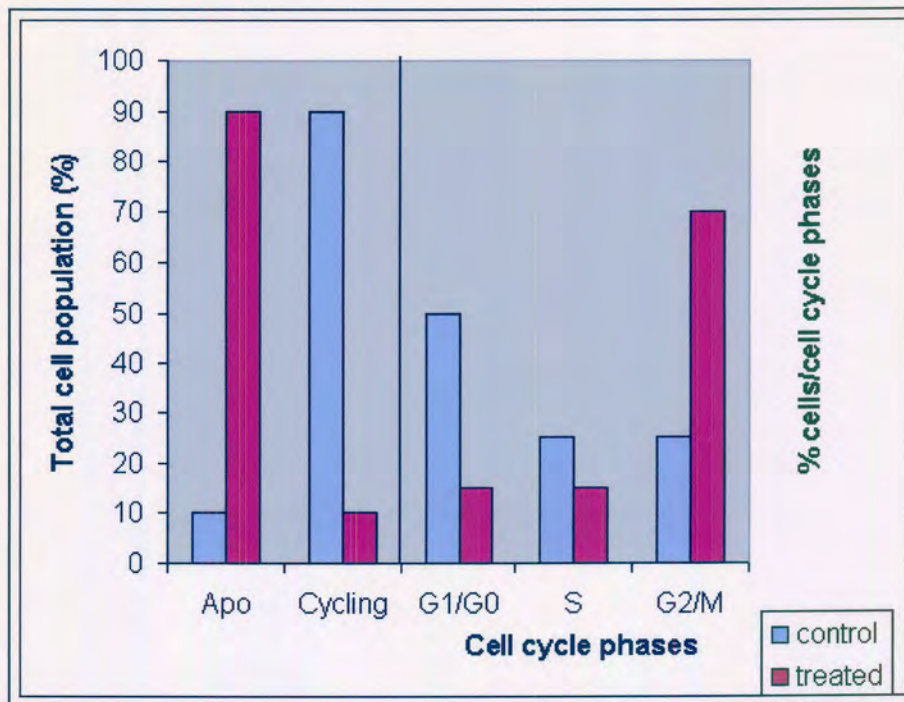


Figure 23a: Flow cytometric analysis of the effects of 24 h exposure to 10^{-6} M 2 ME on cell cycle and apoptosis induction in SNO cells. Percentages of apoptotic cells, including all the events below the G_0/G_1 peak, designated as “apo” and cycling cells are shown in the first panel and percentages of each cell cycle phase are shown in panel 2. In the SNO cells there was a significant difference in the number of apoptotic cells and the number of cycling cells between the control and 2 ME-treated cells. In the treated cells increased apoptotic induction and a subsequent decrease in cycling cells were evident. Decreases were present in the G_1/G_0 and S-phase and an increase was noted in G2/M-phase.

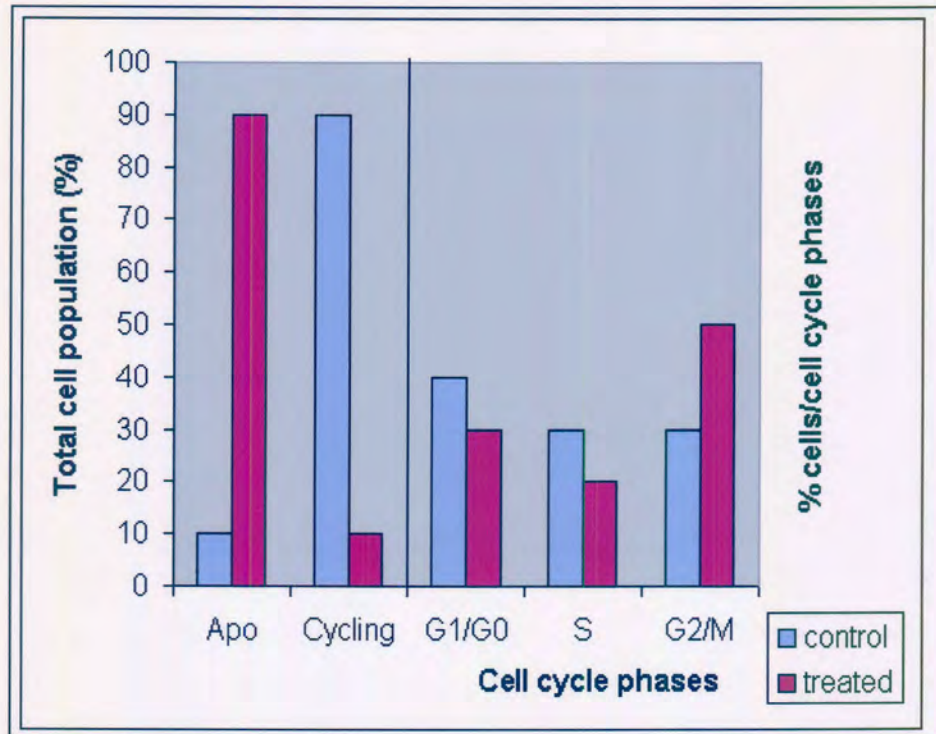


Figure 23b: Flow cytometric analysis of the effects of 24 h exposure to 10^{-6} M dose of 2 ME on cell cycle and apoptosis induction in WHCO3 cells. Percentages of apoptotic cells, including all the events below the G_0/G_1 peak, designated as “apo” and cycling cells are shown in the first panel and percentages of each cell cycle phase are shown in panel 2. In the WHCO3 cells there was a significant difference in the number of apoptotic cells and the number of cycling cells between the control and 2 ME-treated cells. In the treated cells an increase in the “apo” fraction and a decrease in cycling cells were evident. Decreases were present in the G_1/G_0 - and S-phase and an increase was noted in G2/M-phase.

4.4 Apoptotic pathway studies/identification

4.4.1 B-cell lymphoma 2

Having established that 2 ME exerts its anti-proliferative effects by inducing apoptosis, the question remains as to which induction pathway is followed. Since changes have been observed in mitochondrial distribution after 2 ME treatment in the SNO and WHCO3 cell lines (SEM), and since mitochondria play a role in the intrinsic pathway, Bcl2 was chosen as a marker. The Bcl2 family associates with the outer membrane of the mitochondria and consists of both inhibitors and promoters of apoptosis. Initiation of apoptosis requires the activation of pro-apoptotic members of the Bcl2 family. During apoptosis, pro-apoptotic members of the Bcl2 family oligomerize in the mitochondrial outer membrane and this causes a breach in the mitochondrial membrane integrity. This causes pro-apoptotic proteins such as Cyt c to be released, which allows activation of caspase 9 and this initiates apoptosis (84). Bcl2 immunolabeling indicated that the intrinsic or mitochondrial pathway is probably not involved in 2 ME apoptosis induction since it was up-regulated in the treated cells (figure 24a and figure 25a).

In erythromyeloid K 562 cells, 2 ME treatment can trigger Bcl2 phosphorylation (85). This was similar to the action of other microtubule inhibitors and this supported our notion that 2 ME does not trigger apoptosis via the intrinsic pathway.

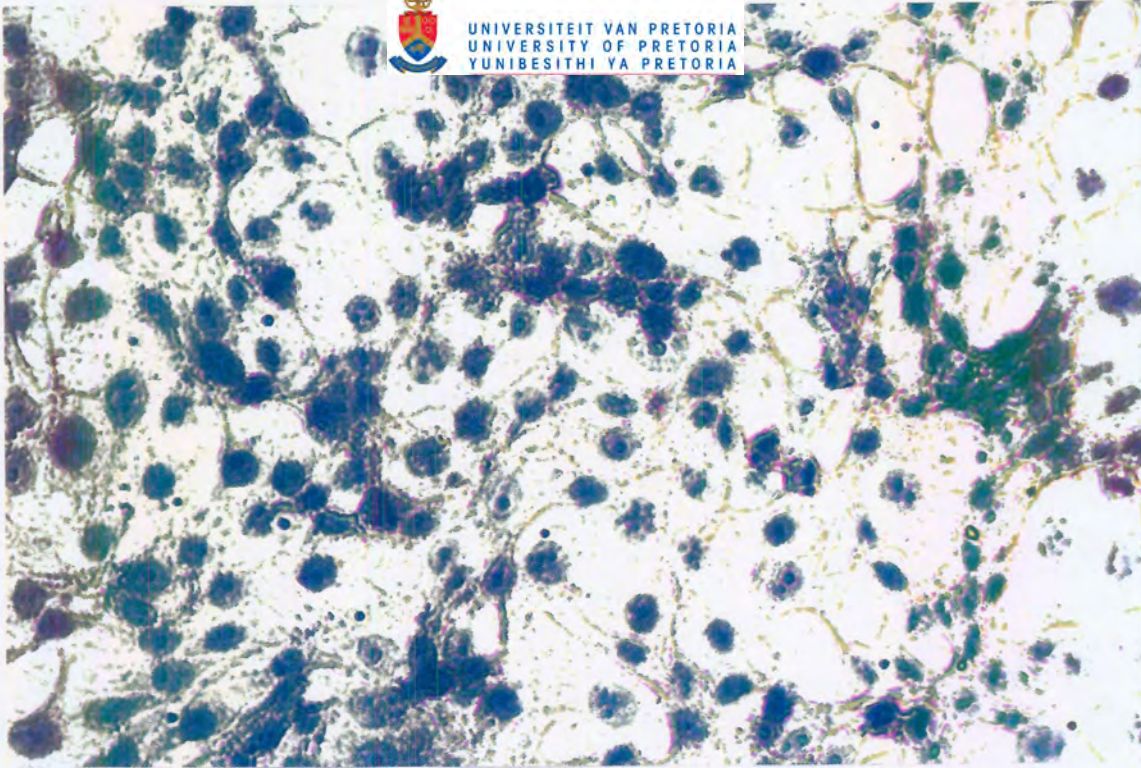


Figure 24a: Bcl2 immunocytochemistry of SNO control cells exposed to 0.1% DMSO (vehicle) for 24 h. Cells remain unstained due to no substrate reaction with DAB.

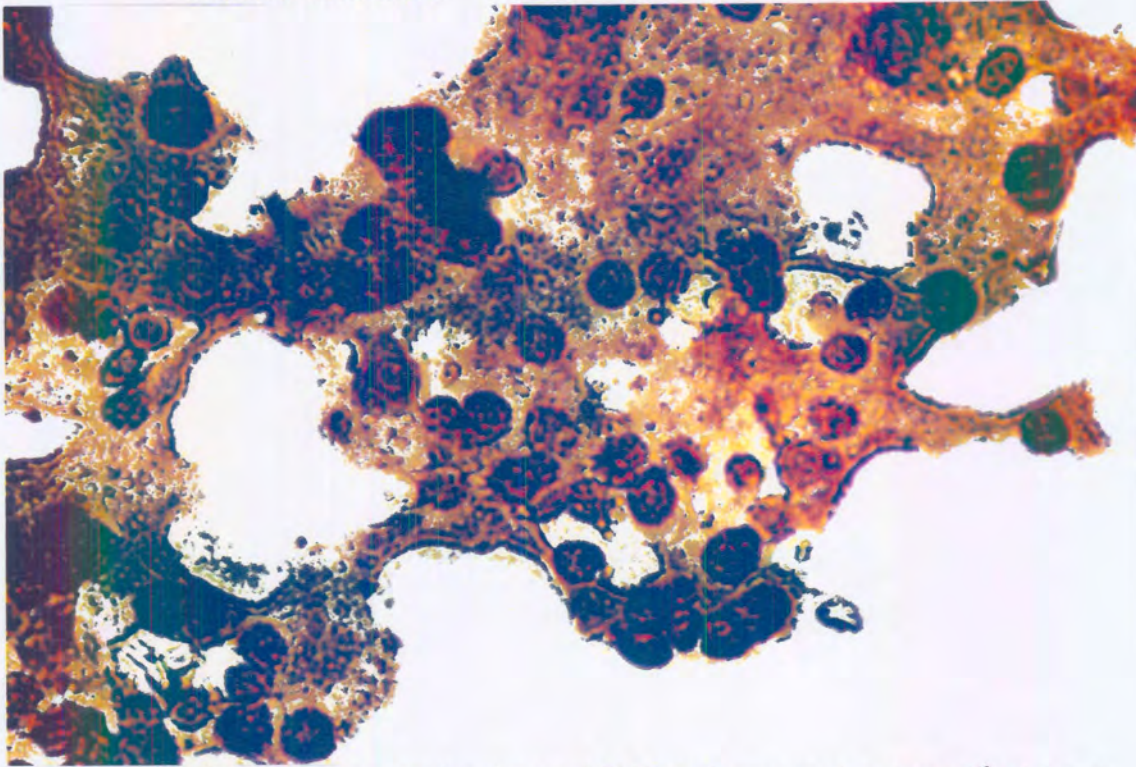


Figure 24b: Bcl2 immunocytochemistry of SNO cells exposed to 1×10^{-6} M 2 ME for 24 h. Cells appearing brown in color, indicating expression/presence of Bcl2.

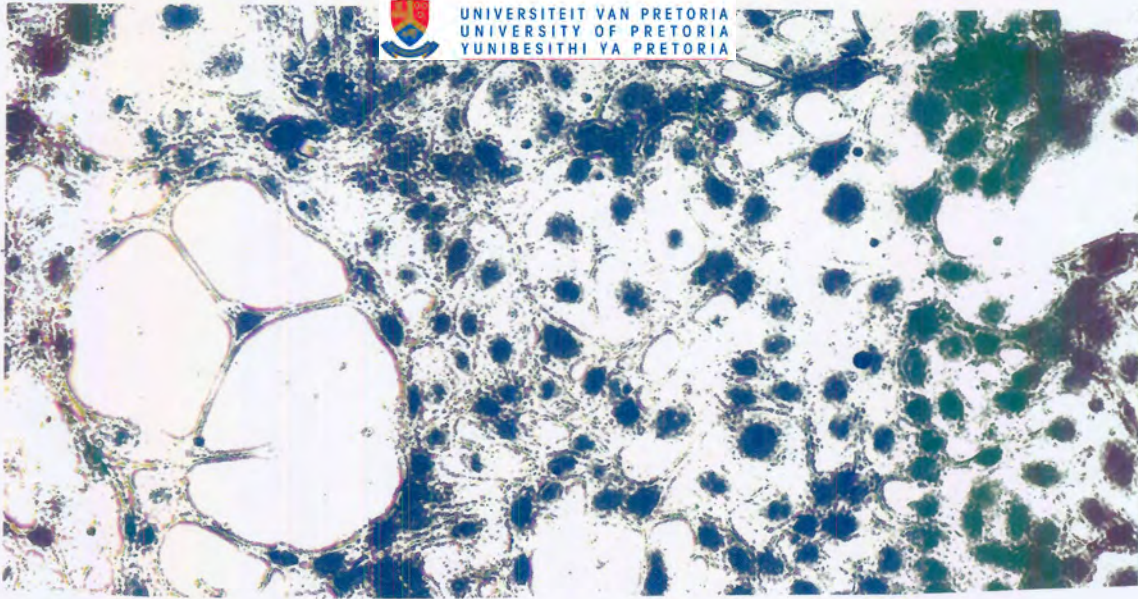


Figure 25a: Bcl2 immunocytochemistry of WHCO3 control cells exposed to 0.1% DMSO (vehicle) for 24 h. Cells do not take up the DAB stain indicating that there is no substrate reaction and that the Bcl2 protein is not present.

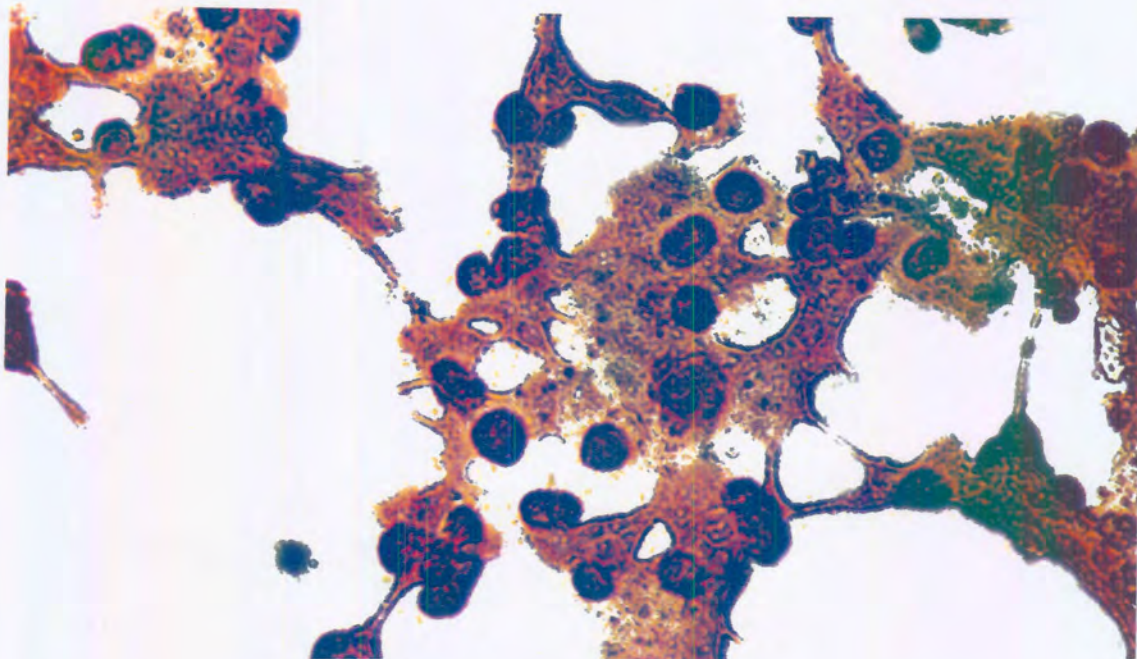


Figure 25b: Bcl2 immunocytochemistry of WHCO3 cells exposed to 1×10^{-6} M ME for 24 h. Cells appearing brown in color, indicating expression/presence of Bcl2.

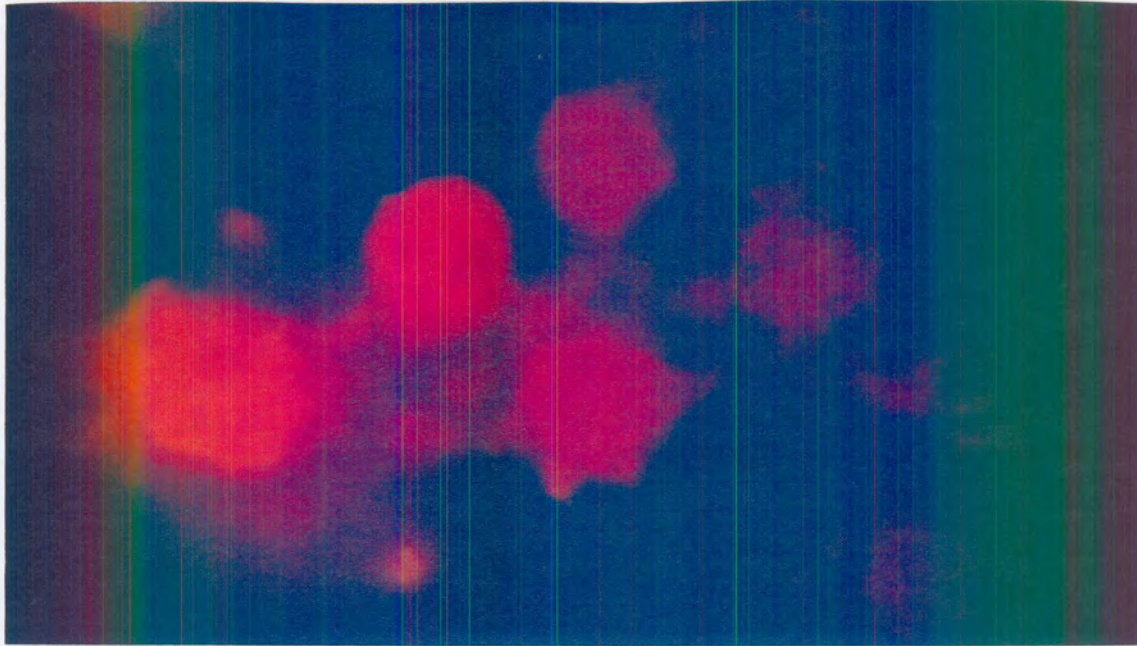


Figure 26a: Death receptor 5 immunocytochemistry of SNO control cells exposed to 0.1% DMSO (vehicle) for 24 h.

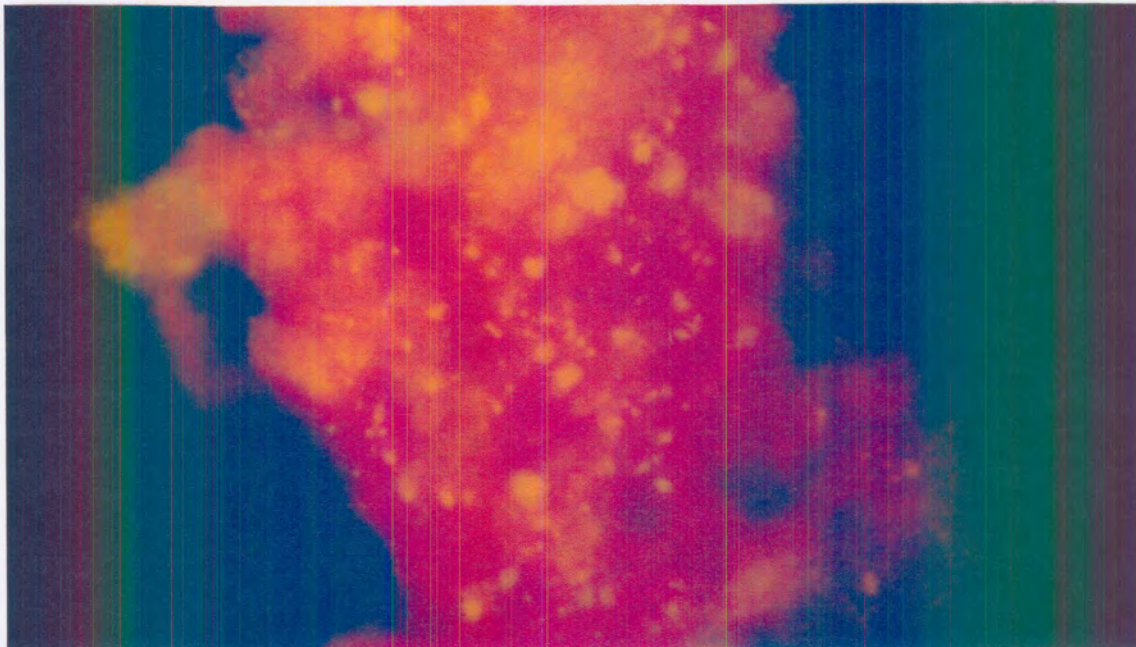


Figure 26b: Death receptor 5 immunocytochemistry of SNO cells exposed to 1×10^{-6} M 2 ME for 24 h. Yellow speckles show an increased density of DR5 on the cell surface suggesting that DR 5 is up-regulated during 2 ME-induced apoptosis.

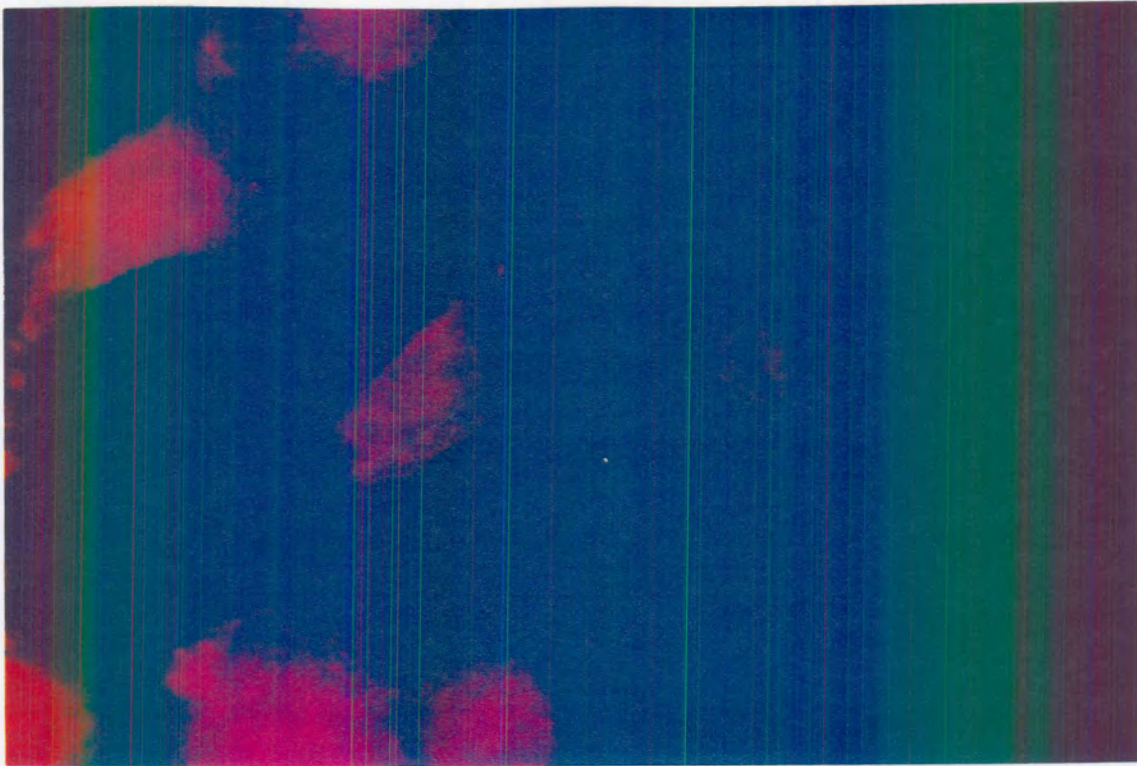


Figure 27a: Death receptor 5 immunocytochemistry of WHCO3 control cells exposed to 0.1% DMSO (vehicle) for 24 h.

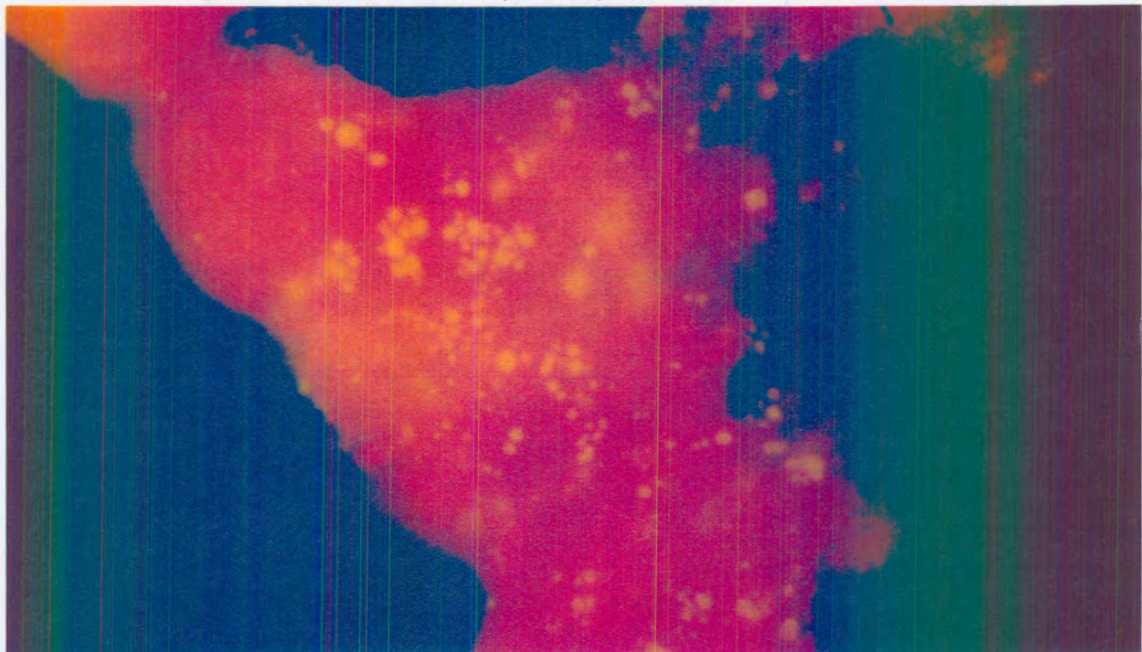


Figure 27b: Death receptor 5 immunocytochemistry of WHCO3 cells exposed to 1×10^{-6} M 2 ME for 24 h. A pronounced increase of DR5 (yellow speckles) on cell surface as compare to control cells is seen, suggesting that DR5 is up-regulated during 2 ME-induced apoptosis.

4.4.2 Death Receptor 5

To investigate whether the extrinsic pathway of apoptosis was activated when cells were treated with 2 ME, we chose death receptor 5 (DR5) as a marker since it is exclusively found in the extrinsic pathway. Immunolabeling of death receptor 5 in 2 ME-treated SNO and WHCO3 cells show possible up-regulation in expression of DR5 and suggested that the extrinsic pathway is possibly being activated during apoptosis induction by 2 ME (figure 26b and 27b). 2 ME has recently been shown to up-regulate DR5 and sensitize cancer cells to TRAIL-induced apoptosis in leukemic cells (85).

Chapter 5

Discussion

The antitumor effects of 2 ME can be divided into anti-proliferative and anti-angiogenic activity (48). 2 ME's antitumor activity can be due to disruption of various steps in the angiogenesis cascade such as migration, invasion, collagen matrix and tubule formation as shown by Pribluda *et al.* (47).

Previous studies suggested various anti-proliferative mechanisms of 2 ME *e.g.* suppression of ribonucleotide reductase enzyme in early S-phase, thereby preventing cells from duplicating their DNA. Lottering *et al.* (20) showed inhibition of ribonucleotide reductase enzyme activation by 2 ME due to suppression of mitogen activated protein kinase and DNA-dependent protein kinase activity during G1/S, delaying cells to enter into S-phase. Both these kinases activate transcription factors by phosphorylation involved in S-phase commencement (20).

In the cell growth study conducted 2 ME has shown anti-proliferative activity in both oesophageal tumor cell lines investigated. The graphs presented on p50 and p51 showed that 2 ME reduced cell numbers significantly in SNO and WHCO3 cells after 72 h. This revealed that 2 ME may display blockage of growth in the SNO and WHCO3 cell lines.

The morphological studies 2 ME caused abnormal chromatin distribution (figure 14b and figure 15b) thereby leading to the formation of multi- and micronuclei. Panzer *et al.*(86) showed that formation of micronuclei and multinuclei in cells treated with Ukrain®. Ukrain is a derivative of alkaloids from the plant, greater celandine (a

poppy-like plant, filled with a bright and acrid orange-colored juice) that has been shown to have potent antitumor properties and causes the blockage of mitosis, with resultant apoptosis (86).

This finding was consistent with the finding by Qanungo *et al.* (43) who showed that 2 ME caused pancreatic cell lines PACa-2 and PANC-1 to undergo apoptosis via a G2/M arrest. G2/M arrest caused by 2 ME could be associated with tubulin disruption. Mukhopadhyay and Roth, D'Amato *et al.* (83) have also reported that tubulin is a molecular target for the anti-proliferative action of 2 ME. This was also shown in 2 ME-treated SNO and WHCO3 cells by means of β -tubulin immunofluorescent detection (figure 18b and figure 19b).

The onset of apoptosis is characterized by shrinkage of the nucleus, as well as condensation of nuclear chromatin into sharply delineated masses that become margined against the nuclear membrane (53). This phenomenon was noted in 2 ME-treated SNO and WHCO3 cells (figure 15b).

Condensed chromatin noted in 2 ME-treated SNO and WHCO3 cells (figure 14b and figure 15b) could be the result of disrupted regulation of chromatin structure or interactions between chromatin and nuclear matrix proteins (87).

Treated cells detached from the surrounding cells and their outlines became convoluted and formed extensions as shown in figure 16b and 17b. Cells also became shrunken. Cell shrinkage could be a result of inhibition of several cellular processes

that maintain cell homeostasis, growth factor signaling and angiogenesis, or induction of apoptosis (46).

All these morphological changes are hallmarks of apoptosis indicating that 2 ME has an apoptosis-inducing action. An intact cell membrane during cell death is also a feature of apoptosis that distinguishes it from necrosis. PI and HO staining confirmed the maintenance of cell membrane integrity in 2 ME-treated OC cells, although blebbing was observed as shown in figures 20b and 21b.

It thus seems as though the anti-proliferative effects of 2 ME can be ascribed to its ability to induce apoptosis, rather than cytostatic effects. SEM revealed increased blebbing on the surface of 2 ME-treated cells as compared to control cells. This could be morphological changes, indicative of apoptosis, occurring in these cells after treatment with 2 ME.

Flow cytometric analysis showed significant difference in the number of apoptotic cells and the number of cells cycling cells between the control and 2 ME-treated cells in both the SNO and WHCO3 cells. In the treated cells increased apoptotic induction and a subsequent decrease in cycling cells were evident. Decreases were present in the G₁/G₀- and S-phase and an increase was noted in G₂/M-phase (figures 23a and 23b). An accumulation of 2 ME-treated cells in the G₂/M-phase could be due to the fact that 2 ME may possibly cause a mitotic block by interfering with spindle formation and chromosome alignment. This in turn will activate “brakes” in the cell such as p53 to prevent the cell from proceeding through the cell cycle and possibly induce apoptosis.

Cells treated with 2 ME showed an increase in mitochondrial numbers aggregating around the nuclear envelope (figure 14b and 15b). Mitochondria have been implicated as an important sensor and amplifier in intracellular death signaling pathways and have a central role as the orchestrator of apoptosis (70). Changes in mitochondrial membrane structure, either by disruption of the outer membrane or by Bax activation (88) can lead to apoptosis induction via the intrinsic pathway (figure 28).

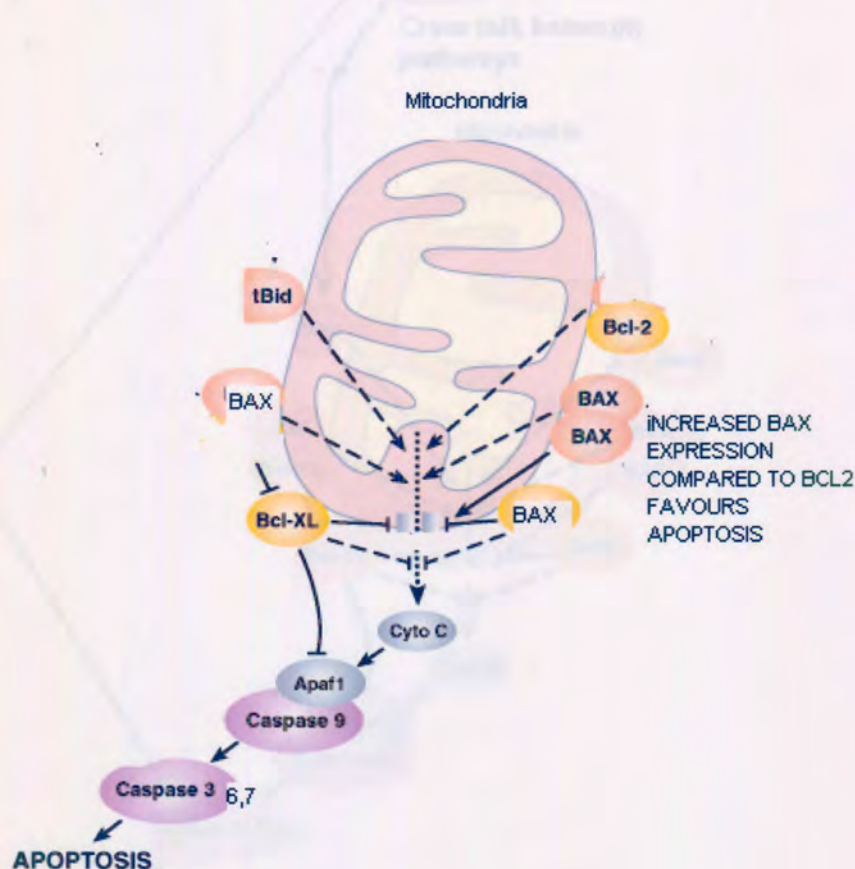


Figure 28: Increased Bax/Bcl2 ratio inhibits the anti-apoptotic function of Bcl2 (figure is adapted from 88).

Although we see Bcl2 expression in OC cells, the Bax expression could be higher and overrides the Bcl2 expression, therefore inducing apoptosis. The omission of the

determination of Bax expression has thus been identified as a shortcoming of this study.

Furthermore, other studies have identified a signaling pathway by which 2 ME causes Bcl2/Bcl-X_L phosphorylation in pancreatic cells (43). Microtubule inhibitor induced Bcl2/Bcl-X_L phosphorylation is known to be detrimental to its anti-apoptotic function (88). Phosphorylation of Bcl2/Bcl-X_L by 2 ME can cause the release of Cyt c from the mitochondria.

2 ME may possibly facilitate Cyt c release by causing the outer mitochondrial membrane to rupture due to causing swelling of the mitochondrial matrix. 2 ME may lead to mitochondrial swelling by the opening of a megachannel called the permeability-transition pore (PTP). This channel spans both the inner and the outer mitochondrial membranes at sites at which the two membranes are apposed. The adenine-nucleotide translocator (ANT), located in the inner mitochondrial membrane and the voltage-dependent anion channel (VDAC), found in the outer mitochondrial membrane are considered to be major components of the PTP. 2 ME could be a potential PTP opener like Bax, and may cause permeabilization of the inner membrane and mitochondrial depolarization by binding to the ANT. This process allows entry of water and solutes into the matrix, leads to mitochondrial swelling and causes the outer mitochondrial membrane to rupture and the release of Cyt c (89).

Increased DR5 expression was observed in 2 ME-treated cells. Expression of DR5 activates the extrinsic pathway. There is, however, opportunity for cross-talk between the extrinsic and intrinsic pathways, which is explained below (see figure 29).

DR5 expression coupled with binding of the complementary death activators FasL and TNF to Fas and the TNF receptors (90) respectively and activation of components of death-inducing signaling complex, such as FADD may trigger cleavage of caspase 8 and 10. Cleavage of caspase 8 and 10 could result in either

- a) the cleavage of caspase 3,6,7 in the extrinsic pathway which leads to proteolysis and apoptosis. This was revealed by LaVallee *et al.* (41) who showed 2 ME-induced apoptosis via the extrinsic pathway in breast carcinoma cells.

Or

- b) the cleavage of Bid in the intrinsic pathway. Bid interacts with Bax on the mitochondrial surface resulting in the release of Cyt c from the inner mitochondrial space (91). This mechanism of action of 2 ME was proposed by Qanungo *et al.* (44), who showed that 2 ME-exposed pancreatic cells exhibit Bid cleavage that is accompanied by the translocation of Bax into the mitochondria leading to release of Cyt c into the cytosol, thus activating the apoptotic signaling cascade.

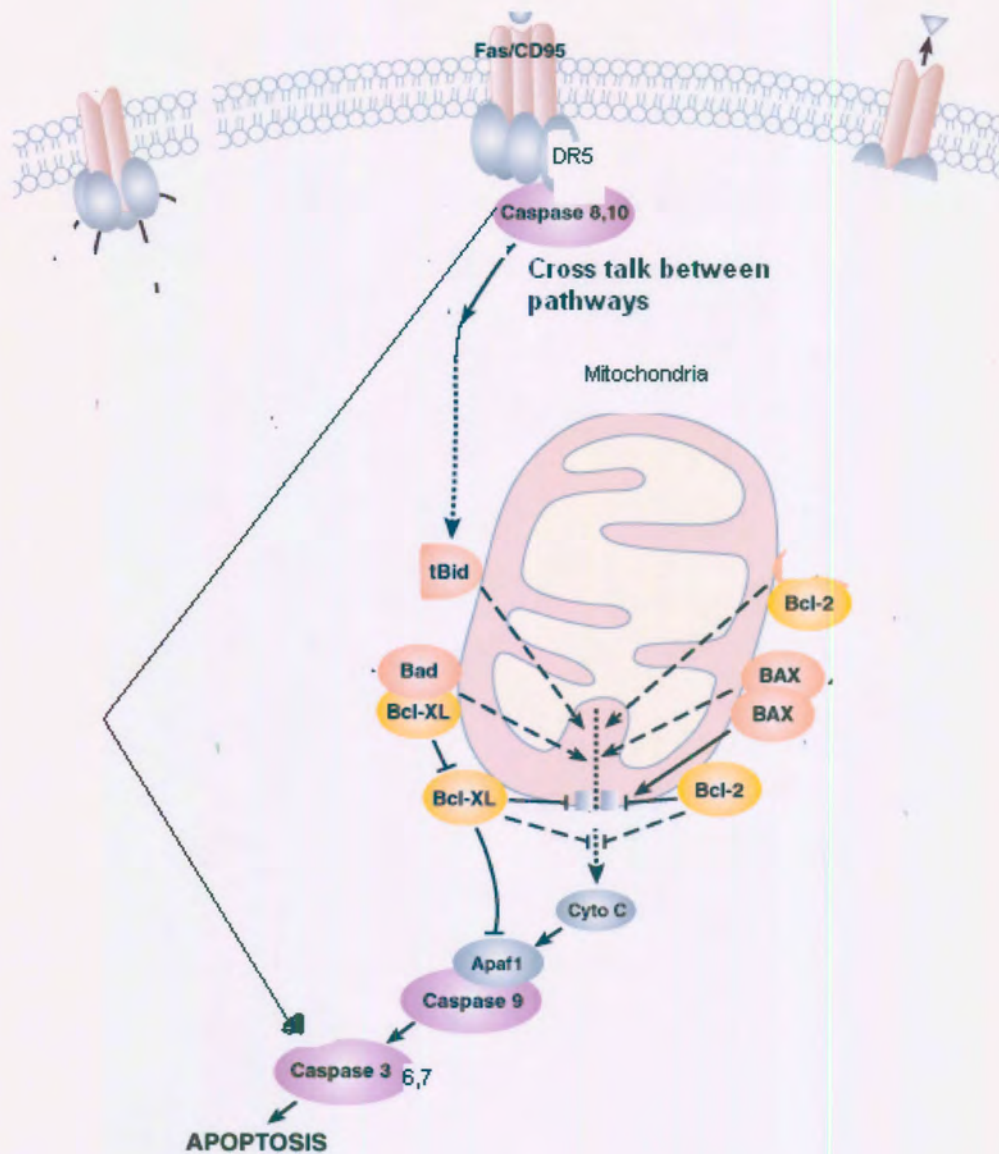


Figure 29: 2 ME may induce apoptosis via the extrinsic pathway and cross-talk between pathways can occur at caspase 8 and 10 cleavage (figure adapted from 88).

As discussed above 2 ME can potentially induce apoptosis in cells by several mechanisms. Our studies showed DR5 expression (figures 26b and 27b), suggesting involvement of the extrinsic pathway in apoptosis with possible cross-talk activity. This is consistent with the finding by Ibrahim *et al.* (92) who showed that 2 ME up-regulates DR5 and sensitizes cells to TRAIL-induced apoptosis.

The activation of caspases, and resultant proteolysis of their substrates lead to a host of morphological changes, many of which were observed in this study. 2 ME could cause DR5 expression and this may account for the nuclear envelope breakdown and blebbing as can be viewed in figures 12b, 13b and 14b in OC the cells. 2 ME could cause activation of caspases. Activated caspases also cleave and disassemble many important cellular proteins. 2 ME may induce caspase-mediated degradation of nuclear lamins A and B, essential proteins that form the nuclear lamina by phosphorylation. Disassembly of the nuclear lamina supporting the structure of the nuclear envelope is also an essential feature of nuclear breakdown in apoptosis (93). Caspases also cleave and activate DFF (94) and CAD, which mediate the DNase activity and genomic DNA degradation into nucleosomal fragments (49).

Substrates of effector caspases *e.g.* actin, Lamin A and B and NuMa (nuclear matrix associated protein) (54) participate in the formation and regulation of membrane-associated cortical microfilament skeleton, which is an important determinant of cell shape. Table 4 summarises the actions of all the proteins involved in maintaining cell shape and integrity. Caspase-cleaved forms of the proteins listed in Table 4 result in dramatic changes in the cell shape, causing cell shrinkage resembling apoptosis as observed in figures 12b, 13b, 14b 17b and 18b. These early apoptotic events are

thought to be responsible for characteristic blebbing of the cell surface (49) as seen in figures 14b and 15b.

Table 4: Summary of structural proteins processed by caspases associated with apoptotic morphology as investigated by researchers (54).

Protein	Function	Author
Actin	Regulation of cell shape in cytoskeleton	(95)
Spectrin/fodrin	Actin cross-linking proteins in cytoskeleton	(96)
Beta-catenin	Intracellular attachment protein in cell junctions	(97)
Gelsolin	Microfilament fragmenting protein	(98)
PAK2	Protein kinase involved in the regulation of cytoskeleton	(97)
MEKK1	Regulates cell morphology at cell matrix	(99)
FAK	Regulates cell adhesion at cell matrix	(100)
Rabaptin 5	Membrane protein that regulates intracellular vesicle traffic	(101)
Lamin A and B	Intermediate filaments that forms the nuclear lamina	(90)
NuMa	Mediator of nuclear chromatin-matrix protein Interactions	(102)

Morphological hallmarks of apoptosis were observed in OC cells treated with 2 ME (figures 13b, 14b and 15b).

Chapter 6

Conclusion

This study has confirmed that 2 ME (at 10^{-6} M) is an anti-proliferative agent causing massive cell death in OC cancer cells. 2 ME may be viewed as a potential apoptotic-inducing agent in OC cells since it caused morphological hallmarks of apoptosis including cell shrinkage, nuclear degradation and blebbing of cell membrane. Whilst the mechanism of 2 ME's apoptosis induction remains unclear, this study has suggested that 2 ME possibly works by activating the extrinsic pathway of apoptosis by causing increased expression of DR5. Indication of possible cross-talk between pathways exists. In summary this study has shown that:

- I) 2 ME induces cell death in OC cancer cells.
- II) the type of cell death induced is apoptosis.
- III) the extrinsic with possible cross-talk to the intrinsic pathway may be used as mechanism(s) of apoptosis induction by 2 ME.

Therefore this study has fulfilled the aims as set out in the beginning of the dissertation.

It also offers answers to the question raised about OC being more prevalent in men than women although they consume the same diet and live the same lifestyle in the Transkei. Since women have higher estrogen levels than men do, it is possible that 2 ME levels would also be higher in women than men. Increased levels of 2 ME in women could be a possible explanation of the lower levels of OC cancer in women

than in men, as this study has shown that the antitumor activity of 2 ME may have protective effects and potential usefulness as a chemotherapeutic agent. However, this study provides preliminary answers and further research, investigating the activity of caspases, mitochondrial damage, Bax/Bcl2 ratios, Bcl2 phosphorylation, cytochrome c release and the nuclear degradation is required to unravel the exact mechanism(s) by which 2 ME works as an antitumor agent.

References

1. Parker MI. Molecular Basis and early detection of oesophageal cancer. Research report. South Africa: CANSA; 2002 Aug.
2. George B, Young B, John W, Paul R, Wheeler P. Wheeler's Functional Histology: A Text & Colour Atlas H. 3rd ed. (NY): Churchill Livingstone; 1999.
3. Coleman MP, Estève J, Damiecki P, Arslan A, Renard H, editors. Trends in Cancer Incidence and Mortality. International Agency for Research on Cancer. No. 121. Lyon: IARC Scientific Publications; 1993.
4. Sagar PM. Aetiology of cancer of the esophagus: geographical studies in the footsteps of Marco Polo and beyond. Gut 1989; 30:561-64.
5. Chetty R, Chetty S. Cyclin D1 and retinoblastoma protein expression in squamous cell carcinoma. Mol Pathol 1997; 50:257-60.
6. Map of South Africa [Monograph on website]-
<http://www.anc.org.za/lists/maplist.html>-20 August 2002

7. Siersema PD, van Lanschot JJ, Fockens P, Tilanus HW. Gastrointestinal surgery and gastroenterology: Diagnosis and treatment of esophageal carcinoma. *Ned Tijdschr Geneeskd* 1999; 143:1947-52.
8. Berrino F, Sant M, Verdecchia A, Capocaccia R, Hakulinen T, Estève J. Survival of cancer patients in Europe. Report. Europe: The Eurocare study; 1995. Report No.: 132.
9. Fuchs CS, Mayer RJ. Gastric Carcinoma. *New Engl J Med* 1995; 142:182-8.
10. Roush GC, Holford TR, Schymura M, White C. Cancer risk and incidence trends: the Connecticut perspective. Washington DC, Hemisphere Publishing Corporation; 1987.
11. Tomatis L. Cancer: Causes, Occurrence and Control. Report. Lyon: International Agency for Research on Cancer; 1990. Report No.: 100.
12. Newberne PM, Schrager TF, Canner MW. Experimental evidence on the nutritional prevention of cancer. New York: New York Plenum Press; 1986.
13. Barch DH, Kuemmerle SC, Hollenberg PF, Iannaccone PM. Esophageal microsomal metabolism of N-nitrosomethyl benzyl-amine in the zinc-deficient rat. *Cancer Res* 1984; 44:5629-33.

14. Myburg RB, Dutton MF, Chuturgoon AA. Cytotoxicity of fumonisin B1, diethylnitrosamine, and catechol on the SNO esophageal cancer cell line. *Environ Health Perspect* 2002; 110:813-5.
15. Lievertz RW. Pharmacology and pharmacokinetics of estrogens. *Am J Obstet Gynecol* 1987; 156:1289-93.
16. Morel Y, Albaladej O, Bouvier J, Andre J. Inhibition by 17 β -estradiol of the growth of the rat pituitary transplantable tumor MtTF 4. *Cancer Res* 1982; 42:1492-7.
17. Anderson BE, Ross RK, Pike MC, Casagrande JT. Endogenous hormones as a major factor in human cancer. *Cancer Res* 1982; 42:1492-7.
18. Paul SM, Hoffman AR, Axelrod J, Martini L, Gananing WF, editors. *Frontiers of neuroendocrinology*. New York: Raven Press; 1980.
19. Knuppen R, Ball P, Emons G. Importance of A-ring substitutions of estrogens for the physiology and pharmacology of reproduction. *J Steroid Biochem* 1986; 24:193-8.
20. Lottering M. Effects of 17-beta estradiol metabolites on cell cycle regulatory mechanisms in MCF-7 cells. [PhD dissertation]. Pretoria: Pretoria Univ.; 1995.

21. Adams JB, Hall RT, Nott S. Esterification-de-esterification of estradiol by human mammary cancer cells in culture. *J Steroid Biochem* 1986; 24:1159-62.
22. Ball P, Hoppen H, Knuppen R. Metabolism of estradiol-17 β and 2 hydroxyestradiol-17 β in rat liver slices. *Hoppe-Seyler's Z Physiol Chem* 1974; 355:1451-62.
23. Ball P, Knuppen R. Catecholestrogens (2- and 4- hydroxy estrogens). Chemistry, biogenesis, metabolism, occurrences and physiological significance. *Acta Endocr Copenh* 1980; 93:1-27.
24. Hoffman AR, Paul SM, Axelrod J. The enzymatic formation of catechol estrogens from 2- methoxyestrogens. *Endocrinol* 1980; 107:1192-7.
25. Purdy RH, Moore PHJ, Williams MC, Goldzieder JW, Paul SM. Relative rates of 2- and 4-hydroxyestrogen synthesis are dependent on both substrate and tissue. *Febs Lett* 1982; 138:40-4.
26. Purdy RH, Merriam GR, Lipsett MB, editors. *Catechol Estrogens: Chemistry and formation of catechol estrogens*. New York: Raven Press; 1983.
27. Lippman ME, Bolam GM. Oestrogen-responsive human breast cancer in long term tissue culture. *Nature* 1975; 256:592-3.

28. Lippman ME, Bolan GM, Huff KK. The effects of estrogens and antiestrogens on hormone responsive human breast cancer in long-term tissue culture. *Cancer Res* 1976; 36:4595-601.
29. Stack G, Gorski J. Relationship of estrogen receptors and protein synthesis to the mitogenic effects of estrogen. *Endocrinol* 1985; 117:2024-32.
30. Seegers JC, Aveling M, van Aswegen CH, Cross M, Koch F, Joubert WS. The cytotoxic effects of 17- β estradiol, catecholestradiols and methoxtestradiols on dividing MCF-7 and HeLa cells. *J Steroid Biochem* 1989; 32:797-809.
31. Bigsby RM, Cunha GR. Estrogen stimulation of deoxyribonucleic acid synthesis in uterine epithelial cells, which lack estrogen receptors. *Endocrinol* 1986; 119:390.
32. Darbre PD, Curtis S, King RJB. Effects of estradiol and tamoxifen on human breast cancer cells in serum-free culture. *Cancer Res* 1984; 44:2790-3.
33. Sabourin JC, Martin A, Baruch J, Truc JB, Gompel A, Pitout P. Bcl2 expression in normal breast tissue during the menstrual cycle. *Int J Cancer* 1994; 59:1-6.
34. Wang TTY, Phang JM. Effects of estrogen on apoptotic pathways in human breast cancer cell line MCF-7. *Cancer Res* 1995; 55:2487-9.

35. Tanaka T, Kato M, Kubodera A. The characteristic binding of catechol estrogens to estrogen receptors in 7, 12-dimethylbenz (a) anthracene-induced rat mammary tumors. *Steroids* 1986; 48:361-8.
36. Davies IJ, Naftolin F, Ryan KJ, Fishman J, Siu J. The affinity of catechol estrogens receptors in the pituitary and anterior hypothalamus of the rat. *Endocrinol* 1975; 97:554-9.
37. Meeriham GR, MacLusky NJ, Pickard MK, Naftolin F. Comparative properties of catechol estrogens. I: Methylation by catechol-*O*-Methyltransferase and binding to cytosol estrogen receptors. *Steroids* 1980; 36:2589-99.
38. Fotsis T, Zhang Y, Pepper MS, Adlcrutz H, Montesano R, Naaworth PP, Schwegerer L. The endogenous estrogen metabolite 2-Methoxyestradiol inhibits angiogenesis and suppresses tumor growth. *Nature* 1994; 368:237-9.
39. D'Amato RJ, Lin CM, Flynn E, Folkman J, Hamel E. 2-Methoxyestradiol, an endogenous mammalian metabolite, inhibits tubulin polymerization by interacting at the colchicine site. *Proc Natl Acad Sci* 1994 ;91:3964-8.
40. Cushman H, He H, Katzenellenbogen JA, Lin CM, Hamel E. Synthesis, antitubulin and antimetabolic activity and cytotoxicity of analogs of 2-Methoxyestradiol, an endogenous mammalian metabolites of estradiol that inhibits tubulin polymerization to the colchicine binding site. *J Med Chem* 1995; 38:2041-9.

41. LaVallee TM, Zhan XH, Herbstritt CJ, Kough EC, Green SJ, Pribluda VS. 2-Methoxyestradiol inhibits proliferation and induces apoptosis independently of estrogen receptors alpha and beta. *Can Res* 2002; 62:3691-7.
42. Qanungo S, Basu A, Das M, Haldar S. 2-Methoxyestradiol induces mitochondria dependent apoptotic signaling in pancreatic cancer cells. *Oncogene* 2002 Jun 13; 21(26):4149-57.
43. Nishigaki K, Minatoguchi S, Seishima M, Asano K, Noda T, Yasuda N, *et al.* Plasma Fas ligand, an inducer of apoptosis, and plasma soluble Fas, an inhibitor of apoptosis, in patients with chronic congestive heart failure. *J Am Coll Cardiol* 1997 May 1; 29(6):1214-20.
44. Wassberg E, Hedborg F, Skoldenberg E, Stridsberg M, Christofferson R. Inhibition of angiogenesis induces chromaffin differentiation and apoptosis in neuroblastoma. *Am J Pathol* 1999; 154:395-403.
45. Kothakota S, Azuma T, Reinhard C, Klippel A, Tang J, Chu K. Caspase-3-generated fragment of gelsolin: effector of morphological change in apoptosis. *Science* 1997 Oct 10; 278(5336):294-8.
46. Pribluda VS, Gubish ER Jr, Lavallee TM, Treston A, Swartz GM, Green SJ. 2-Methoxyestradiol: an endogenous anti-angiogenic and anti-proliferative drug candidate. *Cancer Metastasis Rev* 2000; 19:173-9.

47. Chauhan D, Hideshima T, Pandey P. RAFTK/PYK2-dependent and independent apoptosis in multiple myeloma cells. *Oncogene* 1999; 18:6733-6740.
48. Kuan NK, Passaro E Jr. Apoptosis: programmed cell death. *Arch Surg* 1998 Jul 2; 133(7):773-5.
49. Huppertz B, Frank HG, Kaufmann P. The apoptosis cascade-morphological and immunohistochemical methods for visualization. *Anat Embryol* 1999; 200:1-18.
50. Duke, Richard C, David M, Ojcius C, Young JD. Cell suicide in health and disease [article]. *Scientific American* 1996; 2:48-55.
51. Majno G, Joris I. Apoptosis oncosis and necrosis. An overview of cell death. *Am J Path* 1995; 146:3-15.
52. Saraste A, Pulkki K. Morphological and biochemical hallmarks of apoptosis. *Cardiovascular Research* 2000; 45:528-537.
53. Thompson CB. Apoptosis in the pathogenesis and treatment of disease. *Science* 1995; 267:1456-62.
54. Van Cruchten S, Van Den Broeck W. Morphological and biochemical aspects of apoptosis, oncosis and necrosis. *Anat Histol Embryol* 2002 Aug 1;

31(4):214-23.

55. Kerr JF, Wyllie AH, Currie AR. Apoptosis: a biological phenomenon with wide range-ranging implications in tissue kinetics. *Br J Cancer* 1972; 26:239-57.
56. <http://www.sciam.org>-30 November 2002.
57. Wyllie AH, Kerr JFR, Currie AR. Cell death: the significance of apoptosis. *Int Rev Cytol* 1980; 68:251-306.
58. Liu X, Widlak P, Zou H, Luo X, Garrard WT, Wang X. The 40-kDA unit of DNA fragmentation factor induce DNA Fragmentation and chromatin condensation during apoptosis. *Proc Natl Acad Sci* 1998; 95:8461-66.
59. Enari M, Sakahira H, Yokoyama H, Okawa K, Iwamatsu A, Nagata SA. Caspase activated DNase that degrades DNA during apoptosis, and its inhibitor ICAD. *Nature* 1998; 391:43-50.
60. McCarthy NJ, Whyte MK, Gilbert CS, Evan GI. Inhibition of Ced-3/ICE-related proteases does not prevent cell death induced by oncogenes, DNA damage, or the Bcl2 homologue BAK. *J Cell Biol* 1997; 136:215-77.
61. Fesus L. Biochemical events in naturally occurring forms of cell death. *FEBS Lett* 1993; 328:1-5.

62. Konopleva M, Zhou S, Zhong X, Segall H, Claxton DF, Kornblau SM. Apoptosis: Molecules and Mechanisms. Drug Resistance in Leukemia and lymphoma. New York; 1999.
63. Burns TF, El-Diery WS. The p53 pathway and apoptosis. *J Cell Phys* 1999; 181: 231-9.
64. Zhang X, Takenaka I. Cell proliferation and apoptosis with Bcl-2 expression in renal cell carcinoma. *Urology* 2000; 56:510-5.
65. www.apoptosis-db.org - 10 July 2002.
66. Kidd VJ. Proteolytic activities that mediate apoptosis. *Annu Rev Physiol* 1998; 60:533-73.
67. Martin SJ, O'Brien GA, Nishioka WK, Mahboubi A, Saido TC, Greed DR. Proteolysis of fodrin (non erythroid spectrin) during apoptosis. *J Biol Chem* 1995; 140: 1485-95.
68. www.hokudai.ac.jp/veteri/organization/env/radbiol/apo.html-20 August 2003.
69. Zamzami N, Kroemer G. The mitochondrion in apoptosis: How Pandoras box opens. *Nature Reviews Molecular Cell Biology*. 2002. 2: 67–71.

70. Green DR, Reed JC. Mitochondria and apoptosis. *Science* 1998 Aug 28; 281(5381):1309-12.
71. Srinivasula SM, Ahmad M, Guo Y, Zhan Y, Lazebnik Y, Fernandes-Alnemri T, Alnemri ES. Identification of an endogenous dominant-negative short isoform of caspase-9 that can regulate apoptosis. *Cancer Res* 1999 Mar 1; 59(5):999-1002.
72. Sach JA, Chang L. Irritable Bowel Syndrome. *Curr Treat Options Gastroenterol* 2002 Aug 1; 5(4):267-78.
73. Du Plessis L, Dietzsch E, Van Gele M, Van Roy N, Van Helden P, Parker MI. Mapping of novel regions of DNA gain and loss by comparative genomic hybridization in esophageal carcinoma in the Black and Colored populations of South Africa. Report. Cape Town :Cancer association of South Africa; 2002.
74. Burgher Hester. Environmental and genetic markers markers for the development of esophageal cancer in different population groups in the Eastern and Western Cape Province. Research report. South Africa. Cancer Association of South Africa; 2002.
75. Freshney RI. *Animal cell culture*. 3rd ed. Oxford: URL Press; 1995.

76. Gillies RJ, Didier N, Denton M. Determination of cell number monolayer cultures. *Anal Biochem* 1986; 159:109-13.
77. Ausubel FM, Brent R, Kingston RE, Moore DD, Smith JA, Struhl K, editors. *Current Protocols in Molecular Biology: In situ Hybridization and Immunohistochemistry*. No 4. New York: John Wiley & Sons; 2001.
78. http://www.chemistry.mcmaster.ca/faculty/bader/aim/aim_2.html-2 April 2003.
79. Nias AHW, Fox M. Synchronization of mammalian cells with respect to the mitotic cycle. *Cell Tissue Kinet* 1971; 4:375-398.
80. Schutze N, Vollmer G, Knuppen R. Catecholestrogens are agonists of estrogen receptor dependent gene expression in MCF-7 cells. *J Steroid Biochem Molec Biol* 1993; 46:781-9.
81. Lin M, Chang JK, Shankar D, Sakamoto KM. The role of p53 in cell cycle control and mammalian cell proliferation, differentiation, and apoptosis. *Exp Mol Pathol* 2003; 74:123-8.
82. Schumacher JJ, Upadhyaya P, Ramakrishnan S. Inhibition of vascular endothelial cells by 1,4-phenylenebis (methylene) selenocyanate-a novel chemopreventive organoselenium compound. *Anticancer Res* 2001; 21:1945-51.

83. Mukhopadhyay T, Huober JB, Nakamura S, Meyn R, Roth JA. Oral administration of an estrogen metabolite-induced potentiation of radiation antitumor effects in presence of wild-type p53 in non-small-cell lung cancer. *Int J Radiat Oncol Biol Phys* 2000 Nov 1;48(4):1127-37.
84. Cory S, Adams JM. The Bcl2 family: regulators of the cellular life or death switch. *Nature Reviews Cancer*. 2002. 2: 647-56.
85. Atala A, Pariente JL, Kim BS. In vitro biocompatibility assessment of naturally derived and synthetic biomaterials using normal human urothelial cells. *J Biomed Mater Res* 2001; 55:33-9.
86. www.ukrin.com/ukrainindex.htm-21 October 2003.
87. Panzer A, Joubert M, Bianchi P, Ernest H, Seegers J. The effects of Chelidone on tubulin polymerization, cell cycle progression and selected signal transmission pathways. *EJCB* 2001; 80:111-8.
88. Woodle ES, Kulkarni S. Programmed cell death. *Transplantation* 1998 Sep 27; 66(6):681-91.
89. Martinou JC, Desagher S, Antonsson B. Cytochrome c release from mitochondria: all or nothing. *Nat Cell Biol* 2000 Mar; 2(3):148-55.

90. users.rcn.com/jkimball.ma.ultranet/BiologyPages/A/Apoptosis.html- 21
October 2003.
91. Haldar S, Jena N, Croce CM. Inactivation of Bcl2 by phosphorylation. *Proc Natl Acad Sci* 1995 May 9; 92(10): 4507-11.
91. Ibrahim SM, Ringel J, Schmidt C, Ringel B, Muller P, Koczan D, Thiesen HJ, Lohr M. Pancreatic adenocarcinoma cell lines show variable susceptibility to TRAIL-mediated cell death. *Pancreas* 2001; 23:72-9.
92. Lazebnik YA, Cole S, Cooke CA, Nelson WG, Earnshaw WC. Nuclear events of apoptosis in vitro in cell-free mitotic extracts: a model system for analysis of the active phase of apoptosis. *J Cell Biol* 1993 Oct; 123(1):7-22.
93. Liu X, Peng Li, Widlak P, Zou H, Luo L, Garrard WT, Wang X. the 40-kDa subunit of DNA fragmentation factor induces DNA fragmentation and chromatin condensation during apoptosis. *Proc Natl Acad Sci* 1998 Jul 21;95(15): 8461-66.
94. Brown SB, Bailey K, Savill J. β -Actin is cleaved during constitutive apoptosis. *Biochem J* 1997; 23:233-7.
95. Wang KK, Posmantur R, Nath R, McGinnis K, Whitton M, Talanian RV, Glantz SB, Morrow JS. Simultaneous degradation of alphaII- and betaII-

- spectrin by caspase 3 (CPP32) in apoptotic cells. *J Biol Chem* 1998 Aug 28; 273(35):22490-7.
96. Brancolini C, Lazarevic D, Rodriguez J, Schneider C. Dismantling cell-cell contacts during apoptosis is coupled to a caspase-dependent proteolytic cleavage of beta-catenin. *J Cell Biol* 1997 Nov 3; 139(3):759-71.
97. Kataoka M, Schumacher G, Cristiano RJ, Atkinson EN, Roth JA, Mukhopadhyay T. An agent that increases tumor suppressor transgene product coupled with systemic transgene delivery inhibits growth of metastatic lung cancer in vivo. *Cancer Res* 1998 Nov 1; 8(21): 4761-5.
99. Rudel T, Bokoch GM. Membrane and morphological changes in apoptotic cells regulated by caspase-mediated activation of PAK2. *Science* 1997 Jun 6; 276(5318): 1571-4.
100. Caulin C, Salvesen GS, Oshima RG. Caspase cleavage of keratin 18 and reorganization of intermediate filaments during epithelial cell apoptosis. *J Cell Biol* 1997 Sep 22; 138(6): 1379-94.
101. Cardone MH, Salvesen GS, Widmann C, Johnson G, Frisch SM. The regulation of anoikis: MEKK-1 activation requires cleavage by caspases. *Cell* 1997 Jul 25; 90(2): 315-23.

102. Cosulich SC, Horiuchi H, Zerial M, Clarke PR, Woodman PG. Cleavage of rabaptin-5 blocks endosome fusion during apoptosis. *EMBO J* 1997 Oct 15; 16(20):6182-91.